# The formulation of novel calcium phosphate containing culture beads for cell therapy

By

Parastoo Jamshidi

A thesis submitted to the School of
Chemical Engineering of the
University of Birmingham for the
degree of Doctor of Philosophy

School of Chemical Engineering
University of Birmingham
Edgbaston
Birmingham
B15 2TT

## Abstract

Cell therapy has recently gained much attention as a novel treatment method for a range of diseases. Many early examples of mesenchymal stem cell use have focussed on infusion of a cell population and rely on the cells locating to the area of tissue damage. The development of implantable materials in the form of microcarriers to deliver cell populations to the site of injury could help enhance efficacy of treatment. Such carriers may also be used to expand cell populations *in vitro*. In this thesis, a range of cell culture beads have been formulated using calcium phosphate ceramics, with and without the addition of a hydrogel such as gellan gum. The processing of the calcium phosphate (brushite) cement beads was shown to be critical to cell attachment, with the use of a crystallisation inhibitor in the formulation causing cell detachment. By conditioning the beads post manufacture or by using a process of granulation of brushite crystals, it was possible to generate beads that enable attachment and proliferation of the cells: a ~34 fold increase in the case of post treated beads and ~6 fold in the case of granulated beads. It was also shown that modification of gellan gum with nano-scale HA (nHA) at a concentration of 50 wt% allowed the control of mechanical properties by increasing yield strength and bulk modulus by four- and nine fold, respectively. Finally, it was shown that both ceramic and ceramic-hydrogel beads were conducive to bone formation when culturing MC3T3 pre-osteoblast cells in static and dynamic conditions, respectively.

## Acknowledgments

First and foremost I would like to express my appreciate and thanks to my supervisor, Professor Liam Grover for his invaluable inspiration, supervision, guidance and support throughout my PhD. Without his help I could not be a research scientist. I would also like to thank Dr. Rachel Bridson who has truly made a difference in my life. It was her help and guidance that I could start my PhD.

Great appreciation to all my fellow PhD students who have been great support to me during my PhD. Special thanks to Dr. Gurpreet Birdi who has been a good friend and was always willing to help and for all the fun we have had in the last three years. Great thanks to Dr.Amir Anvarian and Elnaz for all their helps and all the sleepless nights we were working together in the lab and all good memories we have had during my PhD. Thank you to Dr. Maryam Kargar for her pure friendship, advice, support and all the sweet and unforgettable memories we have had during our PhDs. Thank you also to Richard William (My kind brother) for our philosophical debates, fun and exchanges of knowledge. Thanks to Abigail Norton for her kindness, friendship and all her support for taking care of me during the last 6 months of my PhD. I extend my special thanks to Dr. Jennifer Paxton for her insightful comments, her help and her friendship throughout my PhD.

I would also like to thank staff members: Dr James Bowen and Mrs Rooney for their assistance with various laboratory equipment and technical help, specially, Ms Elaine Mitchell for her patience, kindness and her technical help, throughout my research.

I would also like to acknowledge the Biotechnology and Biological Sciences Research Council for financial support and Advanced Materials (AM2), funded by Advantage West

Midlands (AWM) and part funded by the European Regional Development Fund (ERDF), for use of their equipment.

I would also like to thank Birgitta and John for all their kindness and that they always support me like my parents in Birmingham. Thanks also go to my closest friend in Birmingham Marmar who has been a great friend with a great support and lots of fun during my PhD.

My sincerest thanks go to my great parents for their constant emotional support, prayers and encouragement. It was all your good advice in my life that I could reach to this stage of my life. I would also like to thank my sisters Elham and Atefeh and my brothers-in-law Reza and Morteza who have been always there for me for any help and support throughout my study.

Finally I would like to thank my beloved husband, Saeed Khavaninzadeh, for his constant love, all his never-ending support and encouragement throughout my PhD. I would not have been able to complete my PhD without him. Special thanks also to my little princess Sofia who brought joy and luck to my life since her birth and made my life much easier and more joyful.

# TABLE OF CONTENTS

# LIST OF FIGURES

# List of Tables

# LIST OF ABBREVIATION

| | |
|---|---|
| **ALP** | **Alkaline phosphatase** |
| **BC** | **Brushite cement** |
| **BET** | **Brunauer- Emmett-Teller** |
| **BMSCs** | **Bone marrow stromal cells** |
| **BPC** | **Brushite powder compact** |
| **C** | **Cement Casting** |
| **CA** | **Citric acid** |
| **CaP** | **Calcium phosphate** |
| **CPC** | **Calcium phosphate cement** |
| **DAPI** | **4´,6-diamidino-2-phenylindole** |
| **DCP** | **Dicalcium phosphate** |
| **DCPA** | **Dicalcium Phosphate Anhydrous (Monotite)** |
| **DCPD** | **Dicalcum phosphate dyhydrate** |
| **DCP** | **Dicalcium phosphate** |
| **DMEM** | **Dulbecco's Modified Eagle Medium** |
| **ECM** | **Extracellular matrix** |
| **EDX** | **Energy dispersive X-ray** |
| **FBS** | **Foetal Bovine Serum** |
| **FDA** | **Food and Drug Administration** |
| **FP** | **Flat Plate** |
| **G** | **Cement Granulation** |

| | |
|---|---|
| **GG** | **Gellan Gum** |
| **HA** | **Hydroxyapatite** |
| **HEPES** | **4-(2-hydroxyethyl)-1-piperazineethanesulfonic acid** |
| **M** | **Soaking Marble methode** |
| **MCPM** | **Monocalcium phosphate monohydrate** |
| **MeGG** | **Metacrylated gellan gum** |
| **mHA** | **Micro-scale hydroxyapatite** |
| **MSCs** | **Mesenchymal stromal cells** |
| **MTT** | **(3-(4,5-Dimethylthiazol-2-yl)-2,5-diphenyltetrazolium bromide** |
| **nHA** | **Nano-scale hydroxyapatite** |
| **OA** | **Orthophosphoric acid** |
| **OCP** | **Octacalcium phosphate** |
| **OI** | **Osteogenesis Imperfecta** |
| **PBS** | **Phosphate buffer saline** |
| **PHEMAPNIPAAm** | **Poly (hydroxyethylmethacrylate)- poly(N-isopropylacrylamide)** |
| **P/L** | **Powder to liquid ration** |
| **PLGA** | **Poly(lactic-co-glycolic acid)** |
| **PNIPAAm** | **Poly(N-isopropylacrylamide, NIPAAm)** |
| **RGD** | **R: arginine; G: glycine; D: aspartic acid** |
| **SEM** | **Scanning electron microscopy** |
| **SP** | **Sodium pyrophosphate** |
| **SSA** | **Specific surface area** |
| **TEM** | **Transmission electron microscopy** |
| **TTCP** | **Tetracalcium phosphate** |
| **VEGF** | **Vascular endothelial growth factor** |

| | |
|---|---|
| **WL** | **Water Lily** |
| **XRD** | **X-ray diffraction** |
| **α-MEM** | **α-Minimum Essential Medium** |
| **β-TCP** | **β-Tricalcium phosphate** |

# Chapter 1

## INTRODUCTION

Every year millions of people worldwide suffer from cartilage injuries and bone loss due to diseases, trauma, sporting activities, and age related degeneration. As such there is an ever increasing demand for the repair and regeneration of these tissues.

Bone is continuously remodelled during our lifespan and most bone lesions, such as fractures, can heal well with conventional conservative therapy or surgery. In cases where the bone defect is large and unconfined, surgical augmentation using bone graft or bone graft substitute is required. Autologous and allograft bone substitutes have significant disadvantages including inconsistency, the need for a second surgical procedure, donor site pain and in the case of allograft, the risk of disease transmission and rejection (Amini et al. 2012).

Cartilage has limited regenerative capabilities since it is largely avascular, so regeneration requires physical augmentation. Microfracture, the implantation of autologous chonrocytes and osteochondral transplantation are the currently available techniques for cartilage lesion regeneration (Cancedda et al. 2003; Kafienah et al. 2007). These techniques, however, have been only practical for the treatment of focal lesions. For this reason there is a need for the development of alternative techniques for the regeneration of diseased and damaged bone and cartilage tissues.

Tissue engineering using a population of cells can overcome the drawbacks of these existing treatments methods. Tissue engineering approaches, which still have much lower efficacy than autografts, need to be much improved before widespread clinical application. One limiting factor is that it is challenging to provide a sufficiently large number of appropriate cells and localise these within the site of implantation. Bone marrow stromal cells (or mesenchymal stem cells) (MSCs) have considerable potential for expediting the repair of a range of connective tissues including bone and cartilage (Caplan 2007). The clinical application of MSCs, however, due to the low number which can be obtained from a single donor is limited (Caplan and Bruder 2001). Therefore there are still significant challenges that need to be addressed. The development of a culture system which enables the rapid scale- up of MSCs to a number that is feasible for clinical application is currently being investigated. In addition ensuring that the population of MSCs differentiates along the desired lineage without the need for re-seeding the retrieved cells is challenging. The use of microcarriers in the development of implantable material with precisely engineered modulus, can address future challenges in developing large cell expansion processes and in achieving control of desired tissue formation for tissue regeneration (Malda and Frondoza 2006; Park et al. 2013a).

In the design of culture beads, the microenvironment; material architecture, surface chemistry and stiffness of the material to which the cells are attached are key elements that can exert significant influence on cell fate in therapeutic cell delivery. Among the compositions developed, calcium phosphate cements (CPCs), have been widely investigated as materials for bone and (in combination with soft matter) cartilage tissue replacement and have found numerous clinical applications in the last three decades due to their biocompatibility in musculoskeletal tissues, osteoconductivity and the fact that they may be processed in ambient

conditions which are not detrimental to the incorporation of bioactive molecules and therapeutics, (Coutinho et al. 2010; Lin and Yeh 2004; Faleh Tamimi Mariño et al. 2007b; Penel et al. 1999). Cell-attached culture beads formed from these materials could be used for cell therapy. Brushite ($CaHPO_4.2H_2O$) is a calcium phosphate that is several orders of magnitude more soluble than hydroxyapatite (HA; $Ca_{10}(PO_4)_6OH_2$) and as such may be resorbed into the body following implantation. It is surprising; therefore, that few studies have focused on the use of brushite-based materials in the form of culture beads. One of the aims of this project was to develop a method for the fabrication of brushite culture (BC) beads and to investigate cellular attachment to the surface of BC beads systematically in terms of the influence of cement chemistry and the type setting retardant additives used in cement production. The effect of other properties of the beads including surface area and surface topography, which are dependent on manufacturing processes, on cellular behaviour was also investigated.

Another class of implantable materials that could be used to manufacture culture beads are hydrogels. The use of these materials in therapeutic cell delivery has been limited by the fact that they do not readily facilitate cell attachment and their relative fragility (Malafaya et al. 2007). One approach to improve the attachment of cells to hydrogel surfaces and modulate elasticity to direct differentiation appropriately is to incorporate synthetic calcium phosphate particles into the hydrogel matrix. Although several authors have reported the reinforcement of hydrogels with ceramic particles, there have not been any studies that investigate the effect of size and crystallinity of HA particles on the mechanical properties of hydrogel.

In this thesis therefore, nano-sized synthetic hydroxyapatite (nHA) and micro-scale HA (mHA) particles were used to manufacture gellan gum (GG)/HA nanocomposites. The effect of size and crystallinity of HA particles on the mechanical properties of the hydrogel was investigated in order to achieve a more physiologically relevant range of mechanical properties. Additionally, the influence of HA nanocrystal incorporation into the gellan gum (GG) matrix on behaviour of GG/HA culture beads in terms of cell adhesion was investigated in a spinner flask and compared to that of GG/HA disk and static bead cultures.

# Chapter 2

## MUSCULOSKELETAL TISSUES: STRUCTURE AND REPAIR

The human musculoskeletal system comprises bone, cartilage, muscle, ligament, intervertebral discs and tendon, all of which are important building blocks of the human body that support and bind tissues and organs together and allow for movement of the body (Yaszemski and Yasko, 2007). This organ system fulfils important tasks including maintenance of stability, support, movement, protection and storage. The muscles are responsible for giving the body its shape, generating heat, maintaining posture and allowing movement. Bone, the skeletal portion of this system, provides the structure for muscles to attach through tendons. The skeletal system is the framework of the body, and serves as a structure and protection for fragile body tissues and vital internal organs such as the heart, brain, lung, kidney and liver in the human body as well as the main storage system for the two most abundant minerals in the body; calcium and phosphorous. It is also responsible for the production of the blood cells.

All of the aforementioned tissues repair naturally in the human body, however, there are some defects of a critical size that result from trauma, tumour resection, and infection that are too large to regenerate spontaneously and require clinical repair and reconstructive surgery to restore function. Understanding the properties of the musculoskeletal system is essential for the evaluation of current therapies and to allow for the development of more targeted methods of regeneration. In the following sections, therefore, the structure and function of musculoskeletal tissues, bone and cartilage are summarized, along with the appropriate

strategies, traditional and current treatment for the damaged and diseased bone and cartilage defects.

## 2.1. Bone

Bone is a hierarchically complex structured material with remarkable mechanical performance which is responsible for movement and is the main storage system for the most abundant minerals of our body such as calcium and phosphorous. It is also responsible for the production of the blood cells. The basic building blocks of bone are collagen fibrils, providing its tensile strength, and nHA, which give it stiffness in compression (Fratzl et al. 2004).

Bone is continuously being built-up and broken-down during the life span of an individual as a result of the balance between the activities of osteoblasts and osteoclasts, which sequentially carry out formation of new bone and resorption of old bone. The correct balance of this process is critical to bone strength (Cancedda et al. 2003; Clarke 2008).

### 2.1.1. Bone structure

Bone consists of two main types; cortical and spongy. The combination and architecture of these two are responsible for the essential mechanical function of the skeleton. The adult human skeleton is composed of 80% cortical bone (compact type of bone tissue) which is denser than spongy bone and surrounds the marrow space, whereas spongy-bone (cancellous bone) constitutes 20% of the weight of the skeleton (Clarke 2008; Salgado et al. 2004). The outer surface of the bones is covered with a dense layer of vascular connective tissue called periosteum, except at joints where bone is lined by articular cartilage, which contains blood vessels, nerve fibres, and osteoblasts and osteoclasts. Both types of bone are composed of osteons. Osteons, which are known as haversian systems consist of concentric circles

(lamellae) surrounding the central cavity containing blood vessels and nerves (Clarke 2008). They consist of pores containing osteocytes (Figure 2.1.).

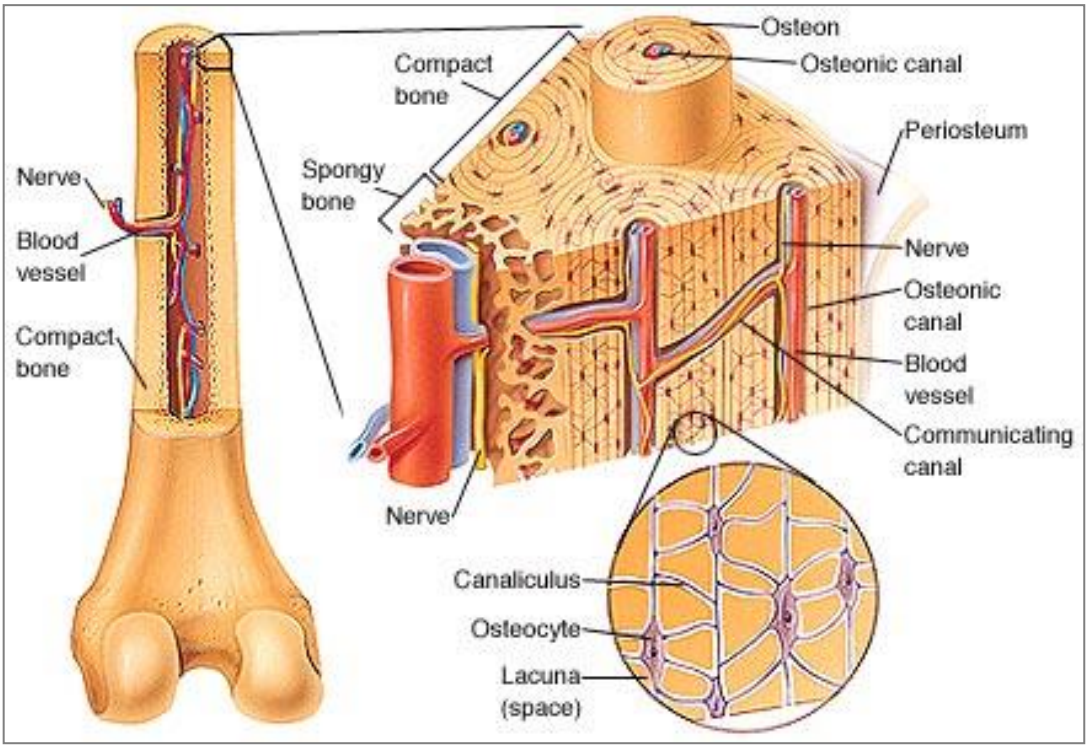


**Figure 2.1: Diagram representation of the main structural features of a typical long bone with a magnified view showing the finer details (http://www.mhhe.com/).**

### 2.1.2. The cells of bone

Bones contain four types of cells; osteoprogenitor cells, osteoblasts, osteocytes, and osteoclasts. The first three cell types are responsible for formation and maintenance of the bone matrix and the role of the osteoclast cells is the degradation of the bone matrix (LeGeros 2008). The least differentiated cells, osteoprogenitors, are located in the periosteum and the bone marrow. These cells divide to produce additional cells, osteoblasts that are responsible for synthesising bone matrix. Osteoblasts that become encapsulated in lacuna within the mineralised matrix differentiate to form osteocytes. The lacunae are connected to each other by small channels called canaliculi (Weiner and Wagner 1998). The exchange of nutrients and

waste products to maintain the viability of the osteocytes is through these channels. Osteocytes are derived from osteoblasts and are thought to maintain the secreted mineralized extracellular matrix (ECM).

### 2.1.3. Bone pathologies and tissue grafting

Bone defects can occur as a result of trauma, tumour resection, resection following infection, biochemical disorders, or abnormal skeletal development (Amit et al. 2006). The ageing population and occurrence of sports-related injuries also enhance the requirement for new bone to replace or to restore the function of traumatized, damaged, or lost bone. A bone graft or a bone substitute is often essential in an orthopaedic and maxillofacial surgery to assist healing of large traumatic or post-surgical defects and of osseous congenital deformities (Kneser et al. 2006). The xenograft, allograft and autograft have traditionally been used for many years as bone grafts for the replacement of lost or damaged bone tissue.

Until recently, the use of autologous bone has been considered the preferred choice to augment bone tissue healing and repair. In an autograft reconstruction, the graft is taken from elsewhere in the patient's body and used as the new bone or to form new bone tissue. This traditional technique has no risk of disease transfer or rejection from the body, in contrast with allografting where the bone graft is transplanted from one person to another presenting a risk of disease transmission and rejection from the patient's body. The use of autologous bone in bone repair has significant problems such as the need for a second surgical procedure, donor site pain, morbidity associated with infection, nerve damage and the limited quality of bone that can be harvested.

Xenografts are organs or tissues transplanted from other species to patient's body (e.g. a graft from a cow to a human) (Richardson et al. 1999). The use of most xenograft tissues is excluded because of a vigorous immune response on implantation leading to a high failure rate (Babensee *et al.* 1998; Garfein *et al.* 2003).

## 2.2. Cartilage

Articular cartilage is composed of a complex, highly organised extracellular matrix (ECM) which principally consists of water, collagen, and proteoglycans, with other non-collagenous proteins, and one unique cell population embedded in the matrix, known as chondrocytes (Bhosale and Richardson 2008; Cancedda et al. 2003; Newman 1998). The cells and the matrix are distributed within four different cartilage layers identified as the superficial zone, transitional zone, middle or deep zone and calcified cartilage zone (Pearle et al. 2005) (Figure 2.2). Together these components are responsible for providing a protective surface for the joint, allowing it to withstand significant load.

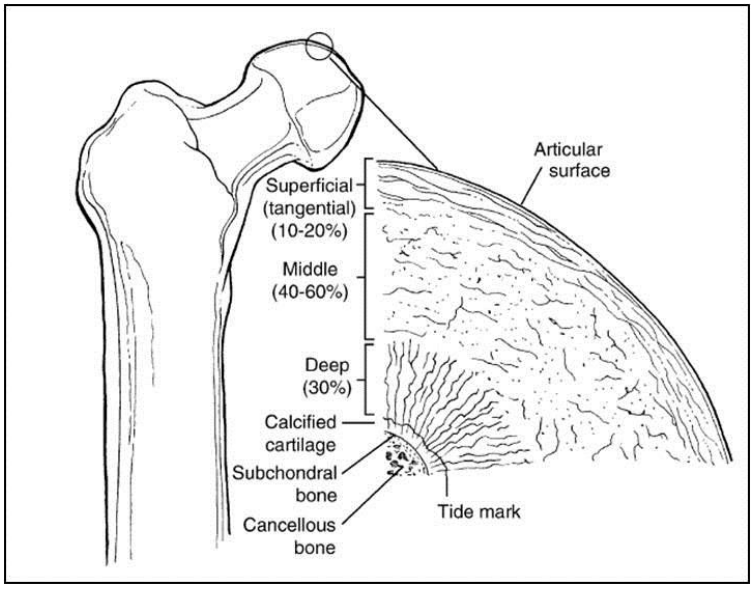


**Figure 2.2: The structure of cartilage demonstrating a zonal arrangement (Pearle et al. 2005).**

There exist three different types of cartilage within different areas of the body such as the knee, shoulder, ribs, ear, intervertebral discs and the nose (Figure 2.3). Articular cartilage, which is also called hyaline cartilage, covers the joint surfaces facilitating smooth movement at joints. The second type of cartilage, fibro-cartilage, which contains a higher proportion of collagen in the ECM compared to hyaline cartilage, is found in many areas in the body such as the intervertebral discs and elastic cartilage forms the ear and nose and is characterized by the presence of elastin in the ECM (Temenoff and Mikos 2000).

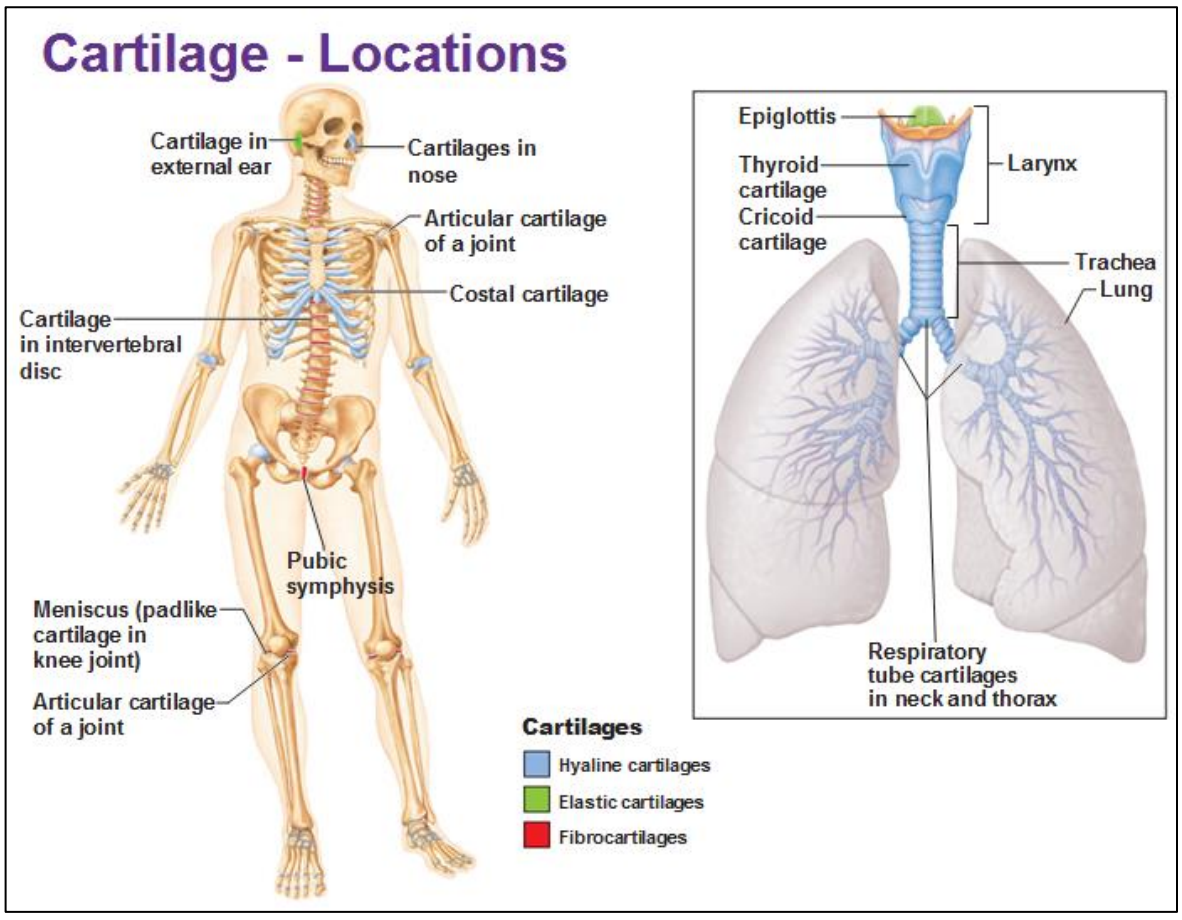


**Figure 2.3: A diagrammatic representation of cartilaginous regions found in different areas of the human body (http://dancehealthier.com/2012/04/).**

### 2.2.1. Damage and repair (strategies for articular cartilage repair)

Cartilage is unique among other connective tissue as this tissue is a poorly vascularized and has limited regenerative capability (Hwang et al. 2007; Malda et al. 2003a). Although the structure appears simple with only one cell type, it has a complex and highly organised ECM. Therefore, the reconstruction of cartilage defects caused by trauma and degenerative joint diseases that may be driven by changes in biomechanics, cytokines, growth factors and cellular responses has been a major clinical problem in the practice of orthopaedic surgery (Chang et al. 2005; Mackay et al. 1998). Several methods including microfracture, the enhancement of chondral resurfacing by providing an environment for new tissue formation and the usage of the body's own healing potential, joint lavage, tissue debridement, implantation of autologous chondrocytes and osteochondral transplantation are currently available for the repair of articular cartilage lesions (Cancedda et al. 2003; Kafienah et al. 2007). These techniques however are often less than satisfactory and they may lead to the formation of fibrous tissue, apoptosis and further degeneration of cartilage. They have been only practical for the treatment of focal lesions. To repair large and unconfined cartilage defects, such as those found in osteoarthritis, the implantation of 3-dimensional engineered cartilage tissue has great potential as a permanent method of regeneration (Mahmouddifar and Doran, 2005). The most effective cartilage engineering protocols are discussed later in the following sections in this thesis.

## 2.3. Cell therapy

Cell therapy has recently gained significant attention for the regeneration of diseased and damaged tissues. This strategy relies on the delivery of cells into a patient's body to aid in the direct formation of new tissue. This novel clinical approach overcomes the complications that can be caused by autologous transplants and allogeneic treatment for bone and cartilage repair.

Currently most bone and cartilage repair methods using cell therapy depend on the cell source, a feasible cell expansion system and the right choice of cell carriers to the site of injury. The transplantation of autologous chondocytes into defect areas such as chondral defects has been used clinically since 1987 and it has been used for approximately 12,000 patients worldwide, however the limitation of this cell based therapy is the low number of the obtained cells from donor tissue (Naveena et al. 2012). Also for large bone defects there are still significant challenges to be overcome to make the therapies clinically feasible.

A system with multifunctional characteristics, comprising the ability of provision of a sufficiently large number of cells for the therapy as well as preservation of cell phenotype following the expansion and delivery to form bone and cartilage tissues is required as a permanent solution for cartilage lesions and large bone defects.

### 2.3.1. Tissue Engineering (TE)

Tissue engineering as an effective alternative to the traditional grafting techniques was defined back in early 1990s (Langer and Vacanti, 1993). This multidisciplinary science aims at restoring damaged and diseased tissues by combining the principles of engineering, biological science, materials, and then manipulating the interactions between them (Eisenbarth, 2007; Leor et al. 2005; Naveena et al. 2012) to develop biological tissue replacements or enhance tissue or organ function. In the last several decades, tremendous advances have been made in the field of tissue engineering, particularly with tissue of simple structure such as skin (Amini et al. 2012). Engineering tissues like bone and cartilage, however, is more challenging as the structure and mechanical strength of these tissues vary by their distinct and dynamic loading conditions, as well as location in the body (Amini et al. 2012). In bone and cartilage, therefore, tissue engineering must consider very carefully

cellular and molecular developmental biology and morphogenesis, bioengineering and biomechanics to ensure that the final product exhibits the appropriate properties.

#### 2.3.1.1. Tissue engineering bone

Bone tissue engineering can be classified into three approaches; the design of the materials that are used as direct bone graft replacements to induce formation of bone from the surrounding tissue (acellular: no additional cellular component), those that act as a carrier for implanted bone cells (cellular systems) and the third group that are designed for delivery of osteoinductive growth factor such as bone morphogenic proteins. The latter group can be also used with cellular bone tissue-engineered constructs which may be loaded with growth factors capable of enhancing bone function (Burg et al. 2000). The success of bone tissue engineering depends on suitability of the selected carriers. Materials must exhibit appropriate mechanical properties and microstructure. In addition, they must be able to facilitate attachment that will initiate bone function (Marolt et al. 2012; Shin et al. 2004; Yuan and Groot 2005). Some bone tissue engineering attempts for repairing bone defects are summarised in Table 2.1. Efforts are still being made to discover new strategies to make bone tissue engineering more clinically feasible. These strategies involve developing mechanically stronger, porous scaffolds to achieve proper vascularization and host integration, designing immunomodulatory biomaterials by incorporating growth factors via the scaffold or genetically modified cells that release increased levels of angiogenic vascular endothelial growth factor (VEGF) to modulate the host's foreign-body response to inhibit fibrous tissue formation (Amini et al. 2012) and recently improving biologics delivery strategies with the use of carriers with appropriate form, function, or fixation (Hollister and Murphy 2011). Many other strategies including the application of stem cells for expediting the repair of bone

tissue are also currently being investigated in the field of bone tissue engineering (A. I. Caplan 2005, 2007; Horwitz et al. 1999; Tuan et al. 2003).

Although much progress has been made, all approaches in bone tissue engineering have been "single-component" and there are still many crucial hurdles for the translation of scaffold and cell-based bone tissue engineering therapies to clinical use (Hollister and Murphy 2011). For bone tissues engineering to become a widespread clinical reality, multi-component strategies consisting of all necessary components (i.e. appropriate carrier, cells, appropriate culture condition and growth factor) are required. For instance, a bioreactor - culture bead system that can combine all these components can be a potential solution for safer and more effective bone tissue engineering.

**Table 2.1: A summary of key bone tissue engineering papers.**

| Scaffold materials | Geometry | Fabrication technology | Cell type | Bone formation | References |
|---|---|---|---|---|---|
| Bioactive glass ceramic | Disk shape | Ready samples supplied by USBiomaterials | Human primary osteoblasts | *In vitro* | Xynos et al. 2000 |
| Bovine Collagen-Hydroxyapatite | Disk shape composites | Dehydration and ϒ-ray irradiated of composite mixture | Human osteoblast cells | *In vitro* & *in vivo* | Rodrigues et al. 2003 |
| Polycaprolactone (PCL) | Cylinders with 3-D orthogonal periodic porous architectures | Selective laser sintering | Primary human gingival fibroblasts | *In vivo* | Williams et al. 2005 |
| Calcium phosphate (HA+β-TCP) | Evacuated microcarriers | Oil-in-water emulsification method | MSCs | *In vivo* | Jin et al. 2012 |
| Modified PLGA | Circular plate | Coating with natural biomaterial solutions of collagen, chitosan, or N-succinyl-chitosan | Rat calvaria stromal cells | *In vitro* | Wu et al. 2006 |
| Akermanite-bioactive ceramics | Disk shape | Sol–gel process | (hBMSC) | *In vitro* | Sun et al. 2006 |
| n-HA/PA | Rectangular shape | Thermally induced phase inversion processing technique | (MSCs) from neonatal rabbits | *In vivo* (defect on rabbit mandible) | Guo et al. 2011 |

### 2.3.1.2. TE-Cartilage

Cartilage tissue engineering similar to TE-bone provides a potential solution for cartilage regeneration (Kafienah et al. 2007). Cartilage tissue regeneration can be more challenging as cartilage cannot self-repair and is avascular (LaPorta et al. 2012). In cartilage tissue engineering approaches, autologous chondrocytes are used to generate the 3-dimensional structure of the tissue. The use of these approaches, however, is limited because of their low quantity and the lack of autologous donor tissue for large and unconfined defects. This has led researchers to explore the use of stem or progenitor cells as a cell source for generation of cartilage tissue (Kafienah et al. 2007). Stem or progenitor cells isolated from foetal and adult cartilage as an alternative cells source are demonstrate significant therapeutic potential for articular cartilage repair (Cetinkaya et al. 2011). The success of cartilage tissue engineering also strongly depends on the specific cell-carrying structures as a supporting matrix for cell expansion as well as providing signals for cell growth and the induction of chondrogenesis (Suh et al. 2000). Hydrogels are a class of polymer-based materials that have been extensively reported as scaffolds for cartilage tissue engineering, due to their similar structure to cartilage with highly hydrated features composed of chondrocytes cells embedded in the matrix. Three-dimensional structures formed from chitosan, agarose, gellan gum, type I and II collagen gels, and alginate have been shown to have potential as cell-laden scaffolds for promotion of chondrogenesis in the presence of defined medium (Hwang et al. 2007; Xi Lu et al. 19999; Suh et al. 2000). Efforts are still being continuously devoted to discover new strategies to make cartilage tissue engineering clinically more feasible. One recent study by Fayol et al. (2013) demonstrated the feasibility of forming cartilage tissue units of defined

sizes and shapes from stem cell aggregates by magnetic condensation in chondrogenic media (Fayol et al.2003).

## 2.4. Cell delivery

The delivery of cells to the site of an injury has been shown to expedite healing for the treatment of many diseases. For examples the most current method for cartilage-repair is an introduction of chondrogenic cells into the defect area (Cetinkaya et al. 2011). The survival and engraftment of directly injected specific cell types into the targeted location, however, can be adversely impacted by various factors including: cellular microenvironment of the implantation site which may not be able to maintain the viability of cells due to the extent of tissue disease and injury, active clearance of the injected cells by the host immune response and mechanical damage of the cells caused by the injection process (Franco et al. 2011). For this reason, cell delivery requires a supporting matrix to provide cell protection during delivery (Kretlow et al. 2009). In order to achieve successful cell delivery, two main critical elements should be considered, including the right choice of biomaterial carrier that serves as a mechanical and biological support for cell growth and appropriate structure in which cells can reside. The supporting matrix for delivery of cells should be able to maintain the phenotype of cells for the formation of desired tissue.

### 2.4.1. Cell types

Cell therapy requires cells that are easy to harvest, isolate and feasible to scale-up to provide a sufficiently large number in a rapid and cost effective manner to expedite tissue healing. For research purposes, animal cells and commercially available cells (e.g. 3T3 fibroblast cells, MC3T3 osteoblast precursor cells) are normally used to validate and improve processing as they are easy to obtain, well-established cell-lines and are reproducible (Griffith 2002). The

outcome between different cells from different species varies due to their metabolic activity and phenotypic stability. It might even vary within a species with different ages, biopsy locations and the health of the donor (Giannoni et al. 2005).

Cell sources for therapeutic applications can be divided into two categories including differentiated cells which can be isolated from the tissue of interest, and/or stem cells from stromal tissues which have this ability to differentiate into various types of cells such as osteoblast, chondrocytes, adipocytes and myoblasts under certain development pathway and also have self- renewal potential (Cancedda et al. 2003). Differentiated cells are preferred as a logical choice in tissue engineering applications as they can build and maintain the tissue of interest *in vivo*, however, their use is limited due to their low proliferation capacity, limited supply of donor tissue, and instability of their phenotype after expansion (Benya 1982; Cancedda et al. 2003). Chondrocytes, for example, lose their phenotype after prolonged expansion in cell culture (Cetinkaya et al. 2011).

The use of undifferentiated (stem/progenitor) cells is favourable due to their higher proliferation capacity compared to differentiated cells for the *in vitro* production of engineered tissue. They can be expanded *in vitro* and their differentiation can be induced by changing culture conditions. Stem cells, such as human mesenchymal (MSCs) have considerable potential for expediting the repair of a diversity of connective tissues (cartilage, bone, and ligament/tendon) (Chen et al. 2013).

#### 2.4.1.1. Mesenchymal stem cells (MSCs)

The potential of Mesenchymal Stromal Progenitor/Stem Cells (MSCs) was discovered by Alexander Friedenstein in the 1960s and now is a key to the development for biological cell-based therapy in tissue repair approaches (A. Caplan and Bruder 2001; Delorme et al. 2006).

MSCs are present in bone marrow aspirates, skeletal muscle connective tissue, human trabecular bone, adipose tissue, periosteum, foetal blood, liver, and umbilical cord blood (Chen et al. 2013; Mackay et al. 1998; Rodrigues et al. 2011). Due to their ability to differentiate into the skeletal connective tissue: osteoblasts, chondrocytes, adipocytes, myoblasts and vascular lineages, they are attracting considerable interest as the source of progenitor cells for research and clinical purposes in the tissue regeneration field (Augello et al. 2010; Cancedda et al. 2003; Caplan 2007; Chen et al. 2013; Deans and Moseley 2000). Clinical trials and applications of MSCs cells in the field of bone and cartilage tissue engineering have been extensively increased. The treatment of Osteogenesis Imperfecta (OI), a bone disease, by MSCs cells went through late stage trial and the promising results showed their potential for bone regeneration (Horwitz et al. 1999). The potential of MSC cells was also shown for the treatment of osteoarthritis with autologous bone marrow derived MSCs injection into the patient's articular cartilage defect. Furthermore results from phase III clinical study of articular cartilage regeneration conducted for the treatment of large defects in the knee joints of elderly patients have shown the safety and feasibility of umbilical cord blood-derived MSCs for this cell therapy (Wakitani et al. 2002) .

The required numbers of MSCs vary depending on the type of treatment, for example, the estimated cell dose needed for cartilage tissue regeneration per patient is between 15 to 45 million (Wakitani et al. 2002) and for treatment of non-union bone defect, estimated cell number needed per patient is between 40 to 100 million. One major drawback of MSCs are their low cell source quantity (Boo et al. 2011). MSCs are typically grown on plastic tissue culture dishes as monolayers with no additional coating. The current two-dimensional tissue culture platform can be used when low cell doses are needed but it becomes impractical when doses above 50 million are needed. There are still significant challenges to be overcome in

this area to make the therapies clinically feasible. The three main key challenges are: rapid scale-up of MSCs to a number that is feasible for clinical application, controlling the plastic nature of the cell ensuring that a population of MSCs differentiates along the desired lineage and preserving MSC phenotype following repeated trypsinisations (Boo et al. 2011). For this reason, a new strategy of culturing of cells with the ability of amplifying the MSCs cell number as well as maintaining their characteristic and delivery of the proliferated cells to the defect site would be needed to address all the aforementioned challenges for successful stem cell-based therapies.

### 2.4.2. Delivery strategy

Strategies to repair bone and cartilage mainly involves the *ex-vivo* culturing and expansion of osteoprogenitor, chondrogenitors or stem cells within the 3-dimensional (3D) scaffolds and then implantation of cell-attached construct into the area of damage. Most developed 3D scaffolds as a carrier to support and deliver cells into defect site in tissue engineering have been fabricated into fibrous meshes, blocks, foams, films, rods, and porous sponges (Brahatheeswaran et al. 2011; Jin et al. 2012). The main disadvantages associated with most of these formulations and scaffold design are their inability to be loaded with bioactive molecules and therapeutics for when drug delivery is required, and the incorporation of these forms of fabricated carriers may be limited due to defect geometry leading to incomplete bone–implant contact and thus to poor osteointegration (Theiss et al. 2005). Also they are impractical for provision of sufficient numbers of cells of desired phenotypes for cell delivery. These disadvantages have limited their use as a delivery system in cell therapy.

An ideal delivery system should be able to successfully deliver cells and or bioactive molecules and therapeutics to a damaged or lost tissue while simultaneously providing a

microenvironment with appropriate material architecture, and stiffness for the cells to which the cells are initially exposed together with the ability to maintain the cell phenotype following implantation (Amini et al. 2012). Furthermore, superior formulations with the ability to fill different shaped cavities efficiently and the capacity to be injectable directly into defective site are other aspects that need to be considered in material selection and design (Habraken et al. 2007). FFSu et al. (2011) fabricated microcarriers with a novel open and hollow shell-like structure which allow the cells to attach and proliferate on both, outer and inner surface of the microcarriers enabling better cell delivery efficiencies (Su et al. 2011). Jin et al. also produced hollow, but empty CaP microspheres as cell carrier for MSCs. The implantation of pre-cultured hollowCaP microspheres-MSCs cell complex in a 6mm-diameter rat calvarial defect for 12 weeks showed a significant improvement in new bone tissue formation (Jin et al. 2012).

## 2.5. Microcarrier technologies

The use of microcarriers was introduced by Van Wezel for the production of viral vaccines and biological cell products in 1967 (Jos Malda and Frondoza 2006; Velden-deGroot 1995; Wang et al. 2008). Since then, the use of microcarriers has gained extensive attention in other fields of medicine. In the pharmaceutical industry, microcarriers with a controlled release profile and defined particle size have an important role for effective drug release in the treatment of various diseases such as treatment of cancer and immune system diseases (M. Oliveira and Mano 2011). In the field of tissue engineering and regenerative medicine, microcarriers have also been adopted as culture systems for cell expansion and differentiation of various tissues like bone (Howard et al. 1983; Qiu et al. 2000), cartilage (Cetinkaya et al. 2011; J. Malda et al. 2003a), skin (Voigt et al. 1999), liver (Davis and Vacanti 1996) and blood vessels (X. T. Sun et al. 2004).

Microcarrier-based cultivation systems in cell therapy can be used as a scalable solution for cell expansion of anchorage- dependent cells and also as a carrier for delivery of cells and/or bioactive molecules. They have also been shown to influence cell behaviour at the diseased bone or cartilage site, eliminating the need for re-seeding the retrieved cells into a delivery system as illustrated in Figure 2.4. (Jos Malda and Frondoza 2006; Jeong-Hui Park et al. 2013a; Jung-Hui Park et al. 2013b). This culture technique offers advantages including: higher surface area for attachment and growth of anchorage-dependent cells in a small volume, enhancement of cell phenotype, maintenance of homogeneous environmental conditions throughout the culture, the ability to monitor and control of various parameters like pH, $CO_2$, levels of nutrient components and agitation of cell suspension in a spinner flask, and/ or rotating chamber system (Jos Malda and Frondoza 2006). The use of microcarriers in comparison with other 3D-structured materials, such as porous sponges or fibrous meshes, can provide greater flexibility for filling different-shaped cavities with closer packing and also minimal invasive handling in surgery in repairing the tissue defect by minimizing the scar formation (Jin et al. 2012).

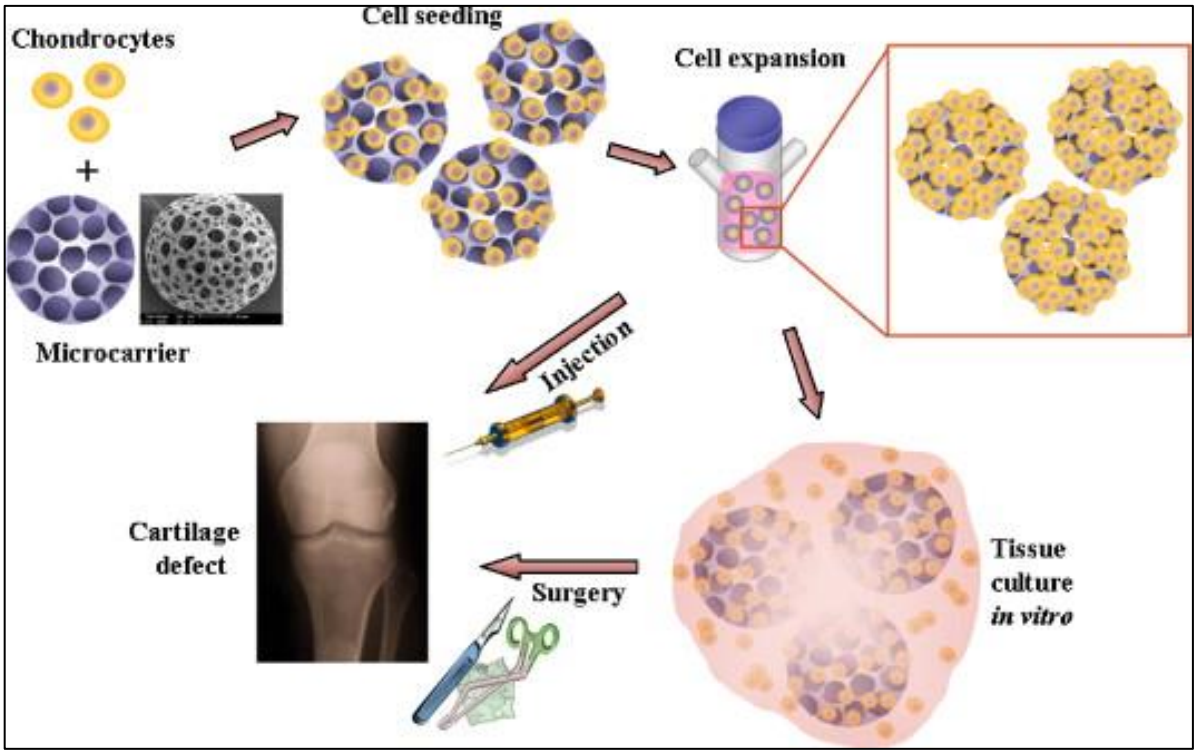


**Figure 2.4. A schematic diagram showing the process for the application of injectable scaffold microspheres for cartilage tissue engineering (Chung et al. 2007).**

The chemical composition, surface topography, degree of porosity and charge density of the microcarriers are key factors that need to be considered during their design as they have a direct effect on the initial cell attachment, growth of the cells and regulating cell fate in therapeutic cell delivery (Jin et al. 2012). The size distribution, density, and their ability to withstand sterilization without compromising structural integrity are other factors which are also important in the design of the microcarriers. In particular recently, in the repair of cartilage and bone, a large number of studies have been conducted on new approaches for development of novel microcarriers in order to improve the delivery efficiency (Malda and Frondoza 2006). The most commonly used and commercially available microcarriers are the dextran-based (Cytodex 1 and Cytodex 2), collagen-coated (Cytodex 3) and gelatine

(Cultispher) microcarriers. These types of commercial microcarriers have been extensively investigated for research purposes and/ or clinical trial for the production of high numbers and a wide range of cell types including foetal chondrocytes, MSCs, and osteoblasts (Baker and Goodwin 1997; Cetinkaya et al. 2011; Freed et al. 1993; J. Malda et al. 2003b; Sautier et al. 1992).

The use of these commercially available microcarriers for bone and cartilage repair, however, might be limited due to some issues such as their problematic ability for delivery of bioactive agents in a controlled manner, their slow degradation, lack of osteoconductivity, limitations in modifying their mechanical properties, and the requirement for cell retrieval from their surfaces by enzymatic methods which compromise cell viability. For this reason, there is still much research in this area for development of the novel microcarriers from other materials to address the aforementioned drawbacks (M. Oliveira and Mano 2011). To address the issue of the traditional enzymatic methods for cell recovery from microcarriers, Cetinkaya et al. (2011) used thermosensitive Poly(N-isopropylacrylamide, NIPAAm) (PNIPAAm), which is FDA approved, to produce microcarriers, and the results have demonstrated that the use of PNIPAAm containing microcarriers overcome the use of toxic enzymes for cell retrieving which was an issue when Biosilon and Cytodex-1 microcarriers were used for cell expansion (Cetinkaya et al. 2011; Ratner and Bryant 2004; J. Sun and Tan 2013). The cells were detached by cold induction. The non-degradable nature of these biomaterials, however, limited their use as implantable materials (M. Oliveira and Mano 2011).

Calcium phosphate based materials, biodegradable polymers, and their composites which have been extensively used in clinical application for bone and cartilage tissue engineering are

promising candidates for production of microcarriers, thus a number of workers recently have attempted to develop microcarriers from these materials either in individual form or in composite form that can make bone and cartilage tissue regeneration clinically feasible. Table 2.2 lists some of the recent developed microcarriers in bone and cartilage tissue engineering research.

**Table 2.2: Examples of microcarriers used as cultivation systems in recent bone and cartilage tissue engineering research.**

| **Microcarriers** | Application | Size (µm) | *In vitro/ in vivo* | References |
|---|---|---|---|---|
| Dextran based-Cytodex & (PHEMAPNIPAAm) Beads | MSC expansion for tissue engineering | ~ 800 | *In vitro* | Boo et al. 2011 |
| Gealtin-based beads | Chondrocytes expansion | ~100-200 | *In vitro* | Glattauer et al. 2010 |
| Bioactive ceramic | Bone regeneration | ~1000 | *In vivo* | Jin et al. 2012 |
| Gelatine-grafted gellan | For musculoskeletal or dermatological fields | 450-600 | *In vitro* | Wang et al. 2008 |
| PLGA | Cartilage regeneration | 60-80 | *In vitro* and *in vivo* | Bouffi et al. 2010 |
| CPC-alginate composite | Bone regeneration | 150-250 | *In vitro* | Jung-Hui Park et al. 2013b |
| Hydroxyapatite | Injectable formulation for bone tissue engineering | 212–300 500–706 | *In vivo* | Fischer et al. 2003 |
| CaP(HA-TCP) | Evacuated morphology for bone tissue regeneration | 200-500 | *In vivo* | Park et al. 2010 |

## 2.6. Common biomaterials used as cell carriers

Numerous classes of biomaterial are used in tissue engineering as support structures, including metals, ceramics, glasses, polymers and various composites. The choice of suitable biomaterials is a key factor to the successful delivery of cells in cell therapy. This is because it serves to reproduce the three dimensional structure of the extracellular matrix and provide signals to the cells that direct new tissue formation. ECM has an important role in the process of cell attachment. Cell attachment on a conventional biomaterial occurs through interaction between ECM components including fibronectin, collagen, laminin, and vitronectin with specific cell surface receptors known as integrins (Bačáková et al. 2004; Hynes 1992). The first binding site for many integrins to be defined is amino acid sequence Arg-Gly-Asp commonly known as RGD which present in firbronectin, vitronectin and in a variety of other adhesion proteins on ECM (Lotfi et al. 2013). In the design of cell-adhesive materials, therefore some specific surface modifications such as the incorporation of RGD peptides or/and immobilization of collagen/gelatin moieties might be required to obtain specific cell surface interaction. The development of tissue engineering is directly dependent on advances in material technology (Burg et al. 2000).

Biomaterials for bone and cartilage repair must be bioactive, osteoconductive (allows the bone cells to adhere, proliferate and form ECM on its surface and pores), osteoinductive (induce new bone formation through recruiting progenitor cells), and biodegrade during application (Porter *et al.*, 2009; Eisenbarth, 2007). The mechanical properties of the biomaterial; material architecture and stiffness of the matrix in which attached cells reside are also important factors that can have a direct impact on cell fate. Biomaterials of biological or synthetic origin have been used as scaffolds for bone and cartilage tissue engineering.

Biomaterials used in tissue engineering and cell therapy may be divided as follows: natural polymers (e.g. aligante, chitosan, chitin, and gellan gum), synthetic polymers (e.g. poly (caprolactone) and poly (lactic-coglycolide), and calcium phosphate- based biomaterials (e.g. hydroxyapatite, β-TCP, and brushite) (Dawson *et al*., 2008) and composites of these. The importance of these materials along with their major advantages and disadvantages are described in the following sections.

### 2.6.1. Calcium phosphate-based biomaterials

The use of calcium phosphate-based materials dates as far as 1920 when it was reported for the first time by Albee and Morison (Bohner 2000; LeGeros 2008). These materials have important advantages of having bone-mineral-like properties, osteoconductivity, biodegradability and the ability to bind directly to bone with no fibrous tissue growth (Qinghong et al. 2007; Solaiman et al. 2013; Tadic and Epple 2004). The degradation products of these materials are non- toxic and they are easily cleared from the body (Kasten et al. 2008) .

There are currently many compositions of calcium phosphate ceramic available on the market. Hydroxyapatite (HA), α- and β-tricalcium phosphate, octacalcium phosphate (OCP), and dicalcium phosphate in the form of ceramics, cements, and thin coatings are examples of calcium phosphate phases that have been used clinically (Habibovic et al. 2008; Langstaff et al. 1999; F. Tamimi Mariño et al. 2007a). These materials have been widely used either as direct bone replacements, thin- coating on metal implants, or as a carriers for implanted bone cells with containing osteoinductive growth factors. Calcium phosphate compounds can be classified as two different categories: 1) calcium phosphates that are obtained by precipitation from an aqueous solution at room temperature, which are also called low temperature calcium

phosphate and 2) those calcium phosphate compounds that are obtained through thermal reactions, which are called high temperature calcium phosphates. All calcium phosphate cements (i.e. brushite) belong to the first category and most other CaP compounds (i.e HA and β-TCP) are categorized in the second group.

#### 2.6.1.1. Calcium phosphate cement

The first hydraulic calcium phosphate cement was discovered by Brown and Chow in the mid 1980's (Brown and Chow 1990; Theiss et al. 2005). Calcium phosphate cement (CPC) can be described as a powder or a mixture of powders that upon mixing with water or an aqueous solution turn into a pasty, mouldable compound that hardens to a firm mass with time at room temperature. CPCs have been widely investigated as materials for hard tissue replacement and have found numerous clinical applications in the last three decades. CPCs, have several advantages over calcium phosphate ceramics that are processed at high temperature. Most importantly processing at room temperature allows the incorporation of bioactive molecules and therapeutics ( Park et al. 2013b).

CPCs typically harden following a dissolution–precipitation reaction which is dependent upon the solubility of the cement reactants. Equilibrium conditions favour the formation of HA above pH 4.2, whereas below pH 4.2, the reaction product is dicalcium phosphate dihydrate ($CaHPO_4.2H_2O$; DCPD; brushite) (Apelt et al. 2004); Barralet et al., 2004; Xia et al., 2006). Brushite cements (BCs) have recently attracted much interest as implantable scaffolds since they are more soluble than HA at physiological pH, and so may be resorbed and replaced by bone more rapidly following implantation (Barralet et al., 2004; Marino et al., 2007b).

Brushite ($CaHPO_4.2H_2O$; dicalcium phosphate dihydrate) cement was first reported in 1987 by Lemaitre et al (1987). As a mineral, it is found in biological systems such as bone, kidney stones and dental calculi (Bohner 2000). It exhibits a relatively high solubility (log $K_{SP}$=6.6) in physiological conditions (Selen and Tas 2010; Tas and Brown 2011). As a consequence, brushite cements recently have been developed and studied as implantable scaffolds in *in vitro* and *in vivo* studies (Uwe Klammert et al. 2010; Penel et al. 1999). Brushite cements (BC) are obtained following a dissolution-precipitation reaction at a pH value lower than 4.2 from either mixing the β-TCP powder and orthophosphoric acid ($H_3PO_4$), or β-TCP and monocalcium phosphate monohydrate (MCPM; $CaH_2PO_4.H_2O$) (Ginebra et al. 2012; Grover et al. 2003). It can be also produced by a mixture of TTCP, MCPM and CaO (Bohner 2000). In the absence of setting inhibitors, the rapid crystallisation of brushite in acidic conditions means that the material can flash-set. This makes it unusable and significantly diminishes the mechanical properties it exhibits. The setting time of brushite cement is strongly influenced by the dynamic solubility of the basic phase and acid concentration. A smaller particle size and the presence of trace quantities of CaO can significantly accelerate setting (Bohner 2000). In order to make brushite cement formulations more suitable as implantable scaffolds and/or injectable cements, significant improvements in setting, mechanical, and handling properties of brushite cement were achieved by using crystallization retardants, such as sodium pyrophosphate (SP) and citric acid (CA) (Barralet et al. 2004; Gbureck et al. 2004). The structure of brushite was illustrated in figure 2.5 including sheets with a composition of $CaHPO_4$ linked together by water molecules.

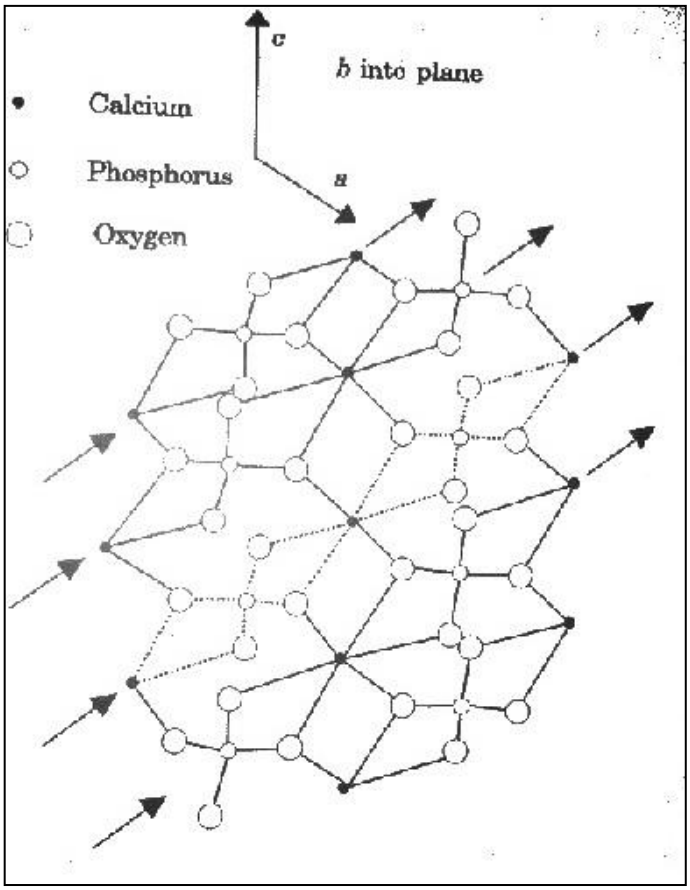


**Figure 2.5: Molecular Structure of brushite illustrating sheets of composition $CaHPO_4$ linked together by water molecules (Elliot J.C., 1994).**

Brushite is known to transform to HA in physiological conditions (pH>7), into dicalcium phosphate (DCP) at (pH<6) and into OCP at pH=6-7 (Bohner 2000). The conversion of large amounts of brushite into precipitated hydroxyapatite after implantation *in vivo* has been reported to reduce the resorption rate of DCPD and also cause an inflammatory reaction due to the release of large amounts of acid from the cement paste (Flautre et al. 1999; F. Tamimi Mariño et al. 2007a). Several studies have prevented this by adding magnesium ions to the cement paste as an inhibitor of apatite crystal growth (Bohner et al. 2003; Theiss et al. 2005). The addition of pyrophosphate ions to brushite cement was also shown to prevent HA formation within the hardened material. Grover et al. (2006) reported that brushite cement

containing a pyrophosphate phase resisted hydrolysis to form hydroxyapatite over 90 days of ageing *in vitro* (Grover et al. 2006).

### 2.6.1.2. Calcium phosphate ceramics

Non-setting calcium phosphate ceramics such as HA have been used widely as implant coating materials for orthopaedic and dental applications due to their compositional similarity with the mineral phase of bone and teeth (Predoi et al. 2008). They have been used in the augmentation of hips, knees, teeth, the stabilization of the jawbone and in spinal fusion (Kalita et al. 2007). This section introduces several important calcium phosphate ceramics that are of interest to the work in this thesis.

#### Nanocrystallie hydroxyapatite (nHA)

Nano-size hydroxyapatite (HA) have been the focus of interest in the area of hard tissue regeneration as it is considered that it exhibits superior biological and mechanical properties and stronger affinity with the mineral component of human bones and teeth than microcrystalline HA (Sprio et al. 2008). It has a structural and chemical composition similar to bone mineral (Pang and Bao 2003). Furthermore, it has been shown that it is osteoconductive and bioactive and can bond well with hard and soft tissues. Its major clinical applications include: surface coating for orthopaedic and dental metal implants, and the fabrication of sponges and granules for the augmentation and regeneration of bone (Lazić et al. 2001). HA ceramic coating of metal implants induces bone formation at the implant surface (osseointegration) and also reduces release of metal ions since its tight association with the bone creates a physical barrier. Since it is highly adsorbent, it has also been used extensively as a drug delivery system agent for the local release of growth hormones, antibiotics, and

antimicrobials molecules to the osseous defect sites in expedite healing or suppress the inflammation process (Zakharov et al. 2004). Furthermore, considerable recent research has focused on the use of these inorganic particles as a filler to adjust the mechanical properties of the structures intended for bone tissue engineering (Lin and Yeh 2004). The use of HA on its own is limited, however, owing to its brittleness and low strength (Kim et al. 2004) and its difficulty in handling and maintaining in the defect sites. As a consequence many studies have recently been conducted on the design of HA composites with polymers to enhance physical properties while maintaining osteoconduction (Rungsiyanont et al. 2011; Swetha et al. 2010). Another disadvantage of HA in comparison with other calcium phosphate compounds (e.g. brushite and octacalcium phosphate) is its slow rate bioresorption *in vivo*. To address this problem Sprio et al (2007) investigated the simultaneous substitution of carbonate, magnesium and silicon into the HA lattice. It was demonstrated that the decrease of crystallinity associated with substitution increased the solubility of the HA in physiological conditions.

There are various techniques of HA powder preparation including chemical precipitation from aqueous solutions, sol-gel procedures, hydrothermal synthesis, electrochemical deposition and emulsion and micro-emulsion routes (Pang and Bao 2003; Salimi et al. 2012). The morphology, crystallinity, and particle size of the synthesized HA are dependent on the route of preparation and these properties will have a direct influence on the effectiveness of the powder on its application. (Pang and Bao 2003). For example Wang et al. (1998) have proposed that the smaller particle size of synthesized HA significantly increased the mechanical properties of the composite compared to that of a powder composed of comparatively large particles. It was also reported that HA scaffolds fabricated with

nanocrystalline-HA enabled more rapid osteoblast growth, and presumably more rapid calcification and bone formation *in vitro* in comparison with the scaffolds prepared with mirco-sized HA crystals ( Smith et al. 2006).

### 2.6.2. Polymeric carriers

Polymeric materials have been used widely in diverse applications as drug delivery systems, orthopaedic fixation devices such as pins, rods and screws, hip joint replacements and bone replacement materials (Nair and Laurencin 2006) . They have great design flexibility as their composition and structure can be tailored to suit various applications (Liu and Ma 2004; Swetha et al. 2010).

The biodegradability of polymers can be adjusted through molecular design; some polymers can degrade by cellular and enzymatic pathways and some, due to their chemical bonds can undergo hydrolysis upon exposure to the body's aqueous environment. Polymers can be fabricated into different shapes with desired porosity contributing to tissue in-growth. Their surface chemistry can be designed by introducing various chemical functional groups to induce tissue formation (Gunatillake and Adhikari 2003). Polymeric materials can be mixed with other polymers or inorganic materials in order to modify and improve their application as composite materials from both mechanical and biological point of views for bone and cartilage tissue engineering. They may be categorized into natural polymers like alginate, gellan gum, collagen, gelatin, chitosan and synthetic polymeric materials like poly(caprolactone), poly(ethylene glycol), poly(vinyl alcohol), and poly(lactic-co-glycolic acid) (Madhumathi et al. 2009).

### 2.6.2.1. Natural polymers

The application of natural polymers as biomaterials dates back thousands of years ago and they are considered among the first biodegradable biomaterials used clinically (Brahatheeswaran et al. 2011; Nair and Laurencin 2006). Natural polymers are used widely in the pharmaceutical and medical industries due to their low cost and biodegradability. They can be categorized as: polysaccharides (starch, alginate, chitin/chitosan, and hyaluronic acid); protein derivatives (soy, collagen, fibrin, and silk) or a variety of biofibres, such as lignocellulose (Swetha et al. 2010). Carriers may be formed from hydrophilic naturally derived polymers in water-based solutions, which allows the polymer network to swell forming a hydrogel. Certain proteinaceous polymers contain extracellular matrix features that may promote better interaction with cells and enhanced their ability to guide migration and growth during tissue regeneration (Malafaya et al. 2007). Due to their biological origin, however, they may contain pathogenic impurities and elicit an immune response. Their weak mechanical properties and uncontrollable degradability has also limited their application as an individual component in bone and cartilage tissue engineering.

### Hydrogels from natural polymers

Hydrogels are physically or chemically cross-linked hydrophilic polymer networks that may be bonded through covalent or non-covalent interactions (cohesion forces such as ionic bond, hydrogen bond and van der Waals forces). The polymeric networks are able to absorb large volumes of water (Drury and Mooney 2003a; Lee and Mooney 2001).

Naturally derived hydrogel forming polymers such as alginate, chitosan, collagen, gelatine, and hyaluronic acid are of great interest for tissue regeneration and cell delivery, due to their tissue-like properties, namely high water content, cytocompatibility and a structure thought to be akin to the ECM. Currently they are being used to deliver cells and bioactive molecules and to engineer various types of tissues like cartilage, bone, liver and muscles (Drury and Mooney 2003a).

Hydrogels have been used widely as cell carriers for cartilage engineering *in vitro* and *in vivo* because they have a similar structure to cartilage. Cartilage is formed from a matrix containing high levels of type II collagen which maintains its physical structure through the absorbtion of high volumes of water. Within the ECM of the cartilage are embedded a population of cells called chondrocytes that do not readily proliferate. Numerous researchers have therefore embedded chondrocytes within hydrogel matrices (Di Martino et al. 2005; Suh and Matthew 2000). For example, Oliveira et al have demonstrated that the encapsulated chondrocytes within gellan gum hydrogel remained viable and produced the hyaline-like ECM *in vitro* and the primary *in vivo* results demonstrated the ability of this natural hydrogel as an injectable system for cartilage augmentation (Oliveira et al. 2010b). Chitosan-based materials have also been shown to be potentially beneficial to wound healing articular cartilage of rats enabling localisation and subsequent proliferation at the site of application (Xi Lu et al. 1999).

Composites of hydrogel and ceramics have also been the focus of interest as they provide an enhanced structure both from mechanical and biological point for tissue engineering of cartilage when compared to the individual materials alone. The following section expands

upon the chemical and physical properties of the hydrogel material used for the fabrication of the culture beads investigated in this thesis.

## Gellan gum

Gellan gum (GG) is a natural polysaccharide manufactured by microbial fermentation of the *Sphingomonas paucimobilis* bacterium (Dai et al. 2008). It forms a strong gel (an elastic gel or a true gel) not a weak gel in the presence of cations in aqueous conditions. GG is formed of a combination of four sugars with a tetrasaccharide repeating unit of α-L-rhamnose, one β-D-glucuronic acid and two β-D-glucose residues as illustrated in figure 2.5.

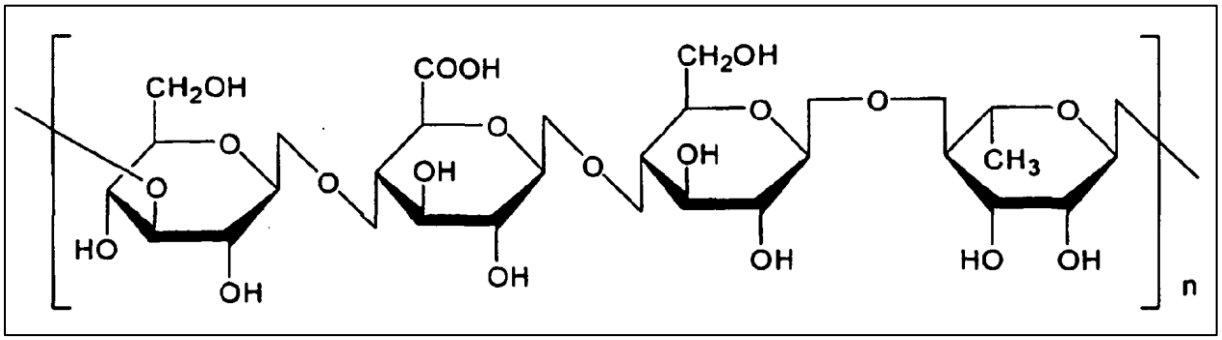


**Figure 2.6: A diagram representing the chemical structure of Low Acyl Gellan gum (Mao et al. 2006)**

The sugar chains subsequent self-organise through the formation of three-fold double helices. The helices then aggregate to form a three-dimensional network upon lowering the temperature under mild conditions (Evageliou et al. 2010; J. Oliveira et al. 2010b). The presence of calcium ions within this matrix enhances aggregation and so enhances mechanical properties. Endotoxin-free GG has been used for drug delivery, for cell immobilisation and as a substrate in tissue engineering (Silva-Correia et al. 2011; A. M. Smith et al. 2007). Although it has been less widely used as other hydrogels such as alginate, it has a number of significant advantages. For example, its gelation occurs in an order of magnitude less calcium

that alginate and so gelation may occur in culture medium or body fluids. It is also substantially more robust than alginate and does not readily disintegrate on immersion in sodium containing solutions (Hunt and Grover 2010; Jahromi et al. 2011). GG, however, does not readily facilitate cell attachment. The lack of cellular affinity is due to its extremely hydrophilic nature, particularly on the outer surfaces which prevents the adsorption of ECM proteins, which are required for cell adhesion (Wang et al. 2008). Several effective strategies have been employed to improve the cellular affinity of this hydrogel such as the incorporation of RGD peptides (which directly mediate attachment), immobilization of collagen/gelatin moieties and protein cross-linking, which has been shown to be successful (T. Chen et al. 2003; Hern and Hubbell 1998). Wang et al have shown that a covalent coating of gelatine on gellan gum microspheres enhanced cell adhesion on the gel surface (Wang et al. 2008). Their investigation demonstrated the potential of these modified microspheres as an injectable vehicle for cell delivery in musculoskeletal or dermatological regenerative medicine. The low mechanical properties of GG (when compared with ceramics or metals) can also be problematic for their further application as templates for tissue regeneration (Coutinho et al. 2010). The mechanical properties of GG can be improved by combining physical (temperature and the presence of cations) and chemical cross-linking mechanisms (chemical modification and UV exposure). One study by Countinho et al investigated the synthesis of a new class of GG by the incorporation of a methacrylate group onto the GG chain in the presence of cations prior to photocrosslinking. It has been shown that their method enabled the development of MeGG hydrogels with highly tunable physical and mechanical properties without affecting their biocompatibility. Another way to adjust the mechanical properties of a hydrogel including GG is to reinforce the structure using inorganic particles such as HA,

which has been shown to be effective in enhancing both mechanical properties and cell attachment (Lin and Yeh 2004).

## 2.7. Composite-based materials for cell delivery in microcarrier design

In order to overcome the properties associated with hydrogel-based materials, research has been undertaken to develop composite materials that exhibit tuneable mechanical properties and, despite consisting largely of hydrogel, may facilitate strong cell attachment. For example composites of natural polymers and ceramics have been fabricated such that the scaffold structure exhibits a composition and microstructure as close to bone as possible (Lin and Yeh 2004, (Zhao et al. 2002).

The hydrogel materials enable the formation of spherical particles of high uniformity, without the need for heat treatment and the use of the ceramic fillers provides sites for the adsorption of molecules that are able to facilitate the cell adhesion process. In addition, it has been shown that the addition of particles fillers may prevent uncontrollable degradation and loss of structural stability of natural polymers (Jeong-Hui Park et al. 2013a). The most widely investigated compositions have utilised HA as a filler with variety of degradable polymers to which has been shown to mediate cell attachment and optimise mechanical properties and degradation rate (Swetha et al. 2010). Various successful nanocomposite microcarrier system has been reported recently. In one study by Shen et al. (2010) HA/PLGA microspheres were developed as an injectable scaffold for bone tissue repair. The authors showed that the inclusion of HA into PLGA increased the cell adhesion, proliferation and subsequent differentiation (Shen et al. 2010). Kim et al. (2007) also demonstrated that collagen–apatite nanocomposite microspheres with similar structure to natural bone structure encouraged cells

to differentiate down an osteogenic lineage in biological conditions and bone mineralized matrix formation (Kim et al. 2007). Spherical substrates of other composites such as inorganic bioactive glass/PLGA (Yao et al. 2004) and bioactive glass/ poly (lactide-co-caprolactone) (Yu et al. 2009) have also been successfully made and the results indicated that the combination of bioactive inorganic phases with the aforementioned degradable polymers enhanced osteogenic differentiation, matrix production and also accelerated their bonding with host hard tissue.

## 2.8. Concluding statement

The importance of cell-based therapy enabled through delivery using materials, which can be implanted into the patients' body for regeneration of diseased and damaged tissue has been discussed. One limiting factor of this novel clinical approach is that it is challenging to provide a sufficiently large number of appropriate cells and localise these within the site of implantation. It has been shown that microcarrier-based cultivation systems in cell therapy in the development of implantable material with precisely engineered modulus can be used as a scalable solution for cell expansion of anchorage-dependent cells and also as a carrier for delivery of cells and/or bioactive molecules. Factors important to the design of microcarriers include the microenvironment; material architecture, surface chemistry and stiffness of the material to which the cells are attached, since these have a strong influence on cell behaviour. One relatively un-investigated material type for the manufacture of culture beads is the CPC, which due to their osteoconductivity and the fact that they may be processed in ambient conditions enable the incorporation of temperature sensitive therapeutics during manufacture. As such, this thesis focuses on the development of cell culture beads containing calcium phosphates synthesised in ambient conditions. It reports how formulation has a strong

influence on bead performance and demonstrates that it is possible to generate culture beads of well-defined properties through a systematic approach to formulation. Two final compositions, a polymer (GG) – HA composite and a brushite ceramic were tested in static and dynamic culture (only in the case of GG/HA composites) to demonstrate and compare the efficacy of the two materials.

# Chapter 3

## GENERAL METHODS AND MATERIALS

### 3.1. Cell culture procedures

Two different cell lines were used in this thesis including: the NIH 3T3 murine fibroblast cell line and the MC3T3 cell line purchased from LGC (Middlesex, UK). One source of primary cells was also used to characterise biological response to the final material formulation. Primary rat bone marrow stromal cells (BMSCs) were extracted from Wistar rats following sacrifice. To isolate these cells, recently the femora were dissected from sacrificed adult albino Wistar rats. The soft tissue was cleaned from the femora using a scalpel and then they were placed into a transport medium that contained: Minimum Essential Medium (α-MEM ;), 10% penicillin/streptomycin, 2.5% HEPES, and 1% amphotericin (all from Sigma Aldrich, UK) until required. Subsequently, the epiphyses were removed and the femora were washed using supplemented α-MEM which contained, 10% Foetal Bovine Serum (FBS) (PAA, Somerset, UK), 10% penicillin/streptomycin,, 2.5% HEPES, 1% amphotericin and 10% L-glutamine (Sigma Aldrich, UK). The resulting suspension of cells was centrifuged at 1000 rpm for 3 min to form a cell pellet. The cells were then incubated in a 75mL flask in a humidified atmosphere of 95% air and 5% $CO_2$ at 37ºC.

All cell lines were grown in D-MEM (Dulbecco's Modified Eagle Medium) (Sigma, UK) which was supplemented with 10% FBS (PAA, Somerset, UK) 2.4% L-glutamine, 2.4% HEPES buffer, and 1% penicillin/ streptomycin. All cultures were maintained in sterile

conditions at 37ºC with 5% $CO_2$ and 100% relative humidity and media was changed every two days.

All culture dishes (12 multiwell plates and petri dishes) for cell culture experiments were coated with 1.5 mL of Sylgard (type 184 silicone elastomer; Dow Corning Corporation, Midland, MI) and left to polymerize for at least a week before use to provide a non-cell-adhesive surface underneath the samples. All samples for cell culture were sterilized with ethanol (70%; Fisher Scientific, UK) and then left overnight under ultraviolet light to complete the sterilization process before cell seeding.

### 3.1.1. Cell culture in osteogenic differentiation media

To determine the functional activity of the grown MC3T3 cells and BMSCs on the culture beads for the synthesis of mineralized matrix, the cultures were provided with supplemented DMEM (as specific in section 3.1) containing 50 μg/ml ascorbic acid 2-phosphate (Sigma-Aldrich, UK), 10 nM dexamethasone (Sigma-Aldrich, UK) and 10 mM β-glycerol phosphate (Sigma-Aldrich, UK).

## 3.2. MTT assay for cell attachment and growth

The cell attachment and proliferation of seeded cells on to the surface of the samples was quantified by using an MTT colourimetric assay after culturing for an appropriate time. MTT solution (5mg/ml) was prepared under sterile conditions in phosphate buffer saline (NaCl 138mM; KCl 27mM, phosphate buffered saline: PBS) (Sigma, UK). At each time, MTT solution (500μL) was added into the sample-cells construct in the DMEM. They were then left in incubator at 37°C for 4 h. Mitochondria of viable cells reduce the yellow, water-soluble MTT (3-(4,5-Dimethylthiazol-2-yl)-2,5-diphenyltetrazolium bromide (Sigma, UK) to

water-insoluble blue crystals of formazan, which was dissolved by acidic isopropanol (MTT solvent) after removal ofthe culture medium. The absorbance of this coloured solution was quantified spectrophotometrically by measuring at a wavelength of 620nm using a microplate reader (BIO-TEK, US), which gives an indication of cell number.

## 3.3. DAPI staining

The adherent cells on the culture beads were labelled with 4´,6-diamidino-2-phenylindole (DAPI), a fluorescent dye. DAPI dye can pass through the intact cell membrane of fixed cells and bind strongly to Adenine-Thymine base pairs in DNA. DAPI (Sigma-Aldrich, UK) stock solution was prepared at 1:1000 in PBS. 300µL of DAPI solution was added to the fixed cells for 5 min. Samples were rinsed with PBS several times. Cell-constructs were placed on a coverslip and one drop of anti-fade reagent was added onto the top of the samples. Samples were visualized using confocal laser microscopy (Leica, UK). The excitation maximum for DAPI bound to double stranded DNA is 358 nm, and the emission maximum is 461 nm.

## 3.4. Alkaline phosphatase activity

The alkaline phosphatase activity was assayed according to the method of Lowry et al. (Lowry et al. 1951). Briefly, culture beads were collected from the media at various time intervals**.** The samples were washed with PBS and then suspended in 500µL PBS containing 100 mM glycine, 1 mM MgCl2 and 0.05% Triton X-100 for 10 min. Aliquots of 60 µl were incubated with 300 µl of *p*-nitrophenyl phosphate solution at 37ºC for 45 min. After adding 900 µl of ice cold 250 mM NaOH, the quantity of *p*-nitrophenol liberated was measured by monitoring absorbance at 405 nm using a UV-Vis plate reader.

## 3.5. Alizarin red staining

The ability of the MC3T3 pre-osteoblast cells grown on culture beads to produce mineralised matrix and nodules was examined by Alizarin Red S staining (Sigma-Aldrich, UK) at specific time points. Alizarin Red S, an anthraquinone derivative, forms as alizarin red-S-calcium in the chelation process with calcium existing in the mineralized matrix. This produces a birefringent staining.

At each interval time, the cell-bead complexes were collected and fixed with 3.7% formaldehyde (Sigma-Aldrich, UK) in PBS for 20 min at room temperature and washed with PBS. The complexes were stained in 40mM Alizarin Red S (Sigma Aldrich, UK) pH 4.2, for 5 min, and washed thoroughly five times with distilled water; the red matrix was visualised using light microscopy (Axiolab, Zeiss, Oberkochen, Germany).

## 3.6. Composition characterisation

### 3.6.1. X-ray diffraction (XRD)

X-ray diffraction was conducted to determine the crystal structure of any inorganic phases. XRD provides a measure of the atomic spacing and the structural properties e.g. preferred orientation, phase composition and grain size of crystalline materials. A fine powder of the sample was mounted between two pieces of a magic tape in an X-ray diffractometer (Bruker D8 Advanced, Karlsruhe, Germany) and diffraction data were collected in the 2θ range between 10º and 60º with a step size of 0.028º/2θ. Short scans (30 min) and long scans (3 h) were conducted depending on the signal from the sample. Diffraction patterns were compared with known standards of each compound from the JCPDS database.

### 3.6.2. Raman microspectrometry

Confocal Raman microscopy, a light scattering technique, was also used to identify chemical properties of the samples by identifying the chemical bonds present within the material regardless of crystallinity. The composition of brushite cement samples after aging was evaluated from absorption bands specific to the mineral using Confocal Raman microspectroscopy (Alpha 300R, WITec, Germany) with a helium neon (785 nm) laser with excitation at a power of 3 mW. The overall spectral resolution was 2 $cm^{-1}$. The spectra were obtained in the 200–2000 $cm^{-1}$ range. The ×100 microscope objective used in a confocal configuration give a micrometric spot size. To enable direct comparison between specimens, all spectra are presented with a normalized intensity.

## 3.7. Specific surface area (SSA) measurement

Specific surface area (SSA) was determined using a Nitrogen Adsorption Apparatus (Micromeritics, UK) with a Brunauer- Emmett-Teller (BET) transform to analyse the data. This method was used to measure the SSA of brushite culture beads prepared with different methods and also synthesised HA particles. The SSA of a biomaterial depends on the shape and size of the particle. The result is expressed in unit of area per mass of sample ($m^2/g$).

## 3.8. Microstructural characterization

### 3.8.1. Scanning electron microscopy

To analyze the morphology and microstructure of the non-aged and aged brushite cement in DMEM solution, scanning electron microscopy (SEM) (quanta200, Fei, CZ) equipped with energy dispersive X-ray analysis (EDX) (INCA x-sight, oxford analytical instrument, UK) was utilized on carbon vaporized samples. SEM operates on the same basis as the light microscope but uses a focused beam of high-energy electrons on the surface of the specimens

in a vacuum state instead of light to generate the image. The surface of the sample is bombarded with electrons and the interaction of electrons with the sample results in the release of signals (i.e. secondary electrons, heat, X-ray, visible light and backscattered electrons) which reveal information about the sample including morphology, chemical composition, crystalline structure and orientation of the materials making up the sample. The signals which include generation of secondary electron from the surface of the sample with lower energy are collected to produce SEM images.

The morphology and microstructure of the GG hydrogel and GG/HA nanocomposites samples was also determined using scanning electron microscopy. The samples were mounted onto a stub and etched at -90ºC, to reduce ice-crystal formation and were coated with gold before being viewed at an appropriate accelerating voltage using scanning electron microscopy (Phillips XL30 ESEM FEG, Netherlands).

#### 3.8.1.1. Biological samples

To observe the morphology of the culture beads and the attached cells on to the beads at required time-points, the cell-bead complexes were fixed in 1.5% glutaraldehyde (Sigma-Aldrich, UK) at 4ºC. Cells were then dehydrated through a series of increasing concentrations of ethanol (50, 70, 80, 90, and 100%) for 10 min at each concentration. This process then was continued by immersing in dry ethanol for 10 minutes. After dehydration, the cell-beads were critical-point-dried with $CO_2$, coated with gold and examined under a scanning electron microscope (SEM; quanta200, Fei, CZ).

## 3.9. Transmission electron microscopy (TEM)

Transmission electron microscopy (TEM) (Jeol 1200EX, Japan) was used to investigate the morphology of the nanocrystalline structures. This technique was based on firing a beam of electrons through the specimen of interest in a vacuum state. The sample must be thin enough to allow the electrons to pass through it. For this reason the powders were first dispersed in ethanol and subsequently ultrasonicated before application to a carbon TEM grid.

## 3.10 Statistical analysis

All data were expressed as mean ± standard deviation of the mean. T-tests were used to evaluate the statistical significance of the differences between groups. Differences were judged significant if $p<0.05$.

# Chapter 4

## NOVEL RESORBABLE BRUSHITE-BASED CELL CULTURE BEADS

Culture beads can potentially be used as three-dimensional scaffolds to allow the localization of a cell population to the site for regeneration and for the successful provision of a sufficiently large number of cells for a therapy (Alfred et al. 2011; Glattauer et al. 2010). This type of culture system has distinct advantages over traditional monolayer culture for the mass production of cells, by providing increased surface area and a better approximation of complex biological processes, enabling cells to behave as they would in the body (E. A. Botchwey et al. 2001; Jos Malda and Frondoza 2006; Nam et al. 2007). An ideal material for manufacturing of the culture beads would be formed from a composition that could be implanted and has a rate of resorption that can match the rate of new bone formation (Glattauer et al. 2010; Shi et al. 2009). During the last three decades calcium phosphate (CaP) cements (CPC) have been widely investigated as materials for hard tissue replacement, and have found numerous clinical applications (Penel et al. 1999; Pina et al. 2010). However, there is little mention in the literature of CPCs being used as culture beads, despite their obvious advantages over calcium phosphate ceramics that are processed at high temperature. CPCs, for example, allow the incorporation of temperature sensitive molecules and give the possibility of fabricating materials of complex morphology (F. Tamimi Mariño et al. 2007a).

Brushite cements have gained more attention recently as implantable scaffolds, as they are more soluble than hydroxyapatite at physiological pH, and so may be resorbed and replaced by bone following implantation (Barralet et al. 2004; F. Tamimi Mariño et al. 2007a). Despite

these attributes, very few studies have focused on the use of these materials in the form of culture beads and cell adhesion capacity of them, something that is of great importance if the materials are to be used in cell delivery. Therefore the first part of this chapter, part a, aimed to investigate cellular attachment to the surface of brushite cement (BC) beads systematically in terms of the influence of cement chemistry and the type of setting retardant used in cement production. The following section, part b, presents a comparison of methods for the fabrication of brushite based culture beads and the effect of manufacturing process of three types of BC beads on cellular behaviour and matrix deposition was investigated.

# Chapter 4A: Brushite cement formulation to maximise cell adhesion

The first reported brushite cement formulations were weak, set rapidly and could not be injected through a needle. Consequently, additives were used to tune their properties for specific applications. In the literature, significant improvements in setting, mechanical and handling properties of brushite cement were achieved by using crystallisation retardants, such as sodium pyrophosphate, and citric acid, which also functions to reduce cement viscosity (Barralet et al. 2004; Gbureck et al. 2004; Faleh Tamimi Mariño et al. 2007b; Tamimi et al.). The use of such retardants would be essential to successfully manufacture brushite cement culture beads. Citric acid has been reported to have a potent viscosity reducing effect on brushite cement formulations and increases setting time. There are several studies that have investigated the influence of citric acid on the properties of calcium phosphate cement, in terms of strength improvement of the CPC, the retardation of the HA formation, and feasibility of the design of fully injectable cements (Barralet et al. 2004; Gbureck et al. 2004; Tamimi et al.). There has not yet been, however, any study to investigate the effect of the use of this retardant on the biological properties of the brushite cement in terms of cellular affinity to the surface of these materials. In order to develop implantable brushite-based culture beads, cell growth is required prior to implantation, therefore in this part of this chapter, cellular attachment to the surface of brushite cement beads was investigated systematically in terms of the influence of cement chemistry and the type of setting retardant used in cement production.

## 4.1. Methods and materials

### 4.1.1. Preparation of brushite culture beads using cement casting method (denoted as sample BC)

β-Tricalcium phosphate (β-TCP) was synthesized by heating a mixture of monetite (DCPA; Mallinckrodt Baker, Griesham, Germany) and calcium carbonate (CC; Merck, Darmstadt, Germany) to 1050ºC for 24 h followed by quenching to room temperature in a desiccator. The product consisted of phase pure and highly crystalline β-TCP as verified by X-ray diffraction (XRD). The sintered cake was crushed using a pestle and mortar and passed through a 355 µm sieve. Milling was performed in a planetary ball mill (PM400 Retsch, Germany, diameter: 400 mm). Brushite cements beads (BC) were synthesised by combining β-TCP with 3.5 M orthophosphoric acid (OA) (Fisher Scientific, Leicestershire, UK) containing citric acid (CA) (200 mM, Fisher Scientific, Leicestershire, UK) and/or sodium pyrophosphate (SP) (200 mM, Sigma-Aldrich, Dorset, UK) retardants at a powder to liquid ratio (P/L) of 3 g/ml. The hardening reaction of the brushite cement used in this study occurs in accordance with Equation 1 (L. M. Grover et al. 2003).

$Ca_3(PO_4)_2 + H_3PO_4 + 6H_2O \rightarrow 3CaHPO_4.2H_2O$ (Equation 4.1)

The resulting paste was cast into a mould to form spherical samples ~1000 µm in diameter. The samples were allowed to harden at $37^0$C for 24 h and afterwards the BC beads (Figure 4.1A) were repeatedly washed in PBS (200 mM, Sigma-Aldrich, Dorset, UK) to eliminate unreacted OA. The samples were sterilized with ethanol (70%) (Fisher Scientific, Leicestershire, UK) and then left overnight under ultraviolet light to complete the sterilization process. As a comparison with brushite cement, a brushite compact (BPC), not hardened

through a cementing process was also characetrised. The BPC (supplied by AstraZeneca) disc shaped samples were prepared by compressing brushite powder using a universal testing machine (Zwick, Germany) at a rate of 1mm/min in a 6mm diameter press to a load of 7000N. Samples were then sterilised using the same method as for the BC beads.

### 4.1.2. Cell culture

3T3 fibroblast cells were seeded onto the sterile BC beads and BPC samples separately in 12-multiwell plates at a final density of $6.0 \times 10^4$ cells per well in 2ml DMEM (section 3.1).

#### 4.1.2.1. MTT assay- non-treated BC beads

Preliminary cytocompatibility testing of BC beads after culturing the BC beads for 7 days following manufacture and repeated washing with PBS was analysed using the MTT assay (section 3.2).

#### 4.1.2.2. MTT assay- treated (aged) beads

To investigate the effect of dynamic *in vitro* aging of BC beads in DMEM on phase composition changes and subsequently on the mechanism of cell adhesion over 7 days culturing, the BC beads were aged in serum-free DMEM at 37ºC over a period of 1 week. The DMEM was refreshed every two days. On day 7, the aged BC beads were seeded with 3T3 fibroblast at the same density that was reported for the non-treated samples ($6.0 \times 10^4$ cells per well) and cell attachment was analysed by MTT assay (section 3.2). Tissue culture plastic (TCP) surfaces with identical conditions were used as controls.

#### 4.1.2.3. DAPI staining

The effect of cement chemistry and the influence of setting retardant upon cell attachment, was evaluated by preparation of brushite cement beads using CA and SP as setting retardants

and brushite cement beads with only SP as a retardant. Cells were seeded at a final density of 6.0 $\times 10^4$ cells per well in 2 ml DMEM and allowed to adhere for 4 h at 37±1ºC until biological characterization (section 3.1). After culturing for one day the number of adherent cells on to the both types of BC beads made with using mixture of retardants were labelled with DAPI (section 3.3). Samples were visualised using confocal laser microscopy (Leica, UK). The cell attachments on the substrates were also quantified using the MTT assay.

### 4.1.3. Determining the presence of intermediate phase in the cement

To determine the effect of citric acid as setting retardant in formation of intermediate phase in the cement matrices, the beads made with CA and SP and only with SP were aged in distilled water for 7 days. To find the quantity of mass lost relating to the presence of intermediate phase from the cement samples with time, samples were removed daily from the aging medium, dried in a freeze dryer and then weighed.

### 4.1.4. Composition and microstructural characterization of non- aged and aged brushite cement

Phase composition of the BC beads made with CA and SP setting retardants before and after aging in distilled water were characterized using X-ray diffraction (section 3.7.1). Short scans (30 min) were conducted for BC samples before and after aging in DMEM solution and long scans (3 h) for the BC samples before and after immersion in distilled water.

Energy dispersive X-ray analysis (EDX) was used to determine the Ca/P ratio of the BC beads before and after aging which was calibrated using known calcium phosphate standards.

Confocal Raman microspectroscopy was conducted (section 3.6.2.) to investigate the

relationship between the cell attachment and the crystalline changes of BC beads before and after aging in DMEM solution for 7 days.

To analyze the morphology and microstructure of the non-aged and aged brushite cement in DMEM solution, scanning electron microscopy (SEM) (section 3.8.1) was utilized on carbon vaporized samples.

## 4.2. Results

### 4.2.1. Preliminary Cytocompatibility test on fabricated BC beads (C)

Initially resorbable calcium phosphate cement beads (brushite) were fabricated (Fig. 4.1A) using a cement casting method (section 4.1.1.) and then the cellular response to the beads was investigated using the MTT assay. Preliminary results from cytocompatibility testing of BC beads after culturing the BC beads for 7 days following manufacture and repeated washing with PBS demonstrated that, there was little or no evidence of cell growth in the period between one and five days of culture, (Fig. 4.1B), however on day 6, absorbance increased and a further significant increase ($p<0.05$) was observed on day 7 (Fig. 4.1B). This large increase in absorbance may be correlated with an increase in cell number.

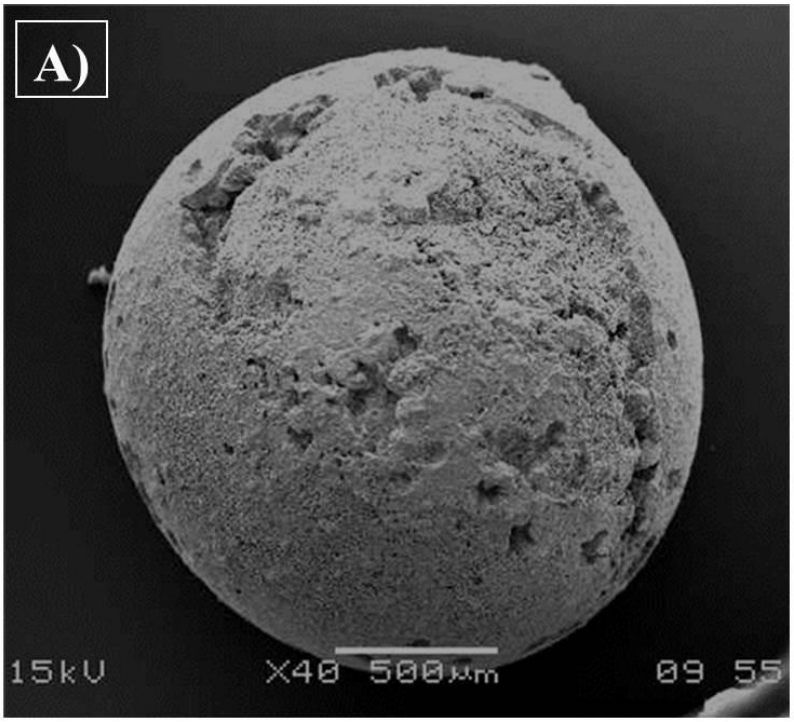


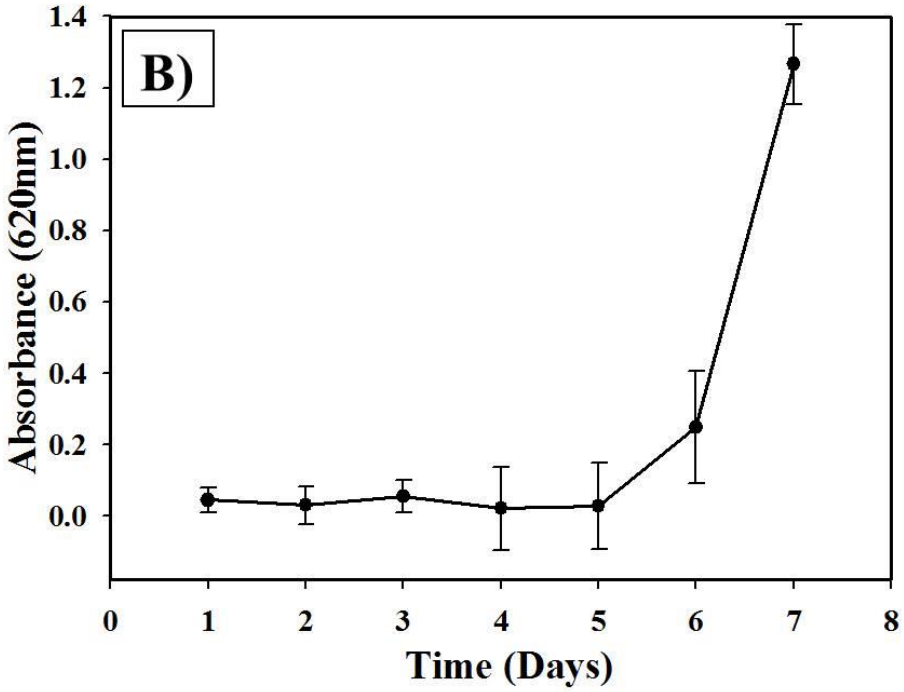


**Figure 4.1: A) SEM micrograph of a BC culture bead, an d B) Results from the MTT assay on 3T3 fibroblasts grown on BC after culturing for 1, 2, 3, 4, 5, 6, and 7 days. Data points represent mean values of n = 9 specimens ± standard deviation.**

To investigate whether this was due to conditioning of the surface with protein or crystalline phase changes within the material in this time, BC samples were aged for 1 week with serum-free DMEM refreshment every 2 days. When the conditioned samples were seeded with cells to the same density under the same culture condition as for non-aged samples, there was considerably more cell attachment after 1 day. Indeed, at this time point, the adhered cell number on the surface of the cement was even higher than on the TCP control (Fig. 4.2).

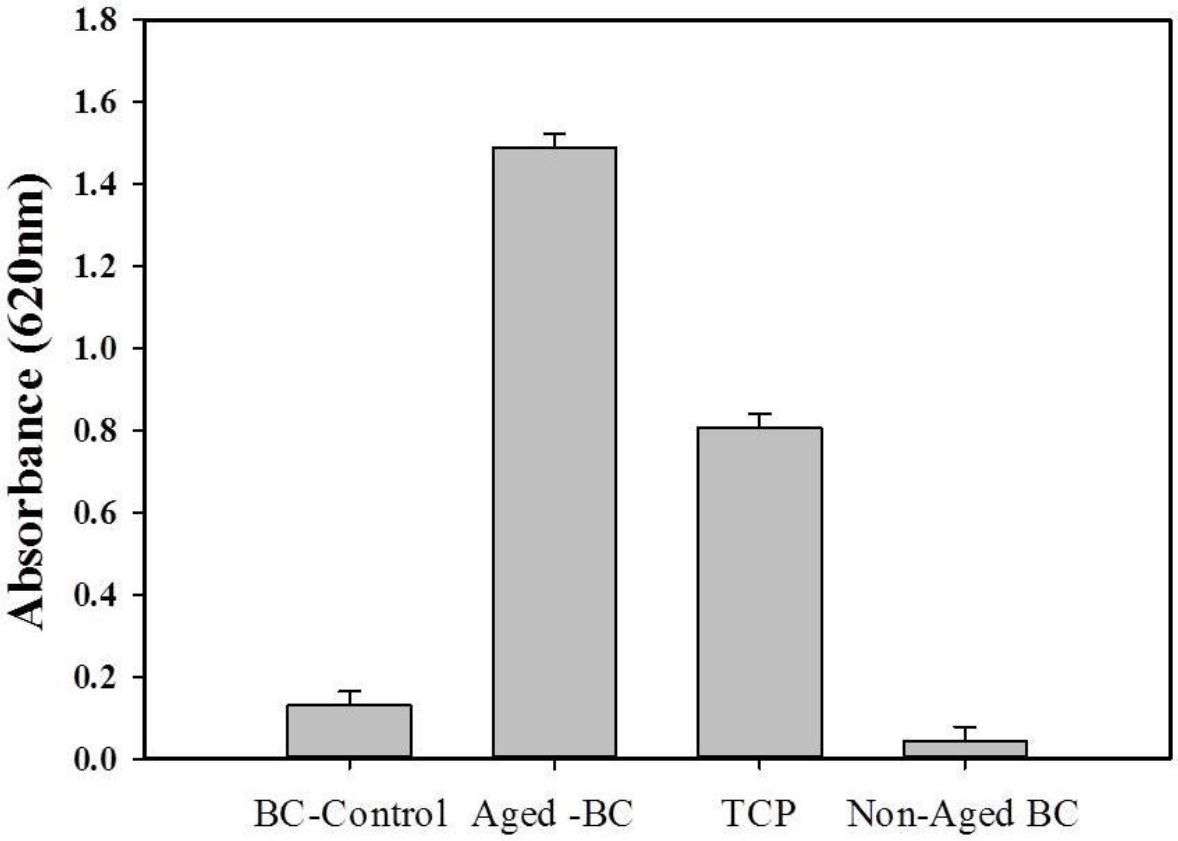


**Figure 4.2: The MTT results of 3T3 fibroblast adhered to aged (7 days) and non-aged BC, after culturing for 1 day. The difference between the two conditions, aged and non-aged BC is significant (*p<0.001). Positive control is tissue culture plastic (TCP). Brushite cement without cell seeding was also used as control sample. Results are displayed as mean of n = 9 specimens ± standard deviation.**

### 4.2.2. Effect of dynamic *in vitro* aging in DMEM on phase composition, morphology and microstructure of BC culture beads

#### 4.2.2.1. SEM and XRD analysis

In order to investigate whether the cell attachment was due to the formation of an apatitic layer on the surface of the cement following immersion in DMEM (as previously reported), the surface of the material was characterised using scanning electron microscopy and X-ray diffraction. Prior to immersion in DMEM, the cement as expected consisted of fully blade/plate-like crystals of ~10 μm in length/diameter (Fig. 4.3A). Following immersion in DMEM, the surface of the material was covered with a finer particulate material, which could have been clusters of octacalcium phosphate (OCP) or Ca-deficient hydroxyapatite (HA) (Fig. 4.3B).

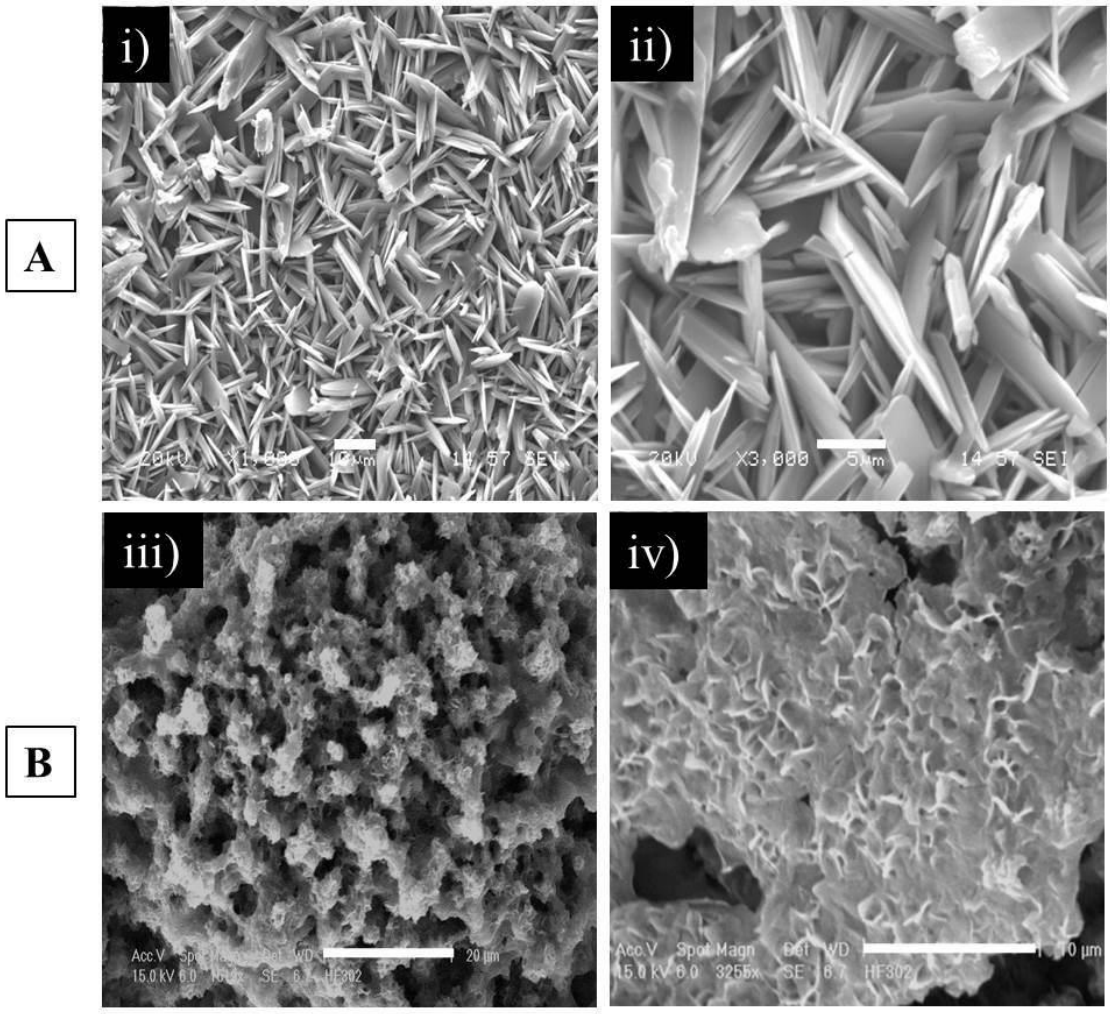


**Figure 4.3: SEM micrographs of A) Non-aged BC beads, B) BC aged in DMEM for 7 days. i) scale bar, 10μm, ii) scale bar 5 μm, iii) scale bar 20 μm and iv) scale bar 10 μm.**

To confirm this, the samples were characterised using X-ray diffraction, which demonstrated the presence of OCP or HA within the cement matrix (Fig. 4.4). OCP is a metastable phase and conversion to HA usually occurs rapidly, consequently the material consisted of both OCP and HA.

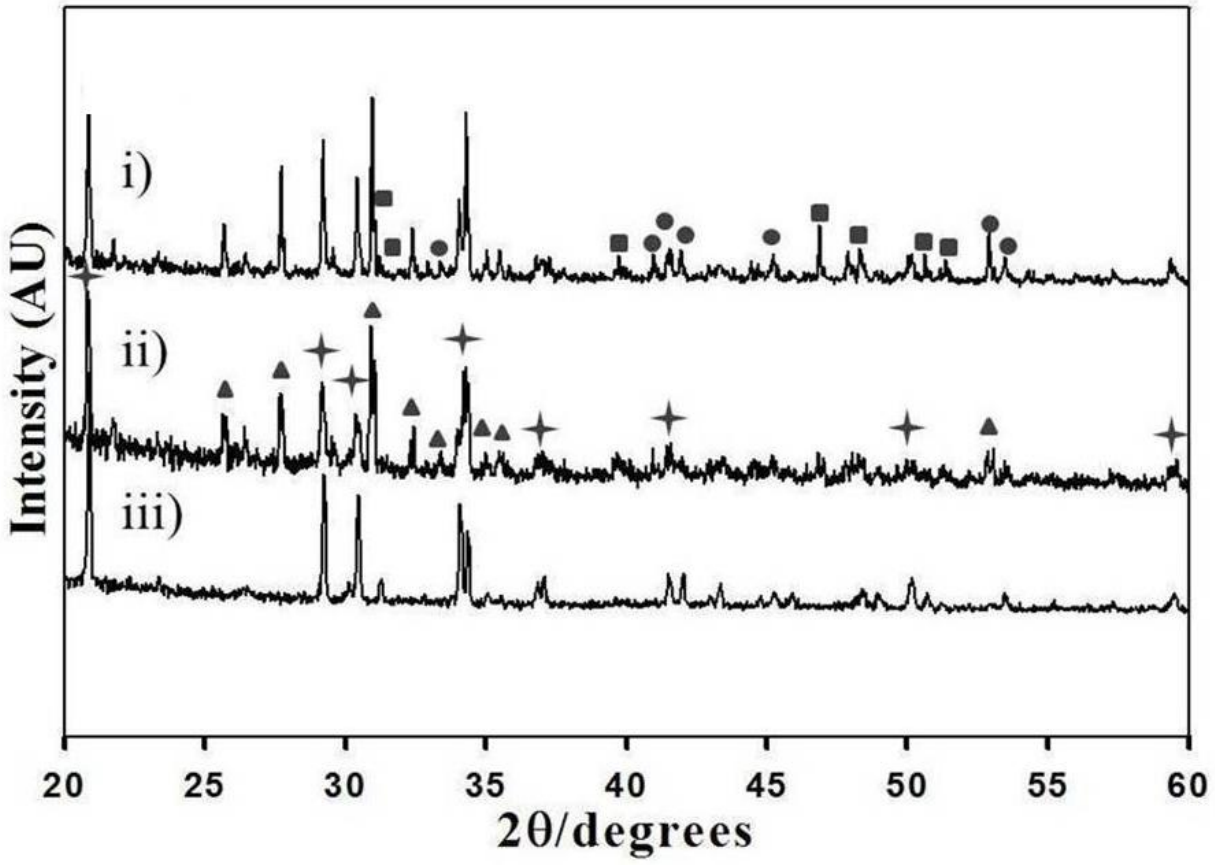


**Figure 4.4: X-ray diffraction patterns of the BC beads before and after aging in DMEM solution for 7 days i) Aged-BC beads, ii) Non-aged BC beads and iii) BPC. Peaks indicative of brushite and β-TCP are marked with asterisks and triangles, respectively. With aging, OCP (closed circles) and HA (closed rectangles) appeared as a new phase suggesting phase transformation of brushite to OCP/HA.**

### 4.2.2.2. EDX analysis

Further evaluation of the cement chemistry demonstrated an increase in Ca/P (Table 4.1), as might be expected with the formation of OCP/HA within the cement matrix. The calculated calcium to phosphorous molar ratio (Ca/P) of the BC beads before aging was different from after aging in DMEM solution. It increased from ~ 1.1 to 1.22 which as may be expected for

the transformation of brushite to OCP/ Ca-deficient HA. The apatite which has been transformed from OCP in *in vitro* physiological condition was a Ca-deficient HA, having a chemical composition with a lower Ca/P molar ratio and higher acid phosphate content (Suzuki et al. 2006).

**Table 4.1. EDX analysis values of the Ca and P atomic composition of the transformed phase of brushite cements before and after immersion in DMEM solution and distilled water for 7 days. Results are displayed as mean of n = 3 specimens ± standard deviation.**

| Sample | Aging medium | Ca /P atomic ratio |
|---|---|---|
| BC | N/A | 1.1±0.06 |
| Aged-BC | DMEM | 1.22±0.01 |
| BPC | N/A | 0.98±0.02 |
| Aged-BC | Distilled water | 1.57±0.03 |

### 4.2.2.3. Raman Microspectrometry

Examination by confocal Raman microscopy was also undertaken to investigate the relationship between the cell attachment and the crystalline changes of brushite cement beads before and after aging in DMEM solution for 7 days. Raman spectra of pure brushite, and β-tricacium phosphate (β-TCP) were compared with the aged cement specimens (Fig. 4.5b). The micro-Raman spectra of non-aged brushite cement beads, and brushite cement beads aged

for 7 days was shown in Figure 4.5a. The absorption bands in the range of 1500-1200 $cm^{-1}$ are representative of pure β-TCP and in the range of 1020-940 $cm^{-1}$ are characteristic to brushite (Figure 4.5b) suggesting that initially the prepared BC beads consisted mostly of β-TCP and brushite. The results of Raman microspectrometry also demonstrated that the aging protocol in DMEM solution led to phase transformation of β-TCP and brushite to OCP/carbonated apatite. The formation of OCP/carbonate apatite can be confirmed by observation of some specific vibrational modes of $PO_4^{3-}$ and $CO_3^{2-}$ which have been reported for these phases (Crane et al. 2006; De Mul et al. 1986; Penel et al. 1998; Penel et al. 1999; Tsuda and Arends 1993).

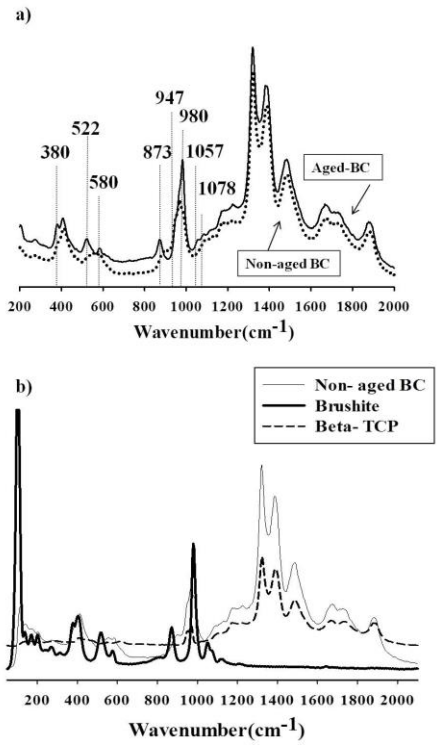


**Figure 4.5: Micro-Raman spectral analysis a) comparing spectra for aged and non-aged BC and b) none-aged BC and pure β-TCP and brushite.**

The main vibrational modes corresponding to composition changes of brushite to OCP/carbonated apatite are listed in Table 4.2.

**Table 4.2. Main micro-Raman wavenumbers observed in aged brushite in DMEM for 7 day.**

| Wavenumbers ($cm^{-1}$) | Micro-Raman vibrational mode | Component |
|---|---|---|
| 380 | $\nu_2 PO_4^{3-}$ | DCPD |
| 522 | $\nu_2 PO_4^{3-}$ | OCP |
| 580 | $\nu_4 PO_4^{3-}$ | OCP |
| 873 | P-OH stretch | Carbonated apatite |
| 947 | $\nu_1 PO_4^{3-}$ | Carbonated apatite |
| 980 | P–O stretch | DCPD |
| 1057 | $\nu_3 PO_4^{3-}$ | Carbonated apatite |
| 1078 | $\nu_1 CO3$ | Carbonated apatite |

## 4.2.3. Effect of dicalcium phosphate–citrate complex present within brushite matrix on cell attachment

### 4.2.3.1. DAPI staining

Since brushite is more soluble than OCP or HA, it was possible that the brushite surface was not sufficiently stable to enable cell attachment. To investigate this hypothesis, compacted

pellets were formed using BPC and cells were seeded onto the surface of BPC samples. As previously reported, following seeding on the surface of brushite cement culture beads formed from the mixture of β-TCP and OA solution; there was no cell attachment after culturing for 1 day (Fig. 4.6a). In the case of the compacted DCPD samples (BPC), however there was cell attachment following seeding (Fig. 4.6b) which confirms the ability of pure brushite to enable cell attachment. This suggested that the poor cell attachment to the surface of the brushite cement prepared using β-TCP/OA with CA and SP retardants (Fig. 4.6a) prior to conditioning could be due to the presence of an intermediate phase within the cement matrix that washed out during aging.

The cell attachment to the surface of the cement beads made using only CA was compared to cell attachment to the surface of cement made only SP as setting retardants and brushite made with CA and SP immersed in distilled water for 7 days (Fig. 4.6c, d, and e). The results from DAPI staining of seeded cells onto surface of the cement beads separately contrasted the ability of cells to attach to their surfaces respectively, which supported the presence of the soluble intermediate phase in the cement made using CA (Fig. 4.6).

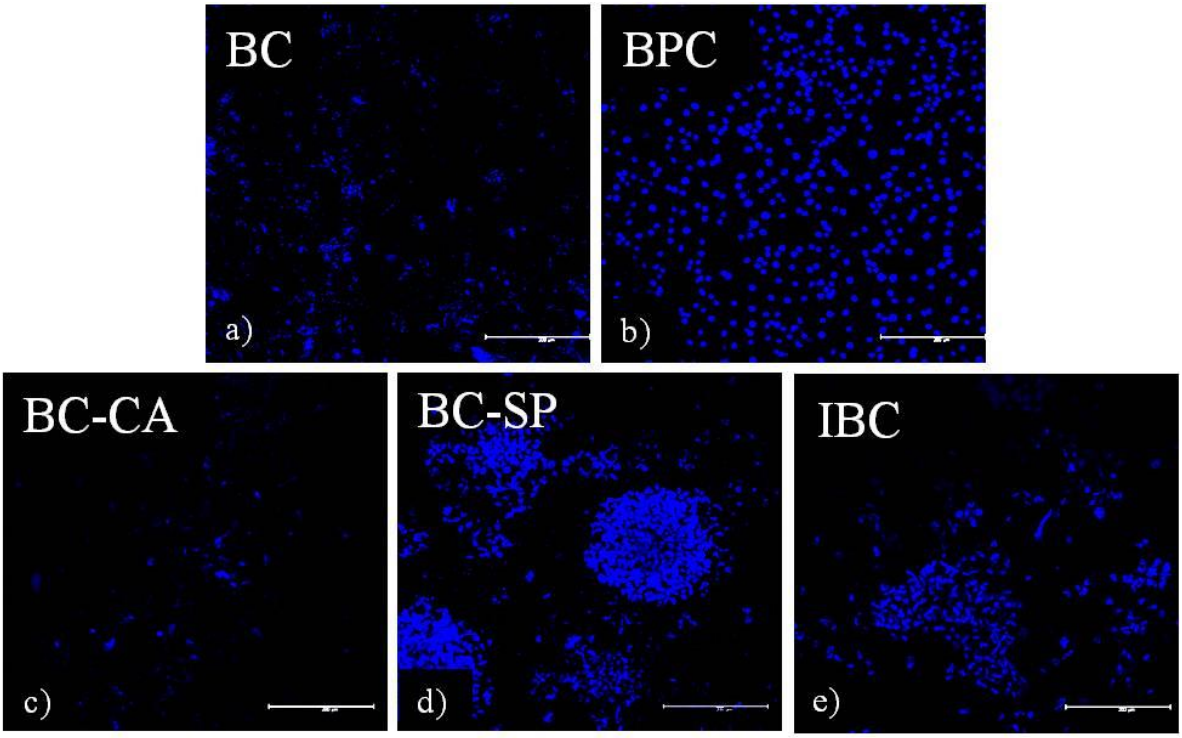


**Figure 4.6: Comparison of the cell adhesion on different brushite cement surfaces after 1-day cell culture using DAPI staining. a)untreated fabricated brushite cement (BC), b) compacted bruhiste powder (BPC), c) brushite cement made using only CA was denoted as BC-CA; d) brushite cement made using only SP was denoted as BC-SP; e) brushite cement made using CA and Sp immersed in distilled water for 7 days was denoted as IBC. Scale bar=200 µm**

The MTT results also quantitatively showed that the brushite cement did not support cell attachment; however the compacted DCPD did (Fig. 4.7). The results from an MTT assay as well as DAPI staining results demonstrated that the immersed BC had a significantly ($p< 0.001$) enhanced cell attachment compared with BC made only using CA and non-aged material ($p<0.01$) (Fig. 4.7).

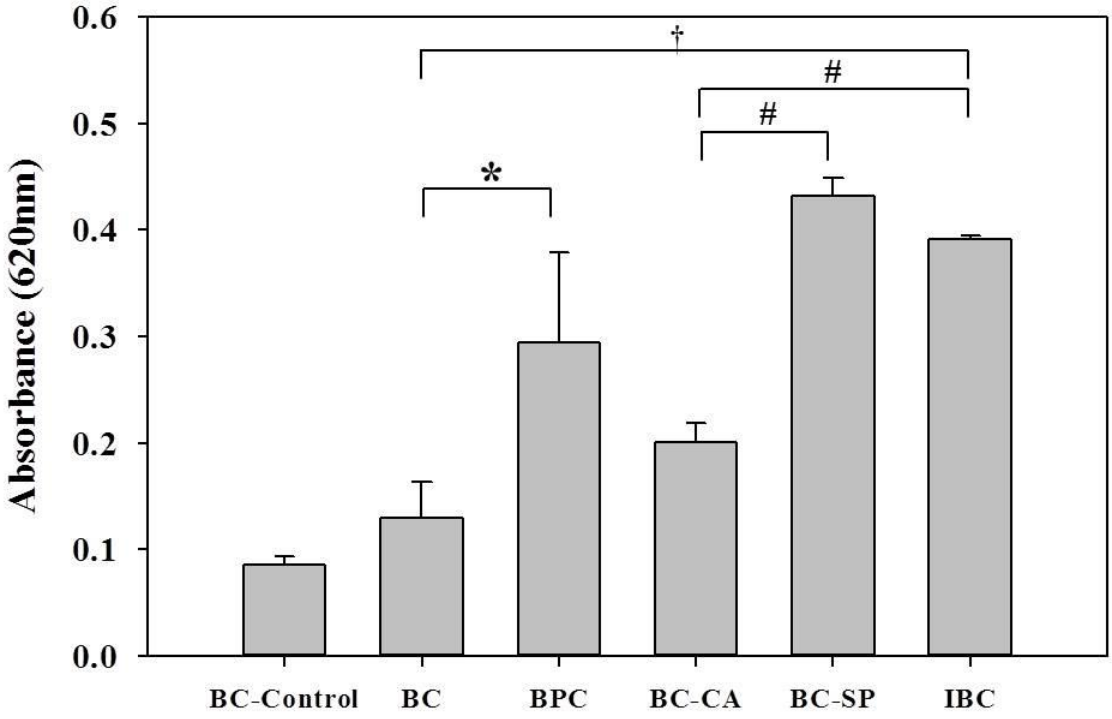


**Figure 4.7: The MTT results of 3T3 fibroblasts attached on the five different substrates at day 1. (Control sample is brushite cement without cell seeding). The cell attachment on the surface of IBC, BC-SP and BPC were significantly higher than that of the BC. *p<0.05 when comparing BPC to BC surface, # p<0.001 when comparing IBC and BC-SP surface to BC-CA. † p<0.01when comparing IBC to non-aged BC. Results are displayed as mean of n = 9 specimens ± standard deviation.**

The presence of an intermediate phase within the cement matrix was determined by measuring mass loss from the cement made using citrate and pyrophosphate or pyrophosphate alone as a retardant. In the case of the brushite cement beads formed using sodium citrate and pyrophosphate as retardants, there was a mass loss of nearly 3wt% within 1 day of immersion (Fig.4.8). In comparison, the cement beads formed using no retardant lost as little as 0.3wt% in the same time period.

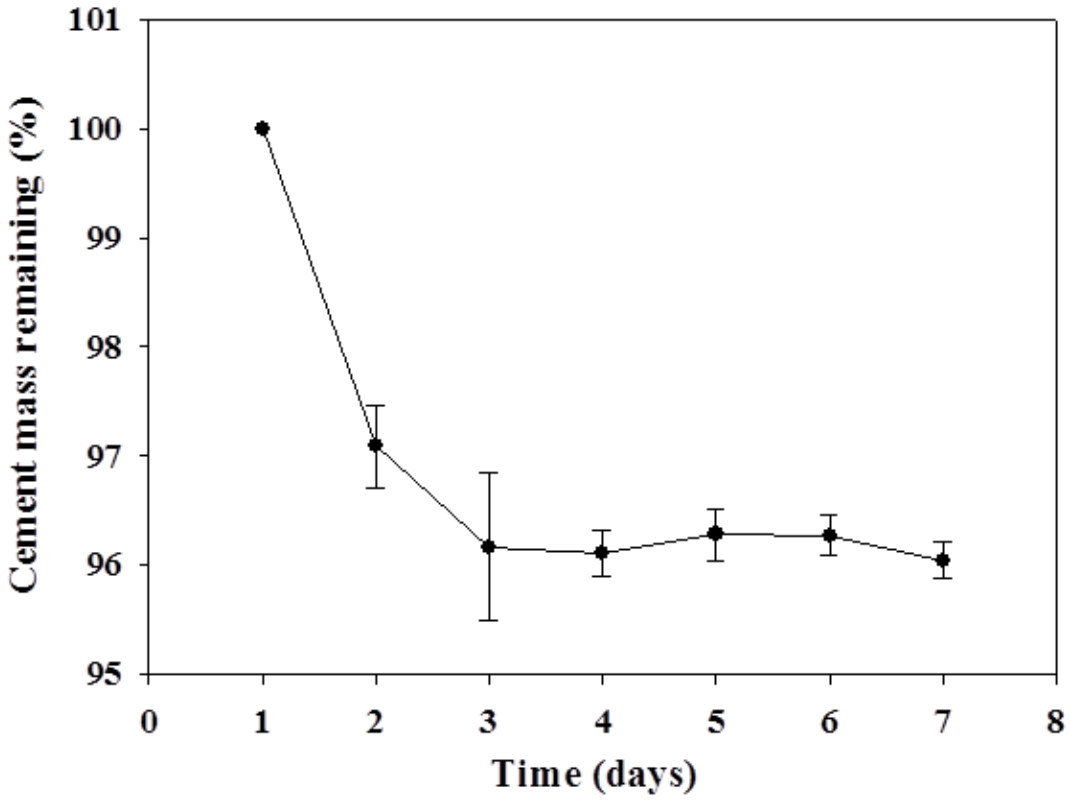


**Figure 4.8: Mass loss of BC samples made from sodium citrate and pyrophosphate retardants in distilled water up to 7 days. Significant mass loss was observed within 1 day of immersion.**

Further characterisation of the cement using X-ray diffraction, showed the presence of broader peaks for the cement prior to immersion (Fig. 4.9b). The peaks width changes of brushite cement before and after immersion were compared by evaluation of the position and full width at half maximum intensity (FWHM) of the peaks. This might suggest the presence of an x-ray amorphous intermediate phase within the cement matrix prior to immersion. Following immersion, the peaks on the X-ray diffraction patterns were significantly narrowed suggesting a higher level of crystallinity which may also correspond to the dissolution of an amorphous intermediate phase (Fig. 4.9a).

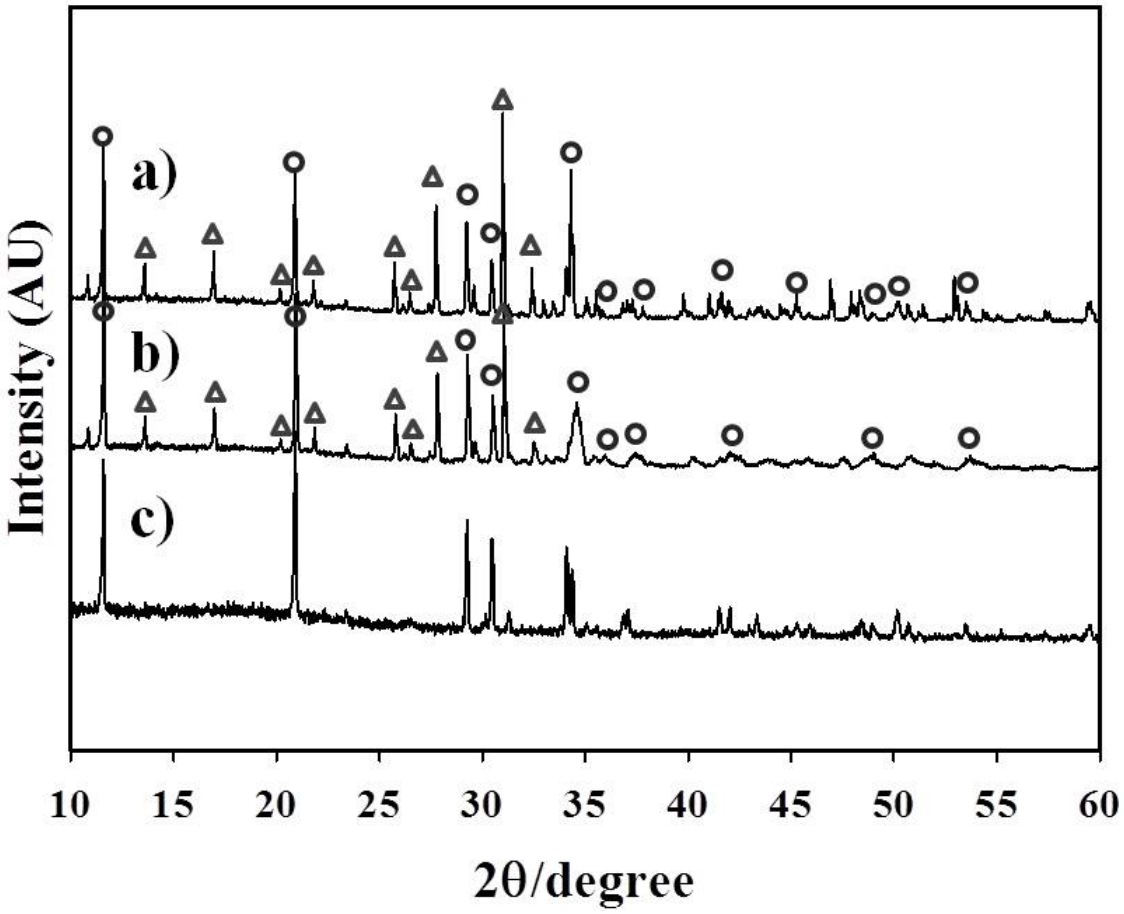


**Figure 4.9: X-ray diffraction patterns of a) immersed-BC in distilled water, b) Non-immersed BC and c) BPC. The peaks on the non-immersed specimen were broader than those on the immersed–BC. The major peaks for brushite and β-TCP are marked with circles and triangles, respectively.**

The XRD patterns of the BC beads made only with SP and without any retardants (Fig. 4.10) as well as BC beads sample after immersion and BPC (Fig. 4.9a and c), showed higher crystallinity compared to BC samples before immersion (Fig. 4.9b). This suggested that the brushite cement formed using SP and /or no retardants showed no amorphous intermediate phase within the cement matrix whereas the use of CA retardant in brushite cement caused

formation of an amorphous dicalcium phosphate-citrate complex that inhibited cell attachment to the surface of brushite.

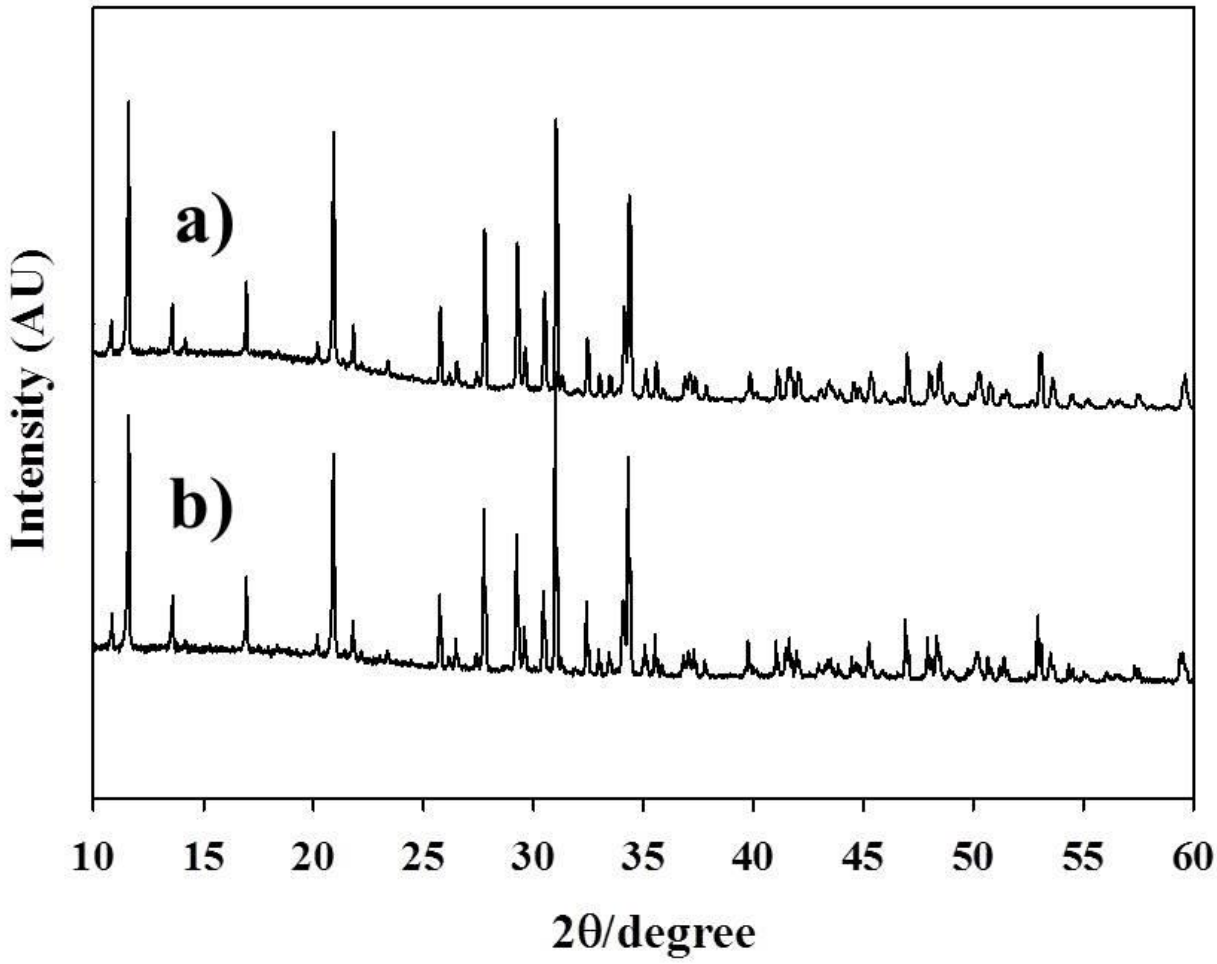


**Figure 4.10: X-ray diffraction patterns of a) BC beads made only with SP, b) brushite cement made without any retardant. The peaks on both samples were narrower than those on the non-immersed BC (shown in previous figure).**

## 4.3. Discussion

Brushite cement based culture beads are ideal carriers for cell delivery, given that they provide a three dimensional scaffold, as well as having a higher surface area for cell cultivation compared to monolayer cultures, they are typically more resorbable than hydroxyapatite ceramics. In this chapter the resorbable brushite cement culture beads (Fig. 4.1A) were formed and it was demonstrated that the cell attachment to the surface of brushite cement beads can be influenced by cement chemistry and the use of setting retardants during cement production. The brushite cement beads formed from the mixture of β-TCP and OA solution using CA and SP as setting retardants didn't facilitate cell attachment (Fig. 4.1B). While some have reported cell attachment to brushite cement, the variety of formulations used and the pre-treatments applied to the materials hinder direct comparison (U. Klammert et al. 2009; Le Nihouannen et al. 2008; Tamimi et al. 2008). This highlights the importance of systematically characterising the chemistry and biological reaction of the cast materials in order to identify formulation parameters that could influence cell attachment.

The first part of this chapter has demonstrated that the dynamic aging protocol of brushite cement beads in DMEM solution at 37º C has a profound effect on the cellular affinity to the surface of cement upon aging (Fig. 4.2) which may have been as a result of changes in phase composition on the surface of the cement following immersion in DMEM (Fig. 4.2 and Fig. 4.3(a)). Brushite is commonly known to be a metastable phase of CaP under normal atmospheric conditions. It tends to gradually transform to HA crystals in aqueous solutions under the normal physiological pH of 7~7.5 (D. Lee and Kumta 2010). Mandel and Tas (2010) recently demonstrated that brushite powders soaked in commercial DMEM solutions, at 36.5 °C for about one week, were able to completely transform into OCP (Mandel and Tas

2010). OCP is also metastable and a precursor to the formation of an apatitic calcium phosphate phase (Dekker et al. 2005; Suzuki et al. 2006). The cell attachment on to the surface of aged brushite samples could be attributed to the formation of OCP or hydrolyzed Ca-deficient HA. Cell attachment to OCP has previously been reported in the literature. (Suzuki et al. 2006). HA also absorbs ECM proteins that support the binding of cells to its surface (Zhao et al. 2006). Since the sample for XRD analysis might be removed near the middle of the hydrolysis process of OCP to HA, the XRD patterns of aged brushite cement in DMEM consisted of both OCP and carbonated apatite (Fig. 4.4). It has been shown that the apatite which has been transformed from OCP in *in vitro* physiological condition was a Ca-deficient HA, having a chemical composition with a lower Ca/P molar ratio and higher acid phosphate content as observed in biological crystals (Suzuki et al. 2006).

The calculated calcium to phosphorous molar ratio (Ca/P) of the non- aged BC beads (Table 4.1) was different after aging in DMEM solution. It increased from ~ 1.1 to1.22 which is further evidence for the transformation of brushite to OCP/HA. Raman spectra as well as XRD evidenced the presence of OCP or HA within the cement matrix after aging (Fig. 4.5a). In order to develop implantable brushite-based culture structures preferably, culture beads, cell growth is required prior to implantation, therefore further investigation was required to optimize the biological properties of these materials in terms of cell attachment and proliferation along with their other properties. To our knowledge this is the first report of investigation of the influence of brushite cement chemistry and setting retardants upon cell attachment on to the surface of these materials. Following seeding on the surface of brushite cements formed using CA and SP as retardants and with only CA, there was no cell attachment after culturing for 1 day (Fig. 4.6a and 4.6c). The mass loss of nearly 3% of the

brushite cement within 1 day (Fig. 4.8) of immersion compared to the cement formed using sodium pyrophosphate alone with ~ 0.9% mass loss in the same period could be explained by the presence of dicalcium phosphate citrate intermediate phase in the cement matrices which prevented cell attachment to the surface of the materials. Therefore this may be why the surfaces of the cements made with CA and SP and with only CA as retardants (Fig. 4.6) did not facilitate cell attachment. Although different studies showed the potent effect of citric acid as setting retardant to increase compressive strength, setting time and injectability of calcium phosphate cements, the formation of an intermediate dicalcium phosphate citrate complex could be problematic for the cell adhesion capacity of brushite cement or may result in a deterioration of compressive strength of the cement in higher concentration (Hofmann et al. 2006) . X-ray diffraction patterns of the cement before and after immersion (Fig. 4.9) displayed peaks typical of brushite and β-TCP and appeared to have a very similar composition – little or no apatite was detected within the material. The peaks on the un-aged specimen were broader than those on the aged material, implying low crystallinity (Fig. 4.9a and 4.9b).

According to the equation (4.1) and the initial quantity of citric acid as a setting retardant used in the preparation of cement paste, the amount of dicalcium phosphate-citrate complex which could be formed was about ~2.6 %, which corresponds well with the mass loss (~3%) we measured from the BC after immersion in water (Fig.4.8). This may suggest that an x-ray amorphous phase was present within the un-aged specimen, which dissolved rapidly following immersion. Therefore our study suggested that the presence of this intermediate phase inhibit cell attachment to the surface of brushite.

## 4.4. Conclusion

In the first section of this chapter, the resorbable calcium phosphate cement (brushite) beads were fabricated and it has been shown that cell attachment to the surface of a BC material can be influenced by retardant type. The use of citrate in the form of CA was shown to hinder cell attachment up to 7 days following immersion, this was shown not to be the case with pure brushite or when SP was used as a retardant. The initial poor attachment of cells to the surface of the cements made with CA could be attributed to the formation of an amorphous dicalcium citrate phase within the cement material which slowly dissolved following immersion in the culture medium. While this prevention of cell attachment if the material is implanted directly is not a significant problem, if the BCs are to be used as culture beads for cell delivery, poor cell attachment is highly undesirable.

# Chapter 4B: A comparison of methods for the fabrication of brushite based culture beads

In this section of this chapter, two other alternative methods; cement granulation technique and soaking Marble granules along with the cement casting method (used in the first section of this chapter) were introduced and used to produce brushite granules. The effect of manufacturing process of three types of BC beads on cellular behaviour was investigated. The granules were characterized with respect to their surface morphology, size, phase composition and specific surface area.

Other properties of culture beads, such as surface topography and surface area as well as surface chemistry are capable of directing cellular responses including initiation of cell attachment, proliferation and induction of bone nodule formation (Amini et al. 2012).

In order to compare the biological behaviour of the granules produced with different methods, preliminary cellular tests on to the beads was carried out using MC3T3 cells. The functional activity of the MC3T3 pre-osteoblast cells grown on three types of brushite-based culture beads to produce mineralised matrix and nodules was also examined by positive bone matrix mineralization indicated with Alizarin Red S staining.

## 4.5. Methods and materials

### 4.5.1. Preparation of brushite culture beads with three different methods

#### 4.5.1.1. Cement casting method (denoted as sample C)

The first of these brushite beads (C) was prepared by cement casting method which consisted of casting a paste of β-TCP and 3.5M orthophosphoric acid (OA) containing 200mM citric acid (CA) and/or 200mM sodium pyrophosphate (SP) retardants at a powder to liquid ratio (P/L) of 3 g/ml in to spherical shape moulds. The hardened beads were post-treated for optimization of cell attachment by immersion in culture media and sterilized with ethanol and then left overnight under ultraviolet light to complete the sterilization process.

#### 4.5.1.2. Cement granulation method (denoted as sample G)

The brushite cement paste was prepared accordance with the method in previous section (3.2.1). The cement paste was allowed to harden at 37ºC for 1 h. The hardened cement was granulated in a high- speed food processor (Kenwood CH180 food processor, 0.35 L, 300W). Granules with different sizes were produced. Granules with the size of ~1000µm were selected by sieving. Afterwards the beads were repeatedly washed in PBS (200 mM, Sigma-Aldrich, Dorset, UK) to eliminate unreacted OA. The samples (Figure 4.11b) were post-treated for optimization of cell attachment by immersion in culture media and sterilized with ethanol (70%) (Fisher Scientific, Leicestershire, UK) and then left overnight under ultraviolet light to complete the sterilization process.

### 4.5.1.3 Soaking marble ($CaCO_3$) granules in phosphate solution (denoted as sample M)

Marble (calcium carbonate) granules (Merck KGaA, Darmstadt, Germany) with the size of ~900µm were soaked in phosphate solution to prepare brushite granules. To prepare the phosphate solution 10g of $NH_4H_2PO_4$ (Merck, Germany) was dissolved in 50mL of double distilled water. Two grams of marble granules were then placed into the phosphate solution and soaked in sealed glass bottles at room temperature for 20h without stirring. The granules were filtered and washed with 1.5L distilled water. They were dried at 37º C overnight (Figure 4.11c).

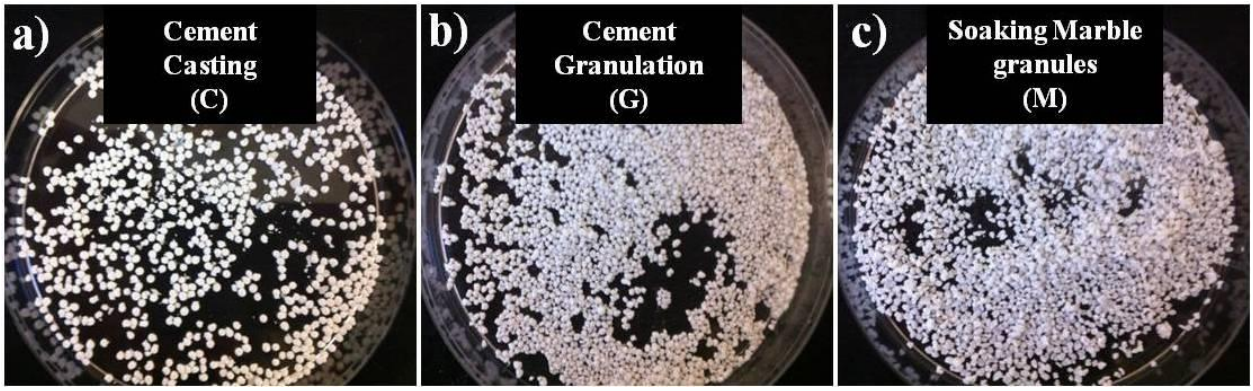


**Figure 4.11: Brushite culture beads prepared with three different methods**

## 4.5.2. Physicochemical characterization of brushite culture beads

Surface morphology and size of all fabricated beads were analysed with scanning electron microscopy (section 3.8.1). The composition and crystallinity of all of them were determined by x-ray diffraction (section 3.6.1). Specific surface area of the beads was measured by BET of nitrogen adsorption data (section 3.7.). Image J was used to analyze circularity of the fabricated granules.

### 4.5.3. Cell culture

MC3T3 osteoblast precursor cells were seeded onto the beads after sterilization (section 3.1) with a density of $10^5$cells/ml in 2 ml DMEM correcting for the surface area of the beads. Cell growth on bead surfaces was recorded by MTT assay (section3.2) on the $1^{st}$, $3^{rd}$, $5^{th}$, $7^{th}$ and $9^{th}$ day of culture. The functional activity of the MC3T3 pre-osteoblast cells grown on brushite beads to produce mineralised matrix and nodules was examined by positive bone matrix mineralization indicated with Alizarin Red S staining (section 3.6.) at defined time-points.

## 4.6. Results

### 4.6.1. Effect of preparation route on brushite culture beads characteristics

#### 4.6.1.1. SEM and XRD

Despite recent significant attention to brushite–based cement in hard tissue repair, there are very few studies that have focused on the use of this material in the form of granules. Accordingly, three different kinds of brushite beads were produced using three different methods. The granules were characterized with respect to their surface morphology, size, phase composition and specific surface area. The size of all three types of prepared beads was relatively consistent (~1000μm) with similar true density (Fig. 4.12, Table 4.3).

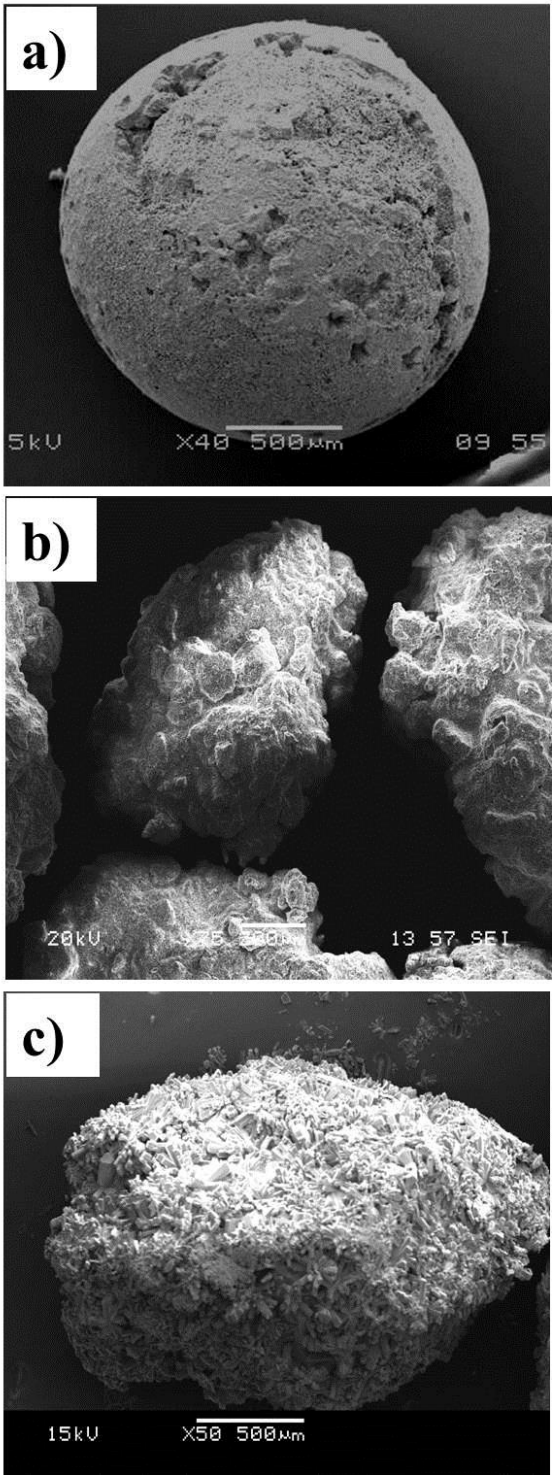


**Figure 4.12: SEM micrograph showing the approximate size of brushite beads, a) (C) beads prepared by cement casting method, b) (G) beads prepared by cement granulation method, and c) (M) beads prepared by soaking marble granules in phosphate solution.**

The XRD patterns of all granules exhibited relatively similar crystallinity. The XRD patterns from (M) beads showed only peaks indicative of brushite and the (G) and (C) beads displayed both peaks typical of brushite and some unreacted β-TCP (Fig.4.13).

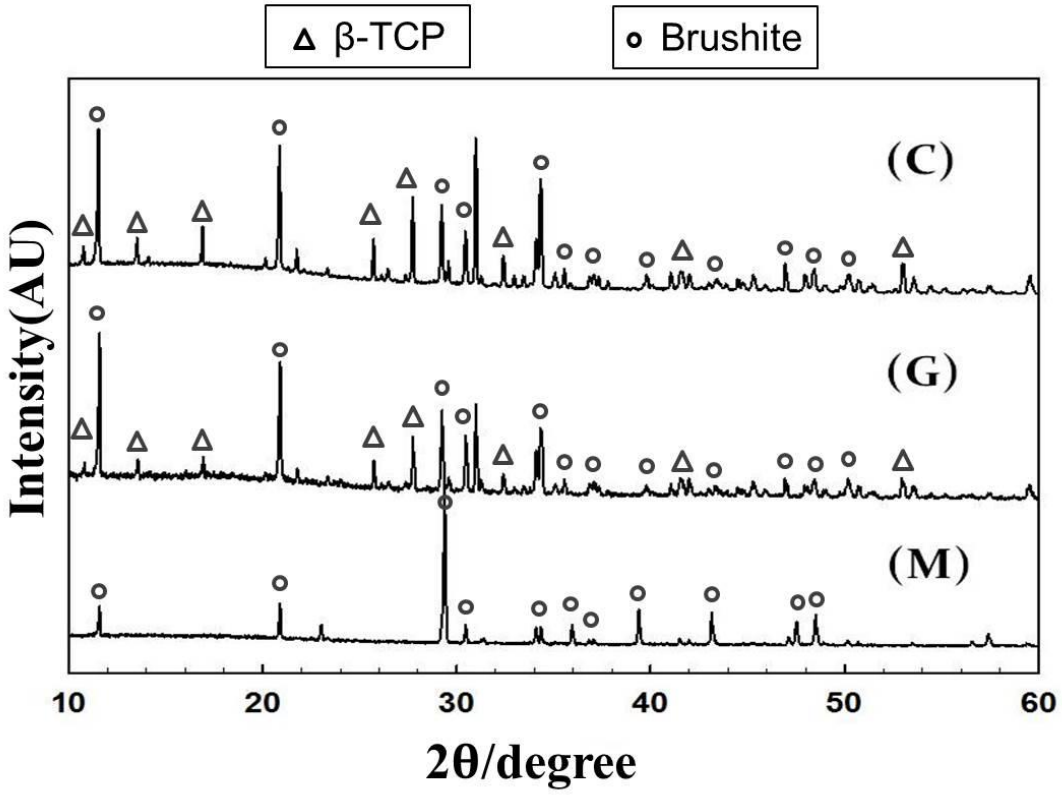


**Figure 4.13: X-ray diffraction patterns of brushite culture beads prepared with three different methods: cement casting method(C), cement granulation method (G), and soaking marble granules in phosphate solution (M).**

SEM micrographs revealed distinct patterns of surface topography of the three kind of prepared beads (Fig 4.14.). The (C) group exhibited relative flat surface composed of sharp plate-like crystals with~10µm length and ~ 0.1µm width (Fig.4.14i). The (G) beads exhibited a relatively rough surface composed of Water lily (WL)-shaped brushite crystals (Miller et al. 2012) about ~100µm in diameter, which consisted of small crystals of approximately 1-2µm ( Fig. 4.14ii). The (M) group also exhibited a relatively rough surface, however fewer (WL)-

shaped brushite crystals and consisted of larger flake-like crystals approximately 25-30µm in length. The difference exist in the surface topography of these beads may be attributed to the dissolution/reprecipitation process used during beads production.

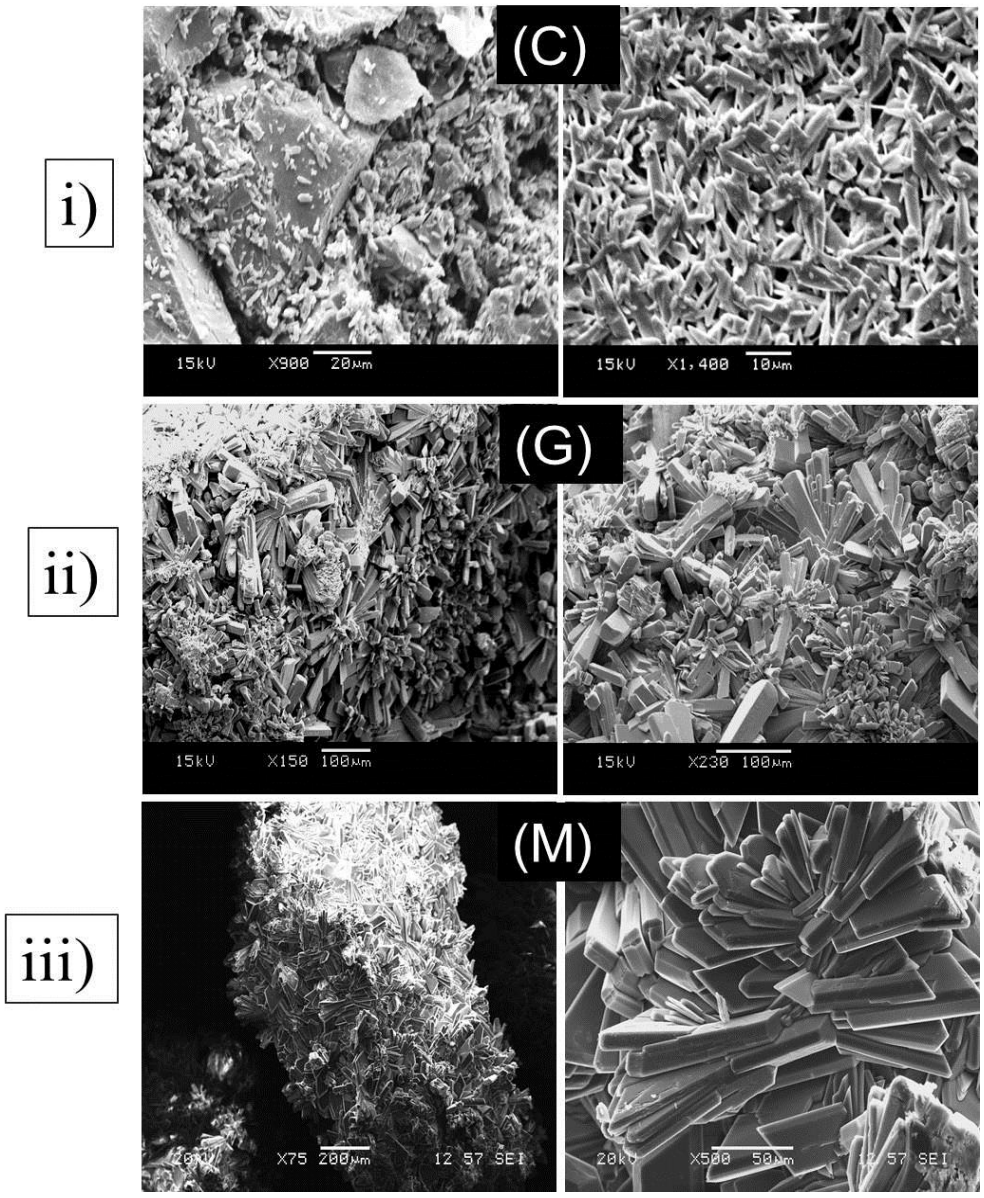


**Figure 4.14: SEM micrograph showing the morphology of brushite beads prepared with three different methods.**

## 4.6.2. A comparison of cellular attachment and proliferation on three types of brushite beads

Following seeding onto the beads, all three types of the brushite cement beads supported cell attachment and proliferation; however there was a significant difference between the attachment of cells to the (M) beads compared with (G) and (C) groups. The cell attachment was significantly ($p<0.001$) higher than that of C and G beads (Fig. 4.15) which may be due to the surface characteristics of the M beads.

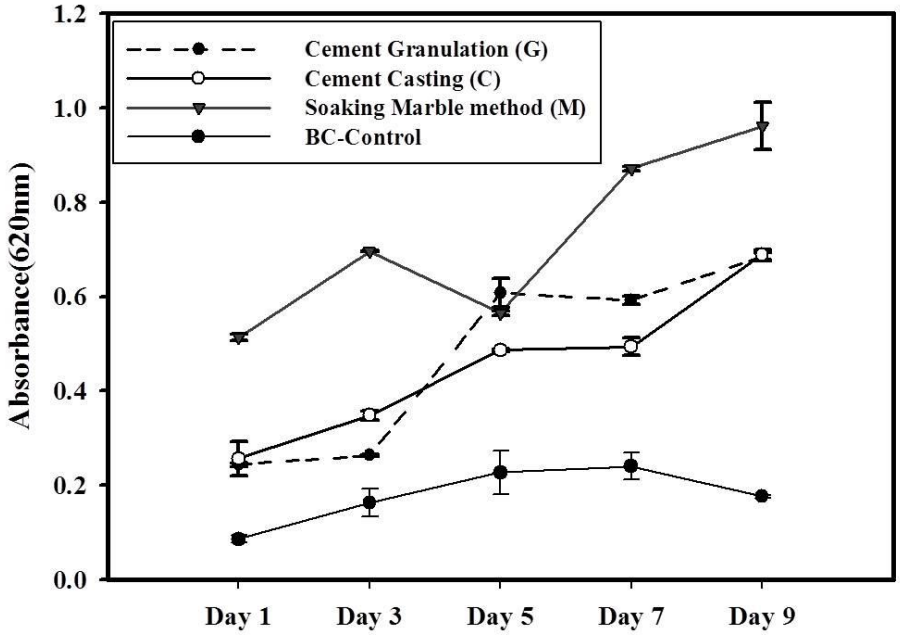


**Figure 4.15: The MTT results of 3T3 fibroblast cultures on three types of brushite culture bead. The cell attachment on brushite beads prepared with soaking marble method (M) was seen to be significantly higher ($p<0.001$) than that of C and G beads. The proliferative activity of cells during the 9 days culture period however was seen to be significantly ($p<0.001$) higher in the case of G beads and C beads respectively compared with the M group. BC samples without cell seeding were used as control. Sample Data points represent mean values of n = 9 specimens ± standard deviation.**

Over the duration of study the increase in cell number at day 9 compared with that at day 1 was significantly ($p<0.001$) higher in the case of (G) beads, and (C) beads respectively compared with the (M) group (Table 4.3). The higher fold-increase of cell number on (G) and (C) beads may be due to the higher specific surface areas of the G and C beads (Table 4.3).

**Table 4.3. Properties of the beads and the percentage of increase in cell number of each bead during the 9-day culture**

| Methods of brushite beads fabrication | True Density ($g/cm^3$) | Circularity | Surface area ($m^2/g$) | % Increase in cell number during 9 day culture period |
|---|---|---|---|---|
| **Cement casting (C)** | **2.75** | **0.91±0.05** | **4.81±0.01** | **168** |
| **Cement Granulation (G)** | **2.72** | **0.79±0.07** | **3.56±0.01** | **181** |
| **Soaking Marble granules (M)** | **2.62** | **0.78±0.06** | **0.65±0.006** | **87** |

## 4.6.3. A comparison of nodule formation by MC3T3-E1 cells grown on three types of brushite culture beads

The functional activity of the MC3T3 pre-osteoblast cells grown on brushite granules to produce mineralised matrix and nodules was examined by positive bone matrix mineralization indicated with Alizarin Red S staining after one week of culture on the beads (Fig.4.16) Alizarin Red staining indicated that (M) and (G) groups of culture beads supported the mineralized nodule formation of pre-osteoblast MC3T3 cells; however little or no red staining was observed in the case of (C) group (Fig. 4.16 a) indicating that these beads do not

stimulate osteogenic activity of MC3T3 osteoblast precursor cells so much as the (G) and (M) groups (Fig.4.16 b &c). It was found that negative control with no cells showed no little alizarin red staining in isolated regions around the beads. The negative control was performed to ensure that the positive staining in the brushite-cell complexes was not because of the presence of the calcium in the material.

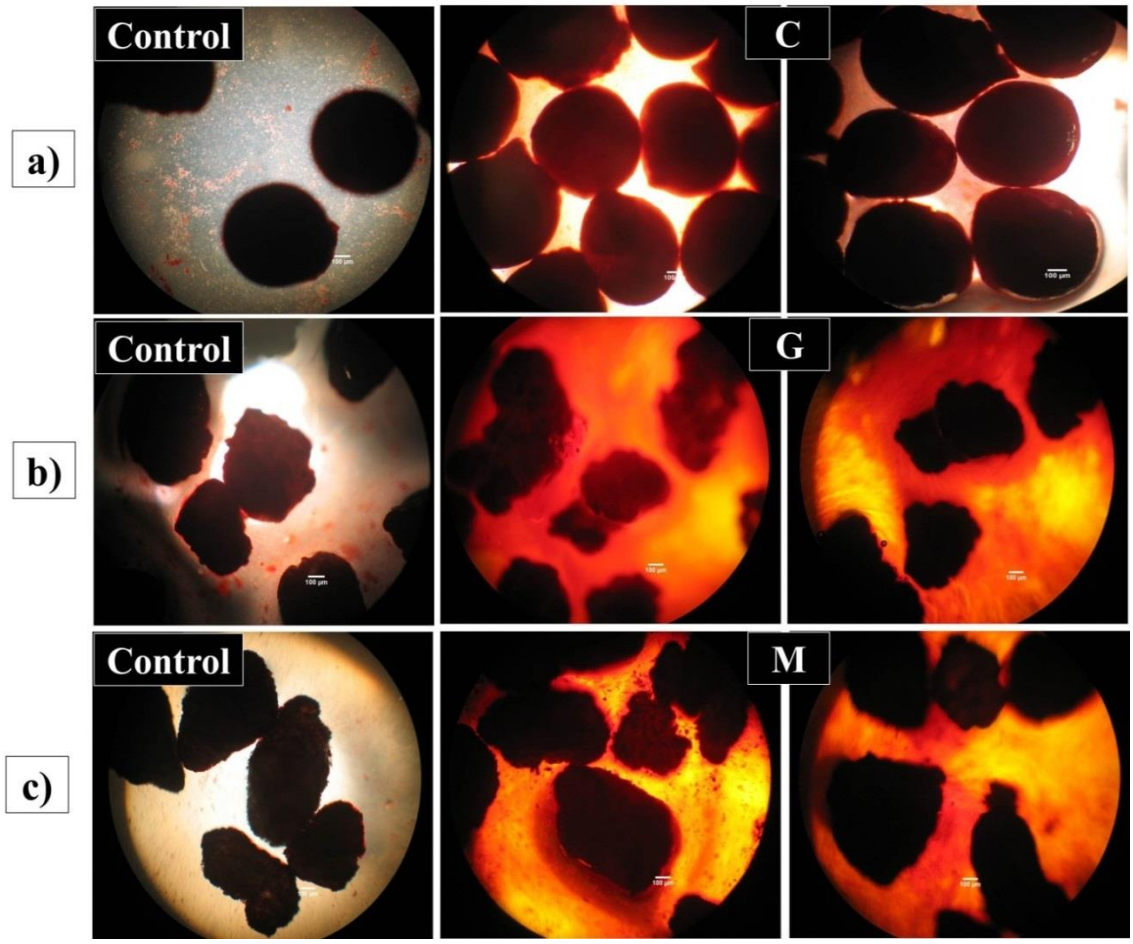


**Figure 4.16: Alizarin Red Staining of MC-3t3 cells indicating of mineralized matrix synthesis. a) cell-beads (C) prepared by cement casting method, b) cell-beads (G) prepared by cement granulation method and c) cell-beads (M) prepared by soaking marble granules in phosphate solution in osteogenic media for 7 days. Control samples are beads with no cells. Scale bar =100µm.**

## 4.7. Discussion

Brushite-based materials are promising candidates for the manufacture of culture beads in cell therapy for bone tissue regeneration as, due to their relatively high solubility, they may be resorbed and replaced by bone following implantation. Despite these attributes, no studies have focused on the methods for the fabrication of brushite culture beads and the evaluation of manufacturing process of the different methods and brushite granules properties on cellular behaviour. Here, three different methods for the fabrication of brushite-based culture bead were evaluated and it was demonstrated that brushite culture bead characteristics are strongly dependent on preparation route. The resulting differences in surface properties and chemistry were shown to strongly influence cell attachment and the proliferation of seeded cells on the three types of brushite culture beads. The tendency of the fabricated beads to initiate bone nodule formation *in vitro* was also shown to be strongly influenced by manufacturing process.

The size of all three type of fabricated beads was relatively consistent (~1000μm; Fig. 4.12) with similar true density (Table 4.3). All granules consisted of predominantly brushite (Figure 4.13). The XRD results confirmed that the samples exhibited a similar level of crystallinity and demonstrated peaks indicative of only brushite in the case of (M) group and peaks typical of brushite and some un-reacted β-TCP in the case of (G) and (C) groups (Fig. 4.13). SEM micrographs, however, revealed distinct surface topographies for the three formulations of prepared beads which may be attributed to the dissolution/reprecipitation process used for producing the beads (Fig 4.14).

All three types of brushite cement bead supported cell attachment and proliferation; however the cell attachment on (M) group beads was significantly ($p<0.001$) higher than that on the (C) and (G) beads (Fig. 4.15) which may be due to the surface characteristics of the M beads.

Surface topography, has been reported to have a strong influence on the initial cellular events at the cell-material interface (Jin et al. 2012; Lampin et al. 1997; Müller et al. 2008). In this study the (M) group beads in comparison with (G) and (C) groups exhibited a relatively rough surface with larger water lily (WL) shaped brushite crystals and this seems to be more supportive for MC3T3 cells attachment compared with the flat plate (FP) like crystals and smoother surfaces that were present on the beads prepared using cement casting and granulation. Osteoblast-like cells have previously been shown to attach to rougher surfaces more extensively than to comparable smoother surfaces (Deligianni et al., 2000; Byon et al., 1996). Surface roughness affects the kinetics of protein adsorption and the structure of the adsorbed protein that influence cell reaction (Lampin et al. 1997).

Over the duration of study, the proliferative activity of the seeded cells was significantly ($p<0.001$) higher in the case of (G) beads, and (C) beads respectively compared with the (M) group (Table 4.3) this could be attributed to different specific surface areas of similar-sized fabricated brushite culture beads. The specific surface areas of the (G) beads and (C) beads were higher than that of (M) beads. Surface roughness might also have an effect on proliferative activity; it is known from the literature that, low cell proliferation was observed on surfaces of the highest roughness (Ponsonnet et al. 2002; Wall et al. 2009). Variations in surface texture or microtopography can influence cells in a wide variety of ways by modifying diffusion through the channels thus influencing the access of nutrients and the escape of their waste products (Ito 1999; Von Recum and Van Kooten 1996). However in this study, as the surface roughness of (M) and (G) groups were similar compared to the surface of (C) groups the higher proliferative activity of seeded cells on (G) and (C) beads must relate to their different specific surface area rather than surface topography.

The capacity of the cells on all three types of culture beads for the synthesis of mineralized matrix was assessed by Alizarin Red staining. Control cultures with no cells showed no alizarin staining (Fig. 4.16). Cell-microcarrier complexes in osteogenic media in the case of (G) and (M) beads showed positive staining indicating the ability of cultured cells on these beads to enable the deposition of mineralized matrix (Fig. 4.16) whereas in the case of the C groups with flat surface composed of sharp plate-like crystals showed little or no alizarin red staining indicating inability to stimulate osteogenic differentiation of seeded cells. Cell aggregate

differentiation and matrix production have also been reported to be altered by surface topography (Boyan et al. 1996; H.-I. Chang and Wang 2011; Kieswetter et al. 1996) . It has been demonstrated that rough surfaces were also superior to smooth surfaces in promoting osteogenic induction of osteoblasts- like cells (Boyan et al. 1996). In this study the circularity of the fabricated brushite granules were evaluated using Image J and it was shown that the cellular behaviour of seeded cells did not depend on the circularity of the granules and no correlation was observed between circularity and cellular attachment and proliferation.

## 4.8. Conclusion

Different methods were used to fabricate brushite based culture beads. Dependence on the characteristics of the granules on the preparation route was studied with respect to cell attachment to their surfaces and proliferation. All three types of beads supported cell attachment and proliferation. The (M) group, however, exhibited the highest extent of initial cell attachment among the groups. The (G) group demonstrated the highest increase in cell population during the 9-day culture period. The (M) and (G) culture beads have been shown to have the ability to stimulate osteogenic differentiation of MC3T3 osteoblast precursor. Surface topography has been shown to be the most important factor in initial cell attachment

and promoting osteogenic induction of osteoblasts- like cells. Among the formulations tested, all have potential for further use as culture supports, however, the beads formed by granulation performed the best with respect to both cell attachment and mineralisation.

# Chapter 5

## THE DEVELOPMENT OF CALCIUM PHOSPHATE/GELLAN GUM NANO-COMPOSITES FOR CELL DELIVERY

Hydrogel materials are widely studied for application in tissue regeneration because of their tissue-like properties. Namely, they have a high water content, can be cytocompatible, and exhibit a morphology akin to that of the extracellular matrix (ECM). Furthermore, they can be injected into the desired site and can gel through relatively mild reactions, causing a minimal inflammatory response (Birdi et al. 2012; J. L. Drury and Mooney 2003b; Malafaya et al. 2007).

Many different hydrogels have been investigated for application in the body; one such material is gellan gum (GG). GG is a natural polysaccharide manufactured by microbial fermentation of the *Sphingomonas paucimobilis* bacterium. It forms a stable gel in presence of cations in aqueous conditions, through the formation of three-fold double helices, which subsequently aggregate to form a three dimensional network upon lowering the temperature under mild conditions (Evageliou et al. 2010; J. T. Oliveira et al. 2010a). Endotoxin-free GG has been used for drug delivery, for cell immobilization, and as a substrate in tissue engineering (Silva-Correia et al. 2011; A. M. Smith et al. 2007). The use of gellan gum is limited, however, owing to their imperfect cell affinity, biocompatibility or other physical characteristics (Wang et al. 2008) . One approach to improve these deficiencies is to incorporate synthetic calcium phosphate (CaP) into the biopolymer matrix. In part a of this chapter, therefore, synthetic HA of two different crystallite sizes: one on the nano and the other on the micro scale have been used to manufacture HA/gellan gum (GG) composites to

achieve a more physiologically relevant range of mechanical properties and in the second section, part b, the influence of incorporation of HA nanocrystals into the GG matrix on behaviour of GG/HA culture beads in terms of cell adhesion, proliferation was investigated in spinner flask and compared to that of static cultures. The ability of the fabricated beads for synthesis of mineralized matrix was also assessed.

# Chapter 5A: Tailoring gel modulus using dispersed nano-crystalline hydroxyapatite

Considerable recent research has focused on understanding the importance of elastic modulus of scaffold materials on the phenotypes of attached or encapsulated cells, indeed researchers are now focussing on controlling new tissue formation by adjusting modulus (Colley et al. 2009; Discher et al. 2005; Engler et al. 2006). For example, it has been shown that an elastic matrix ranging from (20-40KPa) favours the differentiation of naive mesenchymal stem cells (MSCs) to osteoblasts, in contrast an elastic modulus of around 8-17KPa, favours the differentiation of MSCs to myoblasts (Engler et al. 2006). One way to adjust the mechanical properties of a hydrogel is to reinforce the structure using inorganic particles such as hydroxyapatite (HA), the predominant mineral constituent of bone (Swetha et al. 2010). Many researchers have tried to recapitulate this structure using a combination of HA with a variety of biopolymers, for example, Lin and Yeh fabricated a series of alginate/HA composite scaffolds by phase separation. They demonstrated that the incorporation of HA into alginate hydrogel improved both cell attachment and mechanical properties of the composite (Lin and Yeh 2004). The incorporation of HA nanocrystals into chitosan-carboxymethyl cellulose scaffolds has also been reported to improve the compressive strength and modulus of the scaffold intended for bone tissue engineering (Liuyun et al. 2008).

The non-stoichiometric HA crystallites found in bone are nanocrystalline (Rungsiyanont et al. 2011) and it is thought that the impressive mechanical properties exhibited by bone may be partly attributed to the intercalation of these nanocrystals into the collagenous matrix, which would not be possible if the particulate was microcrystalline. Despite the apparent importance of crystallite size to the overall mechanical performance of such a biopolymeric

structure, to date no-one has evaluated the influence of crystallite size on the mechanical properties of hydrogel composite materials. This section of this chapter, therefore, compared the mechanical properties of GG hydrogel reinforced using micro and nanoscale HA crystals at different concentrations. The mechanical properties of the gel were determined using a universal mechanical testing machine and the influence of HA seeding on gel structure was determined using scanning electron microscopy.

## 5.1. Methods and materials

### 5.1.1. Synthesis of nano-sized hydroxyapatite

Nano-sized hydroxyapatite (nHA) particles were prepared by precipitation. Briefly, $Ca(NO_3)_2.4H_2O$ (calcium nitrate, Fisher Scientific, Leicestershire, UK) and $(NH_4)_2HPO_4$ (ammonium phosphate, Fisher Scientific, Leicestershire, UK) were dissolved in double-distilled water. The pH of both suspensions was adjusted to 11 with concentrated $NH_4OH$ (aqueous ammonia, Fisher Scientific, Leicestershire, UK). The $Ca(NO_3)_2.4H_2O$ was added drop-wise to the vigorously stirred $(NH_4)_2HPO_4$, whilst maintaining the pH at 11 by further addition of $NH_4OH$. The final suspension was then left to stir for 1 h at room temperature. This resulted in the formation of a milky white precipitate. The precipitated HA was separated from the solution by centrifugation at 3000 rpm for five minutes, which was repeated five times. The HA slurry was dried at 65°C for 24 h and the dried HA was then ground to powder using a pestle and mortar.

### 5.1.2. Synthesis of micro-sized hydroxyapatite

To compare the effect of the size and crystallinity of the HA particles on the mechanical properties of the hydrogel, micro-crystalline HA (mHA), which consisted of a combination of HA and a small quantity of β-TCP (β-$Ca_3(PO_4)$), was prepared. The microcrystalline material was prepared by sintering half of the nHA in a furnace (Carbolite, CWF, 1300, UK) at 800°C for 1 h. The non-heat treated part of the batch was designated as nHA and the sintered part as mHA.

### 5.1.3. XRD of HA powders

Prior to preparation of the composite, the phase composition and crystallinity of the ‘‘as prepared’’ and calcined HA powder were analysed by using an X-ray diffractometer (section 3.6.1).

The peak broadening of the XRD peaks was used to estimate the crystallite size in a direction perpendicular to the crystallographic plane based on Scherrer’s formula (3.1) as follows (Pang and Bao 2003):

$$X_s = \frac{0.9\lambda}{\text{FWHM}\cos\theta} \tag{5.1}$$

Where $X_s$ is the crystallite size (nm), λ the wavelength of X-ray beam (λ=0.15406 nm for Cu Kα radiation), FWHM the full width at half maximum for the diffraction peak under consideration [rad]; and θ the diffraction angle [º]. The diffraction peak at 2θ=26.04 was chosen for calculation of the crystallite size since it was clearly identifiable in both material types and was relatively uninfluenced by adjacent peaks.

Specific surface area of the both synthesized nano-sacle and micro-scale hydroxyapatite were measured (Table 5.1) by BET surface area analyzer (section 3.7.).

### 5.1.4. Preparation of GG/HA composite

To prepare the pure GG hydrogel, low-acyl gellan powder (Kelcogel, GG-LA, Atlanta, USA) was dissolved in distilled water at 2.5% (w/w) at 90ºC with continuous stirring. The concentration of GG hydrocolloid was kept at a constant 2.5% (w/w) for all the composites. The prepared HA nanoparticles were incorporated into the GG dispersion to make the composite. Five and three composites were prepared with nHA and mHA, respectively (Table 5.1) to investigate the effect of size and crystallinity of hydroxyapatite on composite mechanical properties. The un-sintered (nano-size) and sintered (micro-size) HA were added into gellan solution in the form of a sol and as fine powders, respectively.

In the case of HA sol, the nano-size HAP (un-sintered) was first dispersed completely in double-distilled water with the homogeniser at 26,000 rpm for 3 min. The dispersion was then added to the gellan colloid and stirred continuously, then 5mL of $CaCl_2$ (calcium chloride, Merck, Germany) was added and stirred continuously for 1 min. The resulting solutions were poured into a cylindrical mould of diameter 21mm and height 80mm and transferred to a refrigerator at 4ºC to accelerate gel formation.

The influence of size and crystallinity of the HA in two forms of nano-scale and micro-scale crystallite size on the mechanical properties of the GG hydrogel and composites was determined by compression testing using a Universal Testing machine (5848, Instron, UK) at a cross-head speed of 20 mm/min. The samples were cylindrical with a diameter of 21mm and a height of 20mm and were cut from the previously prepared cylindrical specimens using a razor blade. The mechanical properties (compressive strength and bulk modulus) were the mean of eight measurements. A t-test was used to determine the statistical significance of the differences in mechanical properties.

Compressive strength can be calculated as follows:

$$\sigma = \frac{\mathrm{F}}{A} \qquad (5.2)$$

Where F is the load applied (N) and A is original cross sectional area

And for bulk modulus, initially Strain is given by:

$$\varepsilon = \frac{\Delta \mathrm{L}}{\mathrm{L}_{\circ}} \qquad (5.3)$$

Where $\Delta$L is reduction of length and $\mathrm{L}_{\circ}$ is original length of the samples

And Young's modulus can be calculated as follow:

$$E = \frac{\text{stress}}{\text{strain}} \qquad (5.4)$$

**Table 5.1. Preparation conditions for GG/HAP composite**

| Gellan gum/HA composite | | | | |
|---|---|---|---|---|
| **Gellan gum solution concentration (Wt %)** | **HA content (wt %)** | | **Surface area ($m^2$/g)** | |
| | **Sol (nano-size)** | **Powder (micro-size)** | **Un-sintered (nHA)** | **Sintered (mHA)** |
| **2.5** | **0** | **0** | | |
| **2.5** | **0.25** | **0.25** | | |
| **2.5** | **2.5** | **2.5** | **84.72±0.06** | **7.93±0.02** |
| **2.5** | **25** | **25** | | |
| **2.5** | **50** | **-** | | |
| **2.5** | **75** | **-** | | |

## 5.2. Results

### 5.2.1. Determining phase composition and crystallite size of synthesised HA particles

The XRD patterns from the "as prepared" HA after drying at 65°C (un-sintered) exhibited only peaks indicative of HA and the samples that were sintered at 800 °C displayed both peaks typical of HA and some β-TCP as a result of decomposition of HA during sintering (Figure 5.1).

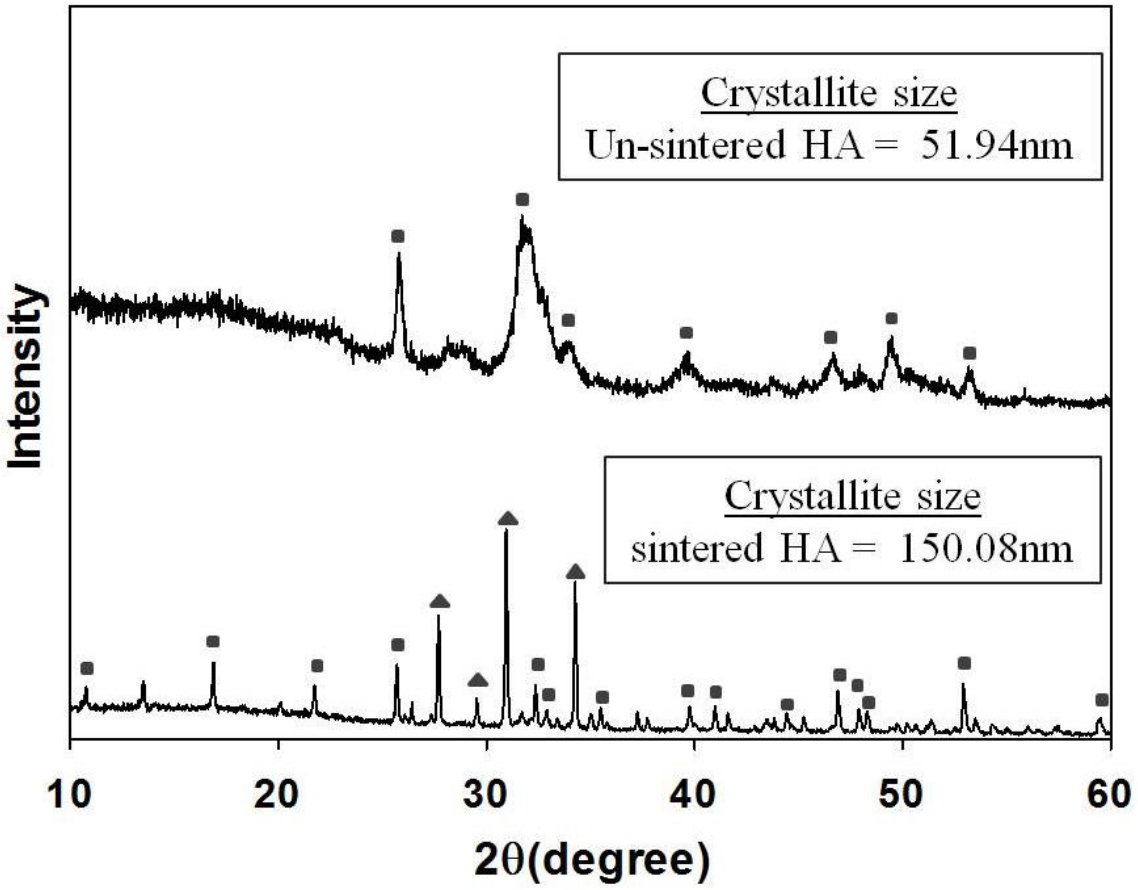


**Figure 5.1: Powder diffraction pattern of nanocrystal synthesised HA 'as prepared HA' at 65°C temperature (top) and micro-scale crystallite HA sintered at 800°C temperature (bottom). Peaks indicative of HA and β-TCP are marked with rectangles and triangles, respectively. The diffraction peak at $2\theta$=26.04 (002) was chosen for calculation of the crystallite size. Inset: the crystallite size of HA calculated by Scherrer's equation.**

In the case of the non-heat treated specimen, the peaks indicative of HA were broader than those of the sintered HA, indicating an increase in particle size following heat treatment. The calculated crystallite size ($X_s$) of the HA before and after sintering using Scherrer's formula were 52 and 150 nm, respectively (Figure 5.1).

### 5.2.2. Determining the morphology of the heated and non-heated HA crystals

TEM micrographs were also used to estimate the average HA crystallite size and morphology of the heat treated and non-heat treated specimens (Figure 5.2). The crystallite size of the HA synthesized at low temperature consisted of elliptical HA crystals of approximately ~50 nm in length and ~20nm in width and the particles on the grid were highly agglomerated. In comparison the HA particles sintered at 800° C appeared to be larger than the nHA particles (as shown in Figure 5.2), but were still in the form of elongated elliptical crystallites. These particles, however, were of a more regular morphology and showed less tendency to aggregate on the grid than the nHA particles.

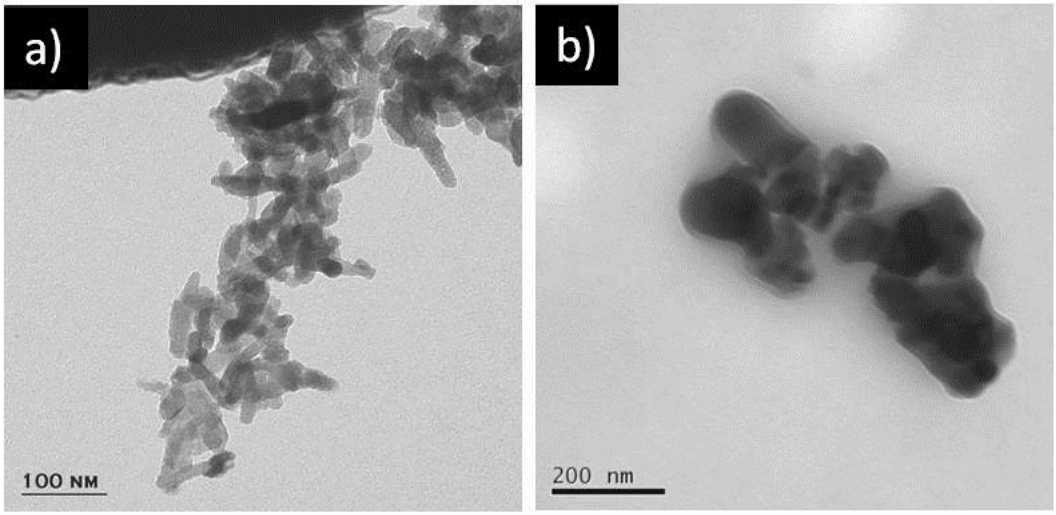


**Figure 5.2: TEM micrograph of the as- prepared HA powder, a) before heat treatment and b) the HA powder after heat treatment.**

### 5.2.3. Effect of size and crystallinity of HA particles on compressive strength and modulus of the composites

Prior to inclusion of HA crystals into the GG matrix, the GG hydrogel exhibited a compressive strength and modulus of 39.9 ± 2.6 KPa and 94.3 ± 7.3 KPa, respectively. Following the inclusion of nano sized HA crystals into GG matrix, the compressive strength and modulus of the composite significantly increased ($p<0.001$) to 70.6 ± 4.5 KPa and 180.9 ± 8.1 KPa, respectively (Figure 5.3A & 5.3B). In the case of mHA crystals, however, there was a significant ($p<0.001$) reduction in the mechanical properties of the composite (Figure 5.3A & 5.3B).

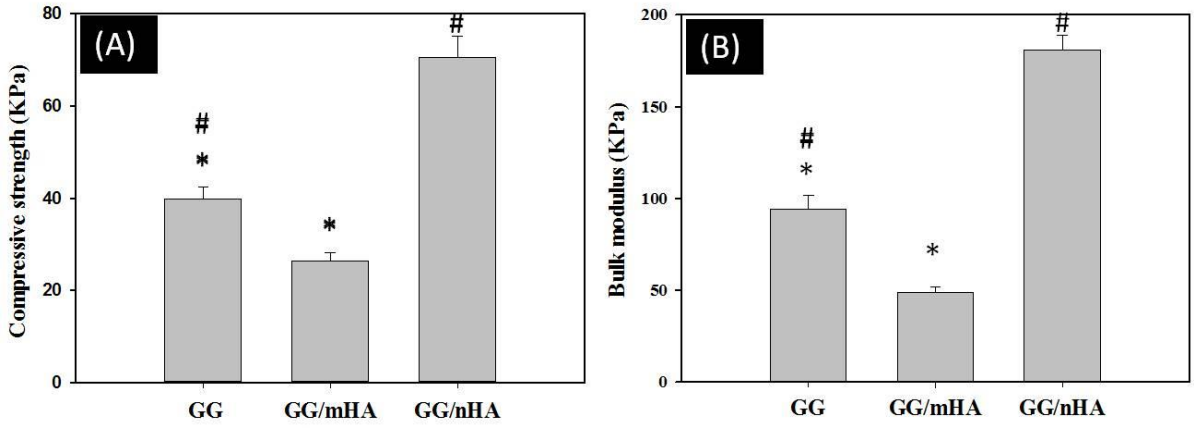


**Figure 5.3: (A) The compressive strength and (B) The bulk modulus of the 2.5%GG, 2.5%GG/2.5%mHA, and 2.5%GG/2.5% nHA (w/w). Results are displayed as mean of n = 8 specimens ± standard deviation. $^{*,\#}$ $p<0.001$**

### 5.2.4 Effect of size and crystallinity of HA particles on the nanostructure of the composite

To further determine the effect of nHA and mHA crystals on the nanostructure of the composite, SEM images of the microstructure of the unmodified GG (Figure 5.4a, 5.4b), GG/m-HA (Fig. 5.4c, 5.4d) and GG/n-HA (Figure 5.4c) were collected. From Figure 5.4 it can be noted that the unmodified GG hydrogel has a nanostructure with pore size diameter of ~0.2-0.5 μm. The inclusion of micro-sized HA crystals resulted in a less dense composite matrix with larger pore sizes of approximately 1 μm compared to GG hydrogel. In comparison, a densely packed mesh with smaller pore size was formed in the case of the gel containing the nHA particles (Figure 5.4e, 5.4f).

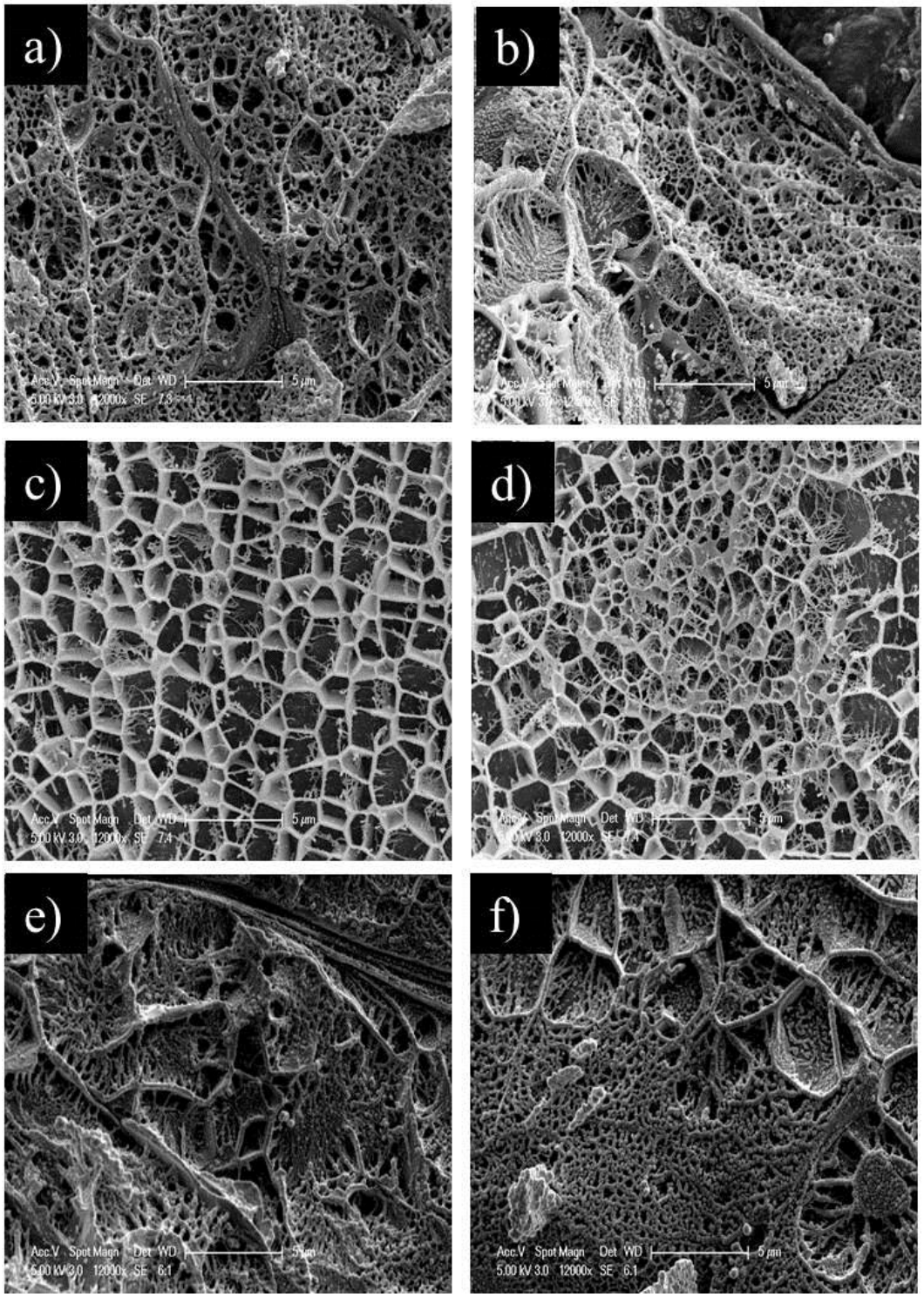


**Figure 5.4: SEM micrographs of a,b) 2.5%GG hydrogel, c,d) 2.5%GG/2.5%mHA (w/w), and e,f) 2.5%GG/2.5%nHA (w/w). Scale bars = 5µm.**

### 5.2.5. Effect of nHA and mHA content on the mechanical properties of composite

To investigate the effect of the HA content on the mechanical properties, further experimentation was carried out with nHA concentrations in the range of 0.25 – 75wt%. The compressive strength and bulk modulus of the composite increased with the nHA content (Figure 5.5A & 5.5B). The maximum value of compressive strength (162.5±9.3 KPa) (Table 5.2) was observed when the nHA content reached 50 wt%. Particle reinforcement of the gel had a similar effect on bulk modulus of the GG/nHA composite as it did to the compressive strength (Figure 5.5B). The bulk modulus of the composite was increased by 9 fold from 94.3±7.3 KPa without nHA addition to 880.8±67.4 KPa (Table 5.2) when the nHA was incorporated at 50 wt.%, however there was a reduction when the HA content was increased to 75 wt%. This suggests that the nHA crystals at high concentration of 75 wt% might not produce a homogenous composite, perhaps as a result of particle agglomeration. It is noteworthy that the incorporation of nHA crystals even at a concentration of 0.25% was effective in improving the mechanical properties of the composite (Figure 5.5A& 5.5B). In comparison, there was no general trend increase in the mechanical properties of the mHA/GG composite when the mHA content was increased (Figure 5.5A&5.5B). In the case of mHA only three concentrations of 0.25% and 2.5% and 25% were examined as the large crystal size of HA at high concentration led to high levels of agglomeration within the gel and subsequently heterogeneity of the samples. As such, it was not possible to make gel samples using mHA/GG at concentrations higher than 25%. The incorporation of mHA crystals even at a concentration of 0.25% decreased both compressive strength and bulk modulus of the composite compared to GG hydrogel and nHA/GG composite. This effect was significant when the concentration of mHA increased to 2.5% (Figure 5.5A&5.5B). An increase in the

compressive strength and bulk modulus of the mHA/GG composite was observed only when the mHA concentration was at 25 wt. %. The large errors associated with the measurement of mechanical properties at a ceramic loading of 25% mHA/GG could be as a result of gel heterogeneity.

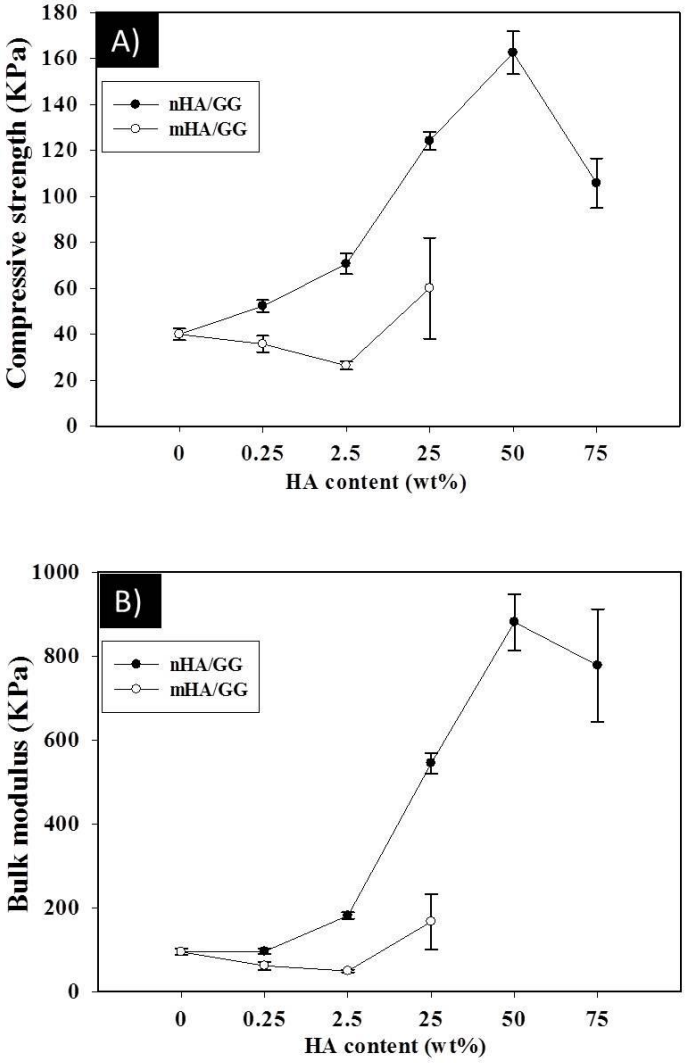


**Figure 5.5: The compressive strength of A) nHA/GG and mHA/GG composites and B) The bulk modulus of the nHA/GG and mHA/GG composites with different HA contents. The GG concentration for all composites were constant (2.5wt%). Results are displayed as mean of n = 8 specimens ± standard deviation.**

**Table 5.2. Compressive strength and bulk modulus of the composites**

| HA content | Compressive strength (KPa) | Bulk modulus (KPa) |
|---|---|---|
| (Wt.%) | GG/nHA | GG/nHA |
| 0 | 39.9±2.5 | 94.3±7.3 |
| 0.25 | 52.2±2.6 | 95.7±6.1 |
| 2.5 | 70.6±4.4 | 180.9±8.1 |
| 25 | 124.1±3.8 | 544.6±24.1 |
| 50 | 162.5±9.2 | 880.7±67.3 |

## 5.2.6. Deformation behaviour of GG hydrogel and GG/HA composites

The stress-strain curves for the unmodified GG, and modified GG hydrogel reinforced using micro and nanoscale HA crystals, are shown in Figure 5.6. From the stress- strain curves one may note that the deformation behaviour of unmodified GG contrasted with the GG/HA composites. In the case of the GG hydrogel the initial fracture initiated at ~40 KPa, followed by a sharp reduction in stress (Figure 5.6a). The deformation behaviour of GG/mHA and GG/nAH, however, differed dramatically from unmodified GG in that the load required to enable deformation of the specimens continued to increase (Figure 5.6b and 5.6c). Crack growth in the material was slow indicating a different failure mechanism.

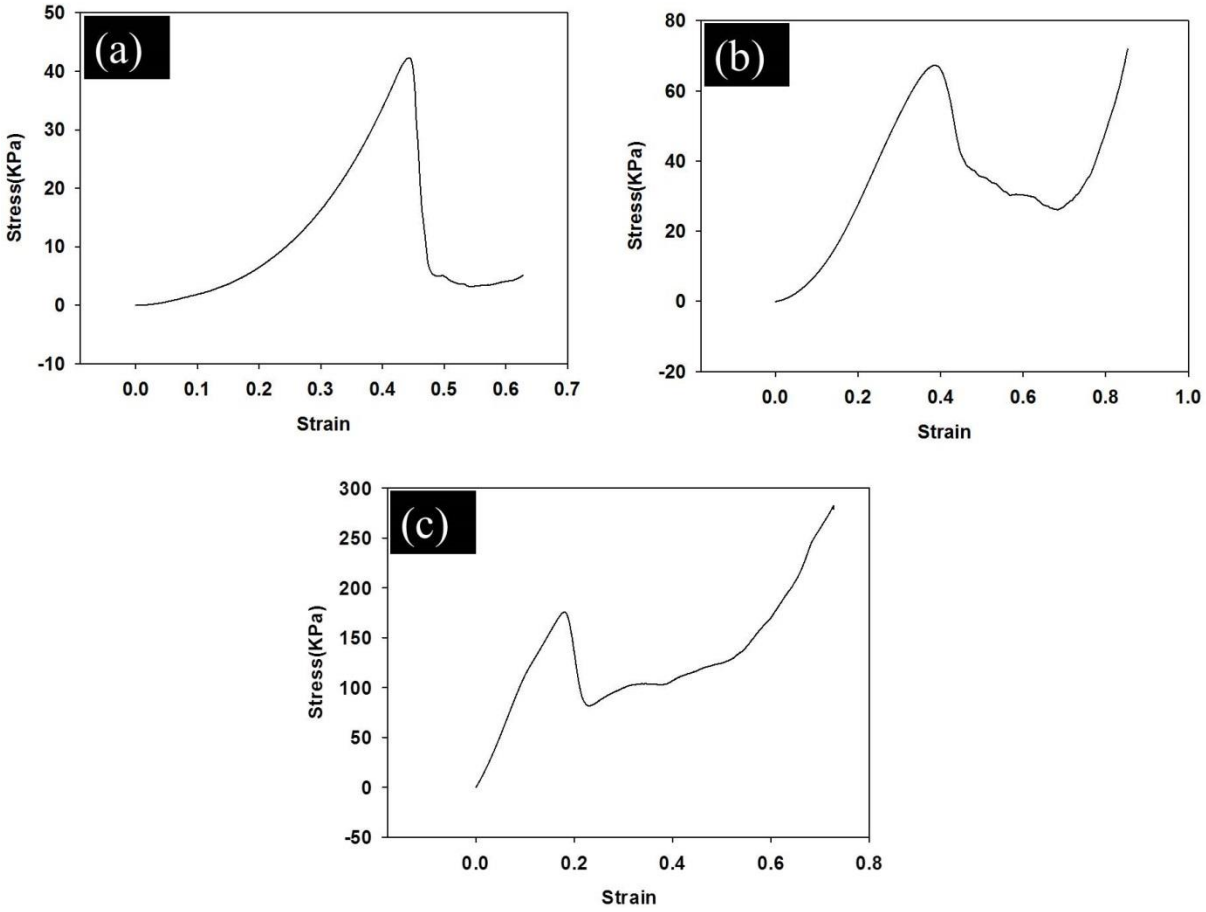


**Figure 5.6: Typical stress-strain curves of a) unmodified GG hydrogel, b) 2.5%GG/ 25%mHA, and c) 2.5%GG / 50%nHA.**

## 5.3. Discussion

Hydrogels are widely used in tissue regeneration since, on the nanoscale, they are of similar morphology to the extracellular matrix (ECM). They also exhibit a high water content enabling mass transport of nutrients to and waste products from encapsulated cells. One important parameter, which has been shown to influence the type of tissue formed around the material, is its elastic modulus. It has been proposed that controlling the modulus of the implanted materials may therefore influence tissue formation *in vivo* (Byrne et al. 2007). As a

consequence several authors have modified the mechanical properties exhibited by hydrogels using hydroxyapatite particles as fillers (Lin and Yeh 2004; Liuyun et al. 2008; Swetha et al. 2010). To date, however, no-one has systematically evaluated the effect of size and crystallinity of the encapsulated HA particles on the bulk mechanical properties of the composite.

The level of crystallinity and the morphology of the reinforcing HA particles used in this study were adjusted by sintering at a temperature low enough to avoid complete phase transformation to β-tricalcium phosphate (β-TCP; $Ca_3(PO_4)_2$). Indeed XRD demonstrated that sintering at 800°C resulted in no phase change, but did result in a significant increase in the crystallite size of the material (Figure 5.1). This was further confirmed using transmission electron microscopy (Figure 5.2) and is in agreement with previous research (Pang and Bao 2003; Santos et al. 2004).

The incorporation of the nHA reinforcement resulted in significant increases in both the bulk modulus and yield strengths of the composite materials (Figures 5.3 and 5.5), yet reinforcement using the mHA resulted in a significant reduction in both yield strength and bulk modulus (Figure 5.3). The mechanical properties of a composite material are determined by factors, including: the mechanical properties of the filler material, the volume fraction of the reinforcing agent, the homogeneity of the composite matrix and stress transfer between the reinforcing particulate and the bulk matrix (Ebrahimian-Hosseinabadi et al. 2011). In the case of the composite investigated in this study, it is likely that the size effect of the reinforcement may be attributed to both nanostructural changes in the gel matrix and also matrix heterogeneity. Indeed, SEMs of the gel nanostructure demonstrate that the mean pore size of the nHA reinforced gel is not significantly influenced by nHA addition (Figure 5.4),

whereas the pore size of the mHA reinforced material is significantly increased (Figure 5.4). The gelation of GG proceeds through the formation of triple helices which subsequently aggregate to form fibres. The presence of the mHA may have disrupted this process, resulting in the formation of fewer cross-links between the polymer fibres and hence a less dense network with a larger mean pore size. Such a nanostructural change has previously been reported to cause a significant reduction in the mechanical properties of chitosan gels (Francis Suh and Matthew 2000) . GG junction zones are thought to be ~1.5 nm in diameter and are formed from four aggregated gellan helices (Yoshida and Takahashi 1993). It may be that the small crystallite size of the nHA prevented any significant change in the molecular organisation of the gel matrix. It may also be that the relatively high specific surface area of the nHA enabled more effective wetting of the crystallites than the mHA crystallites, thus enhancing the interaction between the polymer matrix and the ceramic phase (Rajkumar et al. 2011). Such an increase in matrix/reinforcing agent interaction would result in a significant increase in both the strength and stiffness of the material. Interactions between the gellan and the nHA, may have maintained the dispersion of the particulate during gelation, resulting in a more homogeneous gel matrix than in the case of the mHA reinforcement. Large-scale heterogeneities in gels have been previously reported to cause a weakening of the bulk material (Zhou et al. 2009). Increasing levels of nHA loading in the material resulted in a monotonic increase in both yield strength and bulk modulus up to a loading of 50wt. % after which, there was a significant reduction (Figure 5.5). It is possible, therefore that it is at this point that the weight fraction of particles became sufficient that the GG was not able to maintain crystallite dispersion resulting in the formation of heterogeneities within the composite matrix.

## 5.4. Conclusion

In this part of this chapter it was shown that the size and crystallinity of the calcium phosphate crystals have significant effects on the mechanical properties of a GG matrix. It was shown that while the inclusion of nHA significantly increased the compressive strength and bulk modulus of the GG hydrogel, the microscale (mHA) material acted to weaken it (2.5wt. %HA). Furthermore, it was found that by increasing the content of the nHA in the composite to 50 wt%, the yield strength and bulk modulus was increased by four- and nine fold, respectively. By using different levels of nHA reinforcement in the gel matrix, therefore, it will be possible to produce materials of defined modulus, which may be investigated in the future to control cell differentiation.

# Chapter 5B: nHA/gellan gum nano-composite beads with osteogenic potential

In the previous section it was shown that the incorporation of nano-crystalline hydroxyapatite into a gellan matrix was effective in adjusting the mechanical properties of the nano-composite which would be beneficial for the control of desired tissue formation. In this section of the chapter, nano-sized hydroxyapatite was used to manufacture gellan gum/hydroxyapatite culture beads.

Here we have fabricated uniform pure GG beads and nHA/GG culture beads using a water-in-oil method. The optimum level of incorporated nHA into GG matrix required to initiate cell attachment was determined. MC3T3 cell attachment and proliferation were evaluated to demonstrate cell responses on GG and GG/nHA beads with various nHA loading and compared with that of a GG/nHA disk and conventional tissue culture plastic.

The feasibility of using the GG/nHA beads in spinner flask cultures for cell expansion was also evaluated and compared to that of conventional monolayer cultures and static beads cultures. Furthermore the ALP activity of the MC3T3 pre-osteoblast cells grown on GG/nHA beads and the ability to produce mineralised matrix and nodules was examined. Preliminary experiments were performed with BMSC cells to evaluate the potential of the beads to stimulate osteogenic differentiation,

## 5.5. Methods and materials

### 5.5.1. Synthesis of GG/nHA and GG beads using water-in-oil technique

The GG/nHA beads with an average size of 500μm were prepared using a water-in-oil emulsion method as illustrated in Figure 5.7. Briefly, The GG solution was prepared by dissolving low-acyl gellan powder in distilled water at 2.5% (w/w) at 90°C. HA sol was prepared by dispersing the nHA powder in distilled water with the homogenizer at 24,000 rpm for 3 min. The sol was then added into 2.5% gellan solution at 90°C. The mixture of GG/nHA solution was added into pre-heated 90˚C oil phase under stirring at 500 rpm for 10 minutes. The mixture was finally transferred into an excess amount of 1wt% $CaCl_2$ solution to enhance the gel strength.

The pure GG beads were also prepared with the aforementioned method without addition of HA sol into the GG solution as a control. The fabricated beads were sterilized with ethanol (70%; Fisher Scientific) and then immersed in PBS and left overnight under ultraviolet light to complete the sterilization process for cell culture.

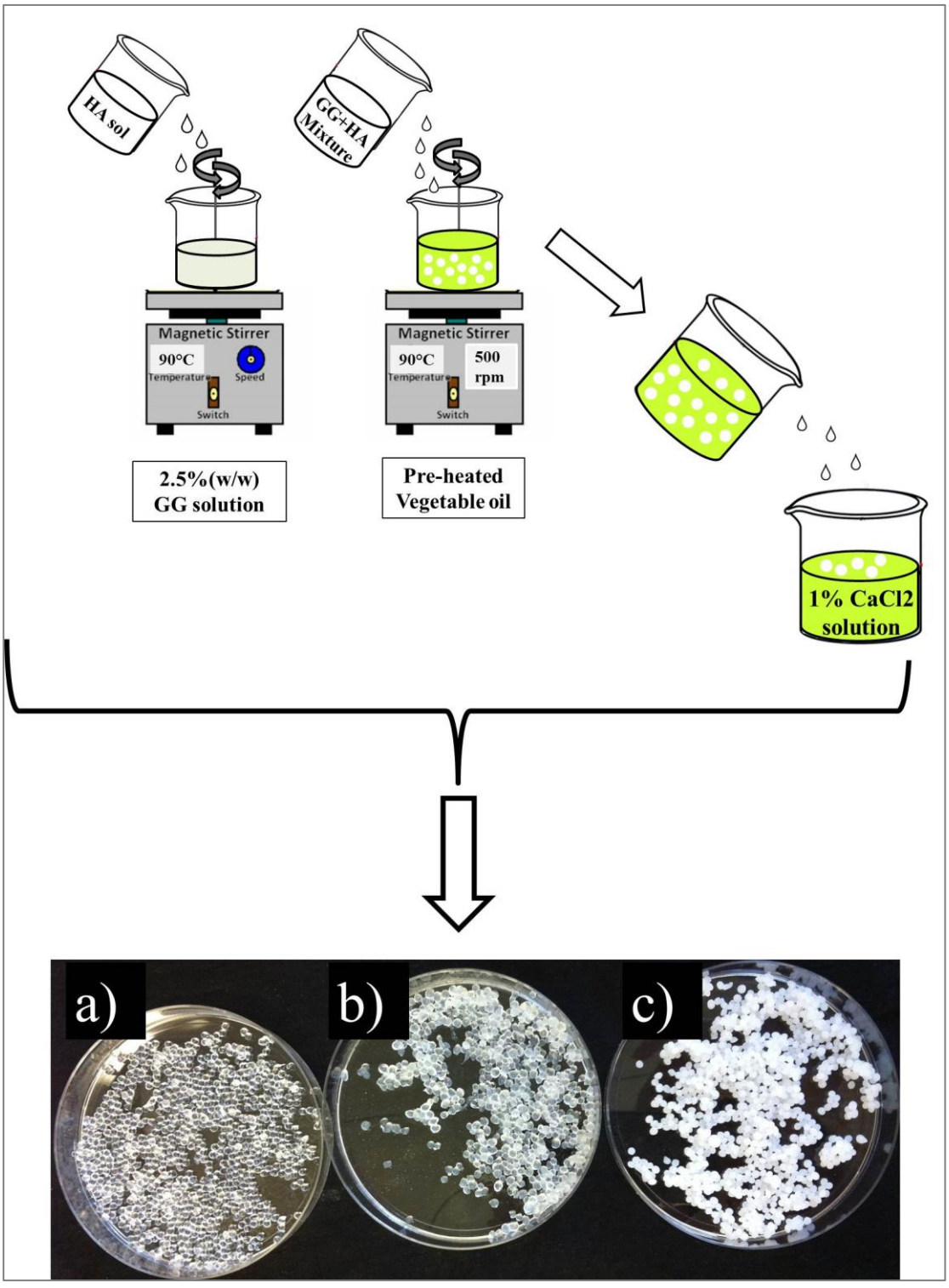


**Figure 5.7: The production of GG/nHA beads by the water-in-oil method and images of fabricated beads a) GG beads prepared without HA sol addition, b) GG/0.25%nHA and c)GG/ 25%nHA beads**

To determine the optimum level of nano-hydroxyapatite in to GG matrix to facilitate cell attachment, various HA contents of 0.25%, 2.5%, 5% and 25% (w/w) were used to manufacture nHA/GG culture beads.

Disc-shaped samples of the GG/HA composites were also prepared by pouring the gellan-nHA mixture into a disk mould of diameter 13mm and thickness of 2mm and transferred to a refrigerator at 4°C to accelerate gel formation. Samples were then sterilized using the same method as for the beads.

## 5.5.2. Cell culture on the GG, GG/HA beads, and GG/HA disk shape samples

### 5.5.2.1. Static condition

Mouse MC3T3 cells were used to evaluate the potentials of GG/HA beads as candidate culture beads for cell delivery. The GG beads and GG/HA beads were used in a concentration of 0.1g approximately of 200 beads, per well of sylgard pre-coated 24-well plate. The total surface area of the beads in each well was around 2.2$cm^2$ (equivalent to the surface area of a well of a 24-well plate as control).

Cells were seeded onto the sterile GG, GG/HA beads and disc-shaped samples separately at final density of 2 x$10^4$ cells /$cm^2$ surface of GG /nHA beads and GG /nHA disks. The viability of cells seeded on to the surface of the beads was analysed using an MTT assay after culturing for 7 days (section 3.2).

The number of adherent cells on to GG /nHA beads was also labelled with DAPI (section 3.3) and samples were visualised using confocal laser microscopy (Leica, UK).

### 5.5.2.2. Dynamic condition-spinner flask

For stirred cultures, 25-ml spinner flasks from Wheaton were used, with a final volume of 25 ml. The spinner flasks were placed on a magnetic stirrer inside a 37°C incubator with 5% $CO_2$. The GG/HA beads were used in a concentration of 180mg, per flask. The total available surface area of the beads in each flask was around 2.2$cm^2$ (equivalent to the surface area in static condition). Cell seeding was performed at final density of 2 x$10^4$ cells /$cm^2$ surface of nHA/GG beads with intermittent stirring for 2 minutes every 30 minutes at 25 rpm for 3 hours, it was then increased to 45 rpm for 1.5 hours. Continuous stirring at 45, 50, 55 to a final 65 rpm was continued at 15 minute intervals (Tebb et al. 2006). Sampling of the cell-beads complexes were performed at required time-points for evaluation of cell adherence and proliferation. The cell adherence and proliferation was determined using MTT assay (section 3.2) and scanning electron microscopy as described in section 3.8.1.1 was used to observe the cell morphology and distribution

## 5.5.3. Cell differentiation

The functional activity of the MC3T3 pre-osteoblast cells grown on GG/HA beads was examined by measuring ALP activity as described in section 3.4. Furthermore mineralised matrix and nodules formation was estimated by Alizarin Red S staining, at interval times (section 3.5). The same experiment was performed with BMSCs to demonstrate the potential of these beads to stimulate osteogenic differentiation.

## 5.6. Results

### 5.6.1. Characterization of fabricated beads

#### 5.6.1.1. Optical and SEM analysis

Pure GG culture beads and nHA/GG composite culture beads with various nHA content of 0.25%, 2.5%, 5% and 25% (w/w) were successfully fabricated using emulsification method. Figure 5.8 is the image of GG/nHA beads taken by bright field microscope. Twenty beads were chosen randomly to measure the beads diameter. As shown spherical composite beads with diameter approximately 300-500 µm could be fabricated using the emulsification method. The SEM micrograph was also used to estimate the average size of fabricated beads confirming formation of uniform spheres and to examine the morphology of the beads (Figure 5.9A). The surface morphology shows the presence of fine nHA particulate material distributed evenly and confirmed that the GG and nHA mixed homogeneously. It can also been shown a relatively smooth surface with a textured surface on the micro-scale (Figure 5.9B).

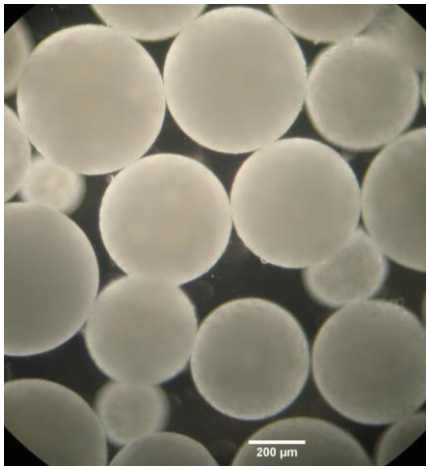


**Figure 5.8. The optical micrograph of composite GG/nHA beads fabricated using emulsion technique. The average diameter of the beads is between 300-500µm.**

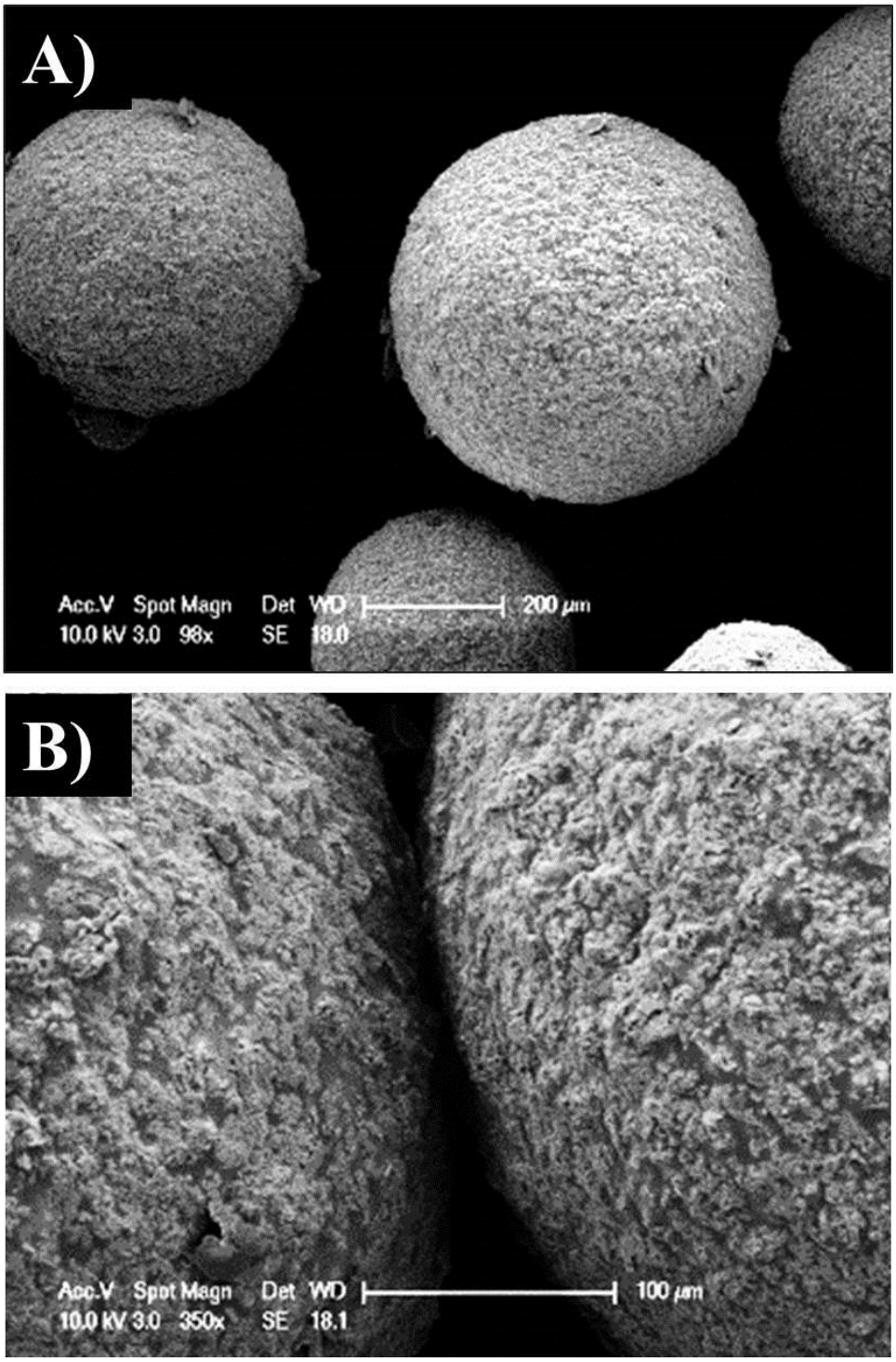


**Figure 5.9: SEM micrograph of GG/nHA composite fabricated beads at different magnification.**

## 5.6.2. Influence of nHA loading on cytocompatibility

After fabrication of the composite beads with various nHA content, the cellular response to the beads was investigated using the MTT assay. Preliminary cellular tests after culturing the beads for 7 days demonstrated that the unmodified GG and the GG/nHA composites with nHA concentration up to 2.5% (w/w) did not support cell attachment and proliferation at any time point throughout the study (Fig. 5.10). The cell attachment and proliferation was initiated when the nHA content was increased to 5wt% and there was a steady increase in cell number over the duration of the experiment (Fig 5.10).

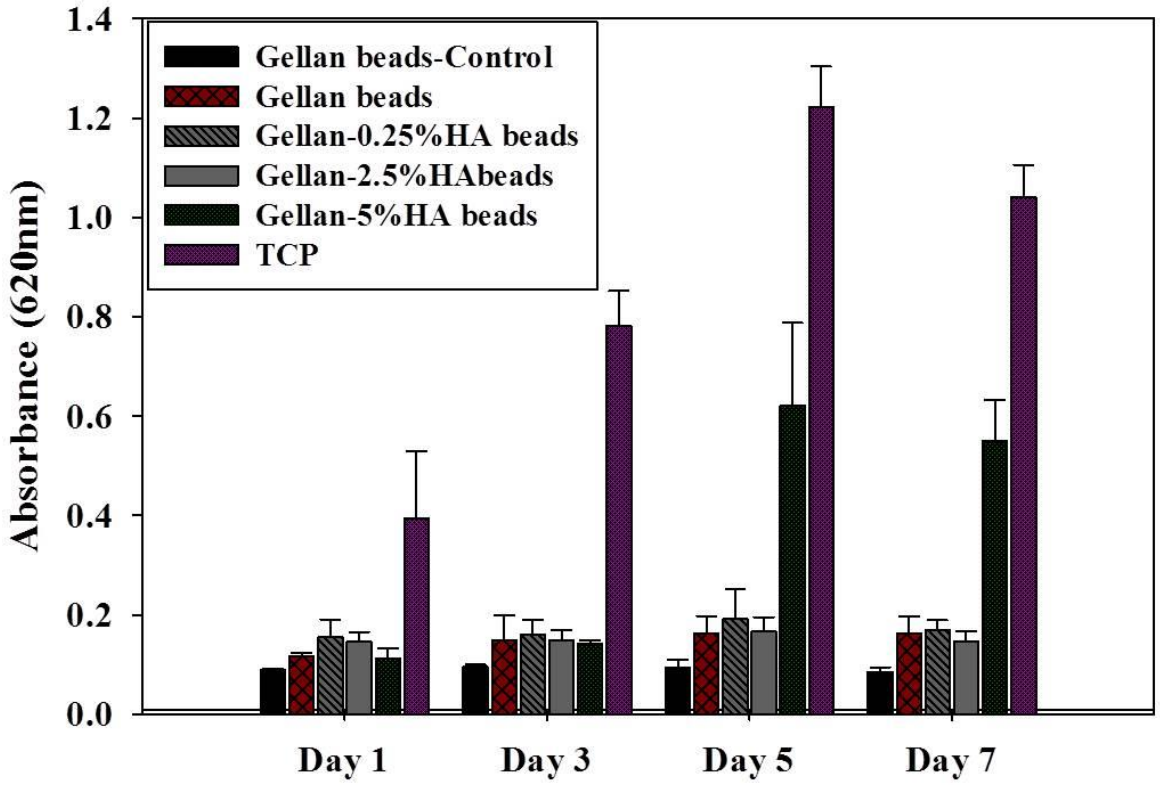


**Figure 5.10: Results from the MTT assay of MC-3T3 cell grown on GG, GG/nHA with various nHA content and tissue culture plastic (TCP). Gellan beads without cell seeding were also used as control sample.**

Increasing the nHA loading of the composite to 25wt% resulted in significant increase ($p<$ 0.001) in the cell number on the culture beads over a cultivation period of 7 days (Fig. 5.11). No significant difference was observed in cell attachment when the nHA loading of the composite was increased however, significant difference (P<0.001) in proliferation of MC3T3 pre-osteoblast cells was found between GG/5%nHA and GG/25%nHA beads. GG culture beads were used as control and it can be seen that they exhibited no cell attachment and proliferation at all over the 7 days of cultivation.

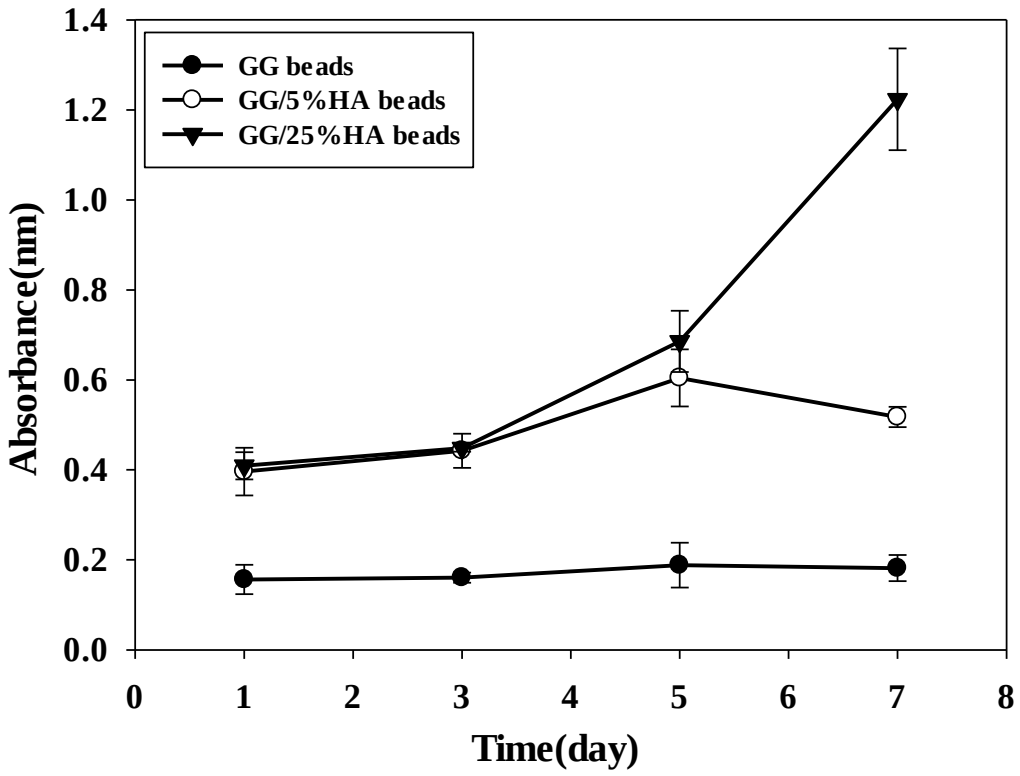


**Figure 5.11: Comparison of cell proliferation on GG/5%nHA and GG/25%nAH culture beads determined by MTT assay of MC-3T3 cell grown on to the beads shown as absorbance. GG beads didn't facilitate cell attachment and cell growth at any time point throughout the study. The number of cells on GG/25%nHA beads was seen to be significantly increased (p<0.001) than that of GG/5%nHA beads over the cultivation period. Data points represent mean values of n = 9 specimens ± standard deviation.**

The cell attachment and cell proliferation on to the GG/5%nHA and GG/25%nHA beads were also visualised and compared at day 5 using DAPI staining. The results have confirmed that the fabricated culture beads supported cell attachment and proved the presence of proliferative cells on to the beads and also as well as MTT results have demonstrated that the culture beads with 25% (w/w) nHA content showed significant increase in cell number and proliferation (Figure 5.12).

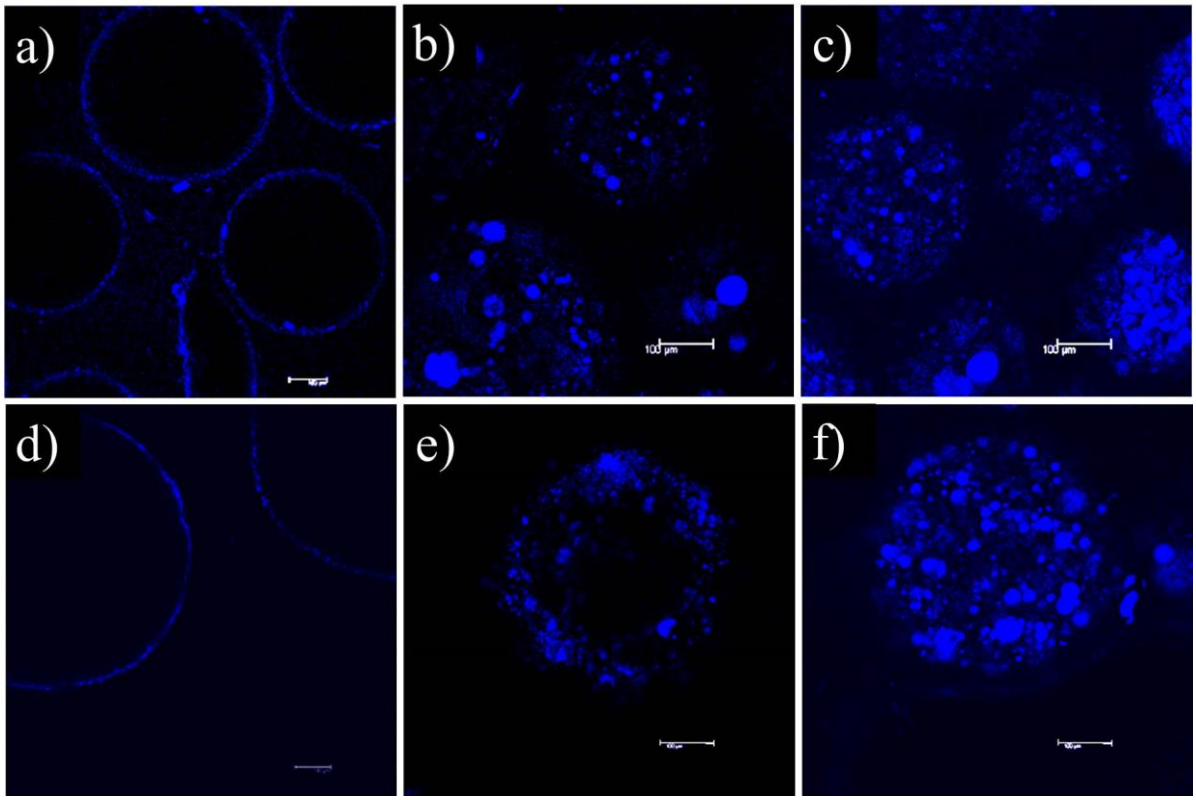


**Figure 5.12: Cell attachment and proliferation was visualized and compared under confocal laser microscopy by using nuclear stain DAPI. a and d) cell- free beads (control samples), b and e) cell-GG/5%nHA beads complexes, c and f) cell-GG/25%nHA beads complexes after culturing for 5 days. The images confirms significant increase in cell number and proliferation of MC3T3 cells on GG/25%nHA beads compared to that of GG/5%nHA beads**

### 5.6.3. Comparison of cell growth in static and dynamic culture condition

As a result the GG/25%nHA was selected and considered ideal for further cell culture study in spinner flask. The feasibility of using these beads in spinner flask cultures for cell expansion was evaluated and corasedmpared to that of conventional monolayer cultures and static beads cultures (Fig 5.10). Following seeding onto the beads at various conditions, there was a significant difference between the attachment and proliferation of MC-3T3 cells to the dynamic GG/25%nHA culture beads as compared to monolayer culture and static culture beads (Figure 5.11). In dynamic culture conditions, the cells after the inoculation enter a lag phase from day 0 to 3 days followed by a log phase of cell proliferation (day 4-6) leading to the maximum cell growth at day 7. In contrast the proliferation in static monolayer (control sample) proceeded as might be expected, the cell number increased slowly (day 1-5) and was in stationary phase by day 7 (Figure 5.11).

The static culture beads followed the same trend as dynamic condition however with significantly lower cell increase during the cultivation time. The better cell attachment and proliferation in stirred suspension cultures can be explained by the homogeneous culture environment created in the stirred culture and more availability of the entire free surface of beads in suspension culture, thus cells had a greater chance of coming into contact with microcarriers.

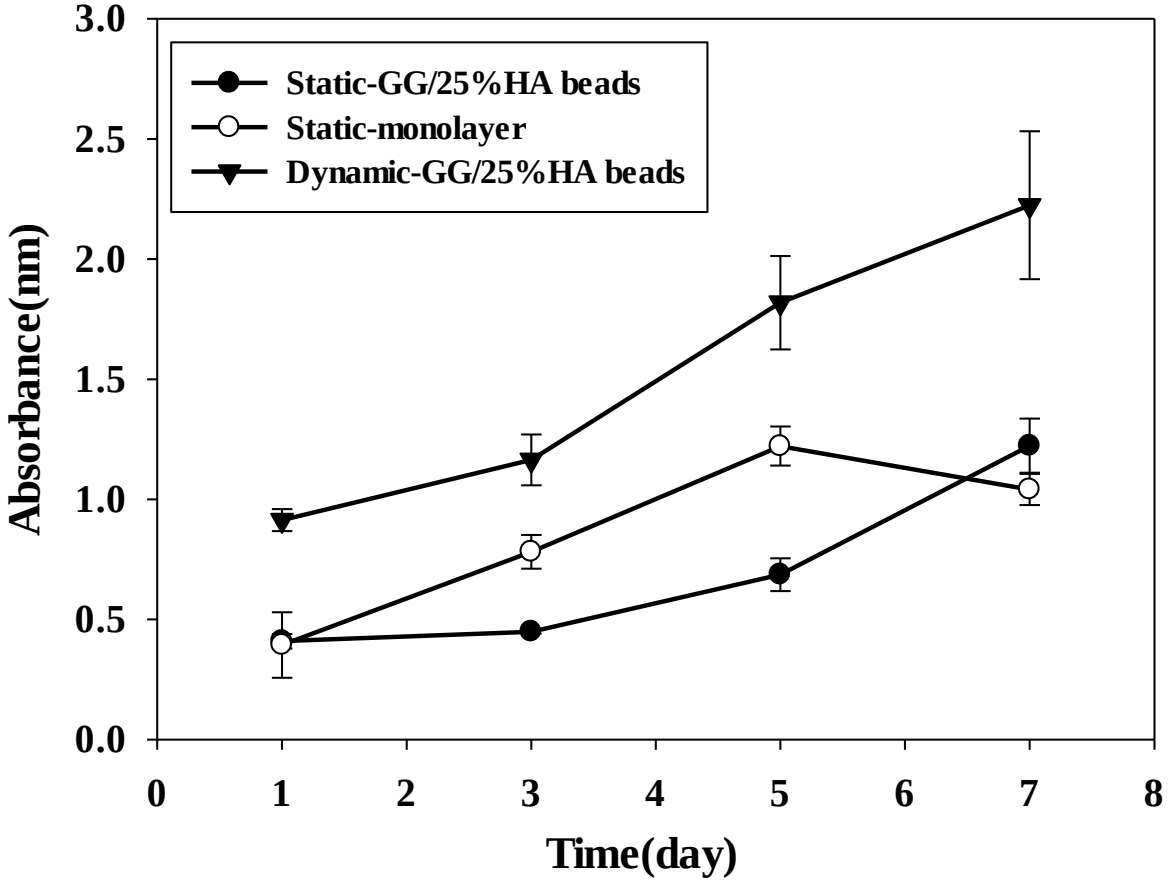


**Figure 5.13: Comparison of cell proliferation on GG/25%nHA beads with various culture conditions; static and dynamic culture condition (spinner flask). There was a significant difference ($p<0.001$)between the attachment and proliferation of MC-3T3 cells to the dynamic GG/25%nHA beads as compared to monolayer culture and static GG/25%nHA beads were seen at all-time points. Data points represent mean values of n = 9 specimens ± standard deviation.**

### 5.6.3.1. SEM analysis of cell- beads complexes

In stirred suspension cultures, the cell adherence, distribution and proliferation on to the beads were further observed by SEM. The results show that the cells grew favourably on composite beads. It was shown that the cells appeared to attach to the beads firmly and became flattened on day 3 (Figure 5.14a, b) and started to form cell bridges with the adjacent beads to form an aggregate of cells (Figure 5.14c). On day 5, active proliferation of cells was observed over the surface of the beads (Figure 5.14d).

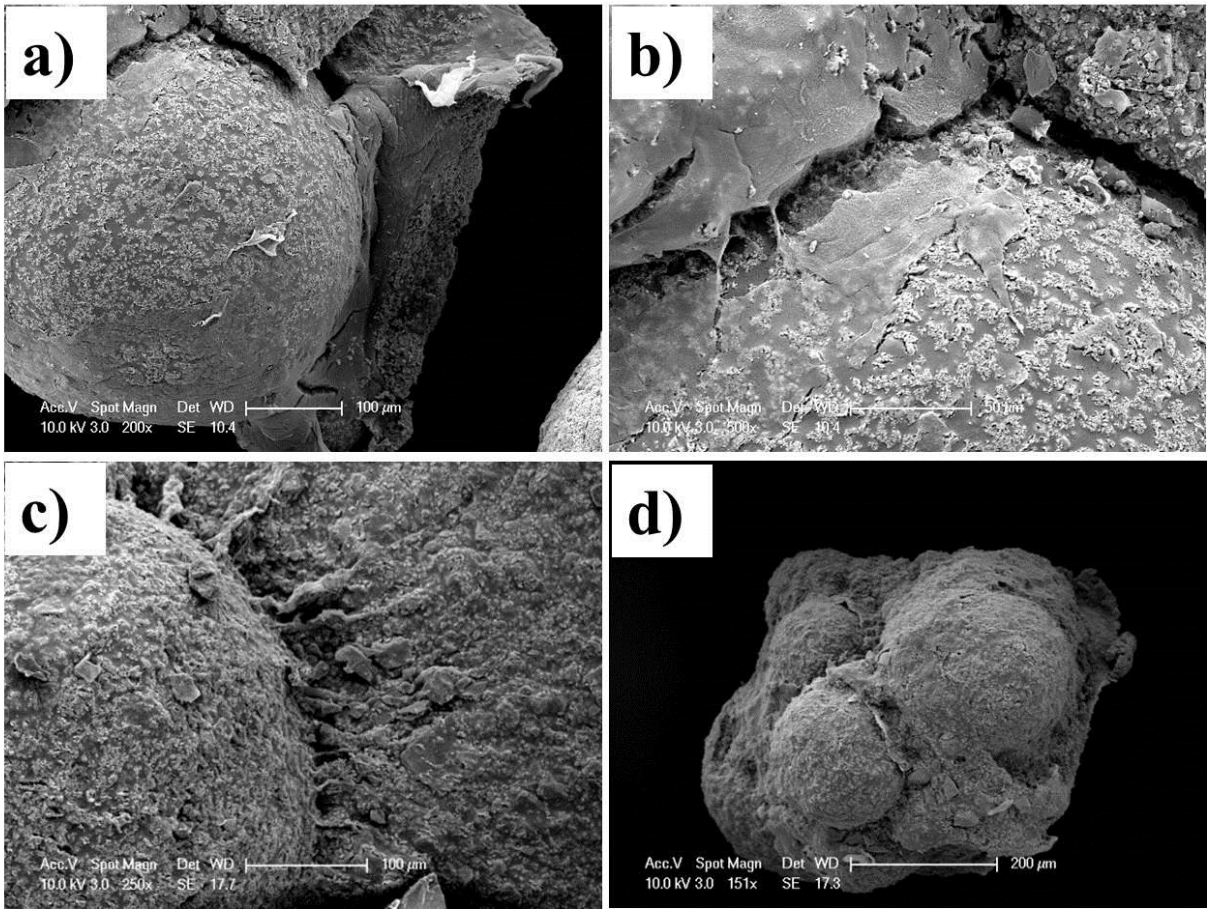


**Figure 5.14. SEM micrographs of the MC-3T3 cells grown on the surface of nHA/GG culture beads; a, b, c) day 3, and d) day 5.**

### 5.6.4. Quantitative and qualitative analysis on cultured cells differentiation

The functional activity of the MC3T3 pre-osteoblast cells grown on GG/25%nHA beads was examined by measuring ALP activity after culturing for 7 and 14 days as shown in Figure 5.15. The ALP activity was enhanced at each time point in cells cultivated on GG/25%nHA beads both in conditioned and un-conditioned culture media without requiring exogenous addition of biochemical factors compared with the cells cultured on TCP in un-conditioned culture media. The ALP activity on control cultures on TCP are only found to be increased when the culture media was supplemented with ascorbic acid, dexamethasone and β-glycerol phosphate as biochemical factors. There was a significant difference ($p < 0.001$) between ALP activity in cells on beads in un-conditioned media and un-conditioned TCP on day 14. (Figure 5.15). The increase of ALP activity in cells cultivated on beads in un-conditioned culture media suggest that the fabricated GG/25% nHA nanocomposite in the form of 3D culture beads alone might be sufficient to induce osteogenesis without the presence of biochemical factors.

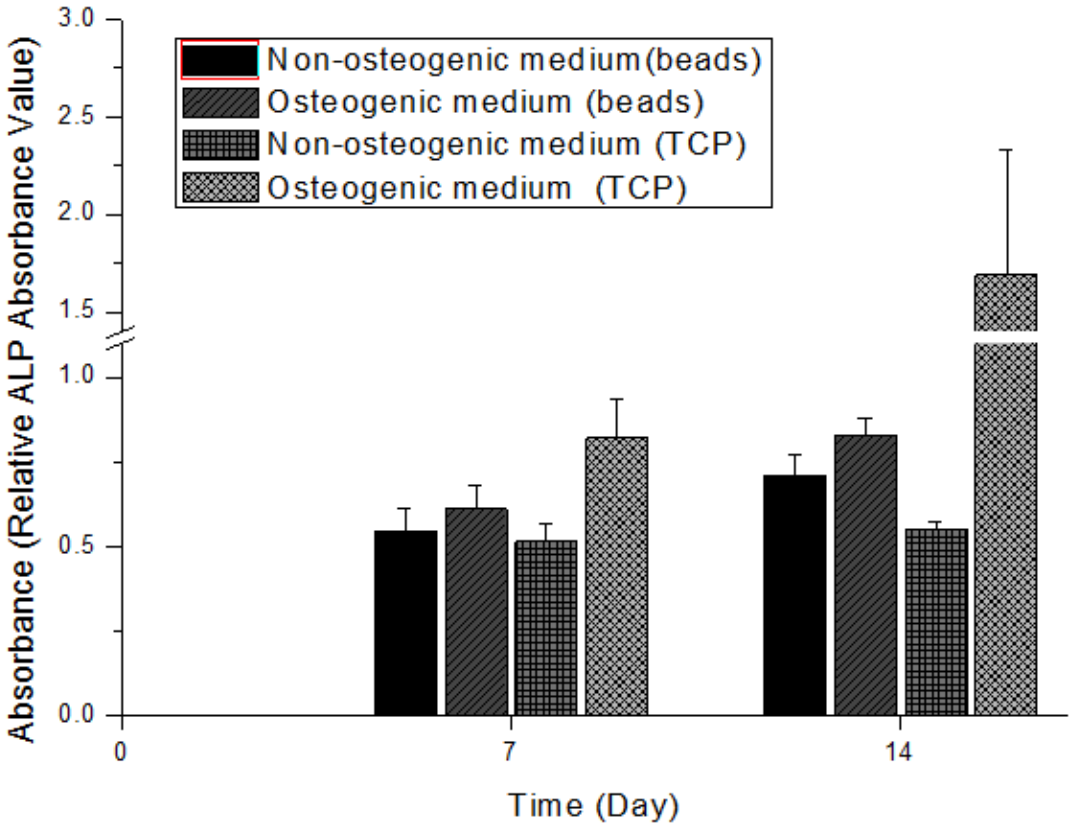


**Figure 5.15: Comparison of Alkaline phosphatase (ALP) activity of the MC3T3 cells on the GG/25%nHA beads after culturing for up to 7 and 14 days in osteogenic and non-osteogenic media. Tissue culture plastic was used as a control. ALP activity was normalised to cell number. Interestingly the ALP activity increased in cells cultivated on beads in the media without requiring exogenous addition of biochemical factors as well as in osteogenic media. The difference between ALP activity in cells on beads in un-conditioned media and in un-conditioned TCP at day 14 was significant *p<0.001.**

Furthermore mineralised matrix and nodules formation was assessed qualitatively by Alizarin Red staining (Figure 5.16). Control cultures with no cells showed no alizarin staining (Figure 5.16a, d). Cell-beads complexes in osteogenic media showed positive staining indicating the

ability of cultured cells on GG/HA beads in deposition of mineralized matrix (Figure 5.16b, c- top row) as it was confirmed with ALP activity measurement. Moreover, the culture beads without osteogenic media appeared to be able to induce differentiation and matrix mineralization (Figure 5.16e, f - bottom row).

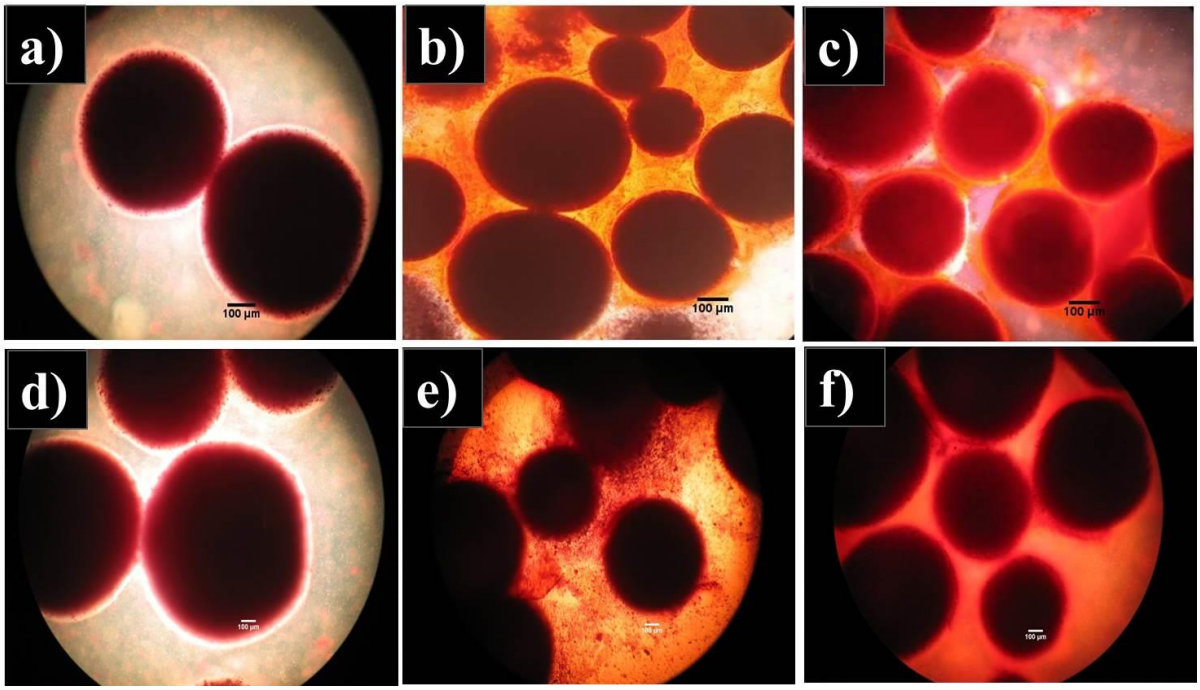


**Figure 5.16: Alizarin Red Staining of MC-3T3 cells indicating of mineralized matrix synthesis. a and d) Control-beads with no cells, b and e) cell-beads complexes in osteogenic media for 3 days , c and f) cell-beads complexes in osteogenic media for 5 days. Top row is cell-beads complexes in osteogenic media and bottom row is in non-osteogenic media. Scale bars=100µm**

In order to demonstrate the potential of these fabricated beads to stimulate osteogenic differentiation in BMSCs, preliminary experiments were undertaken with BMSCs. The ALP activity of cultured BMSCs on GG/25%nHA beads were measured after culturing for 7 days (Figure 5.17A).The ALP activity in BMSCs as well as in MC3T3 cells was found to be

increased both in osteogenic and non-osteogenic media without the need for addition of biochemical factor compared with control (Non-osteogenic media TCP). There was a significant difference between ALP activity in cells on beads in both conditioned and unconditioned media and in cells in un-conditioned TCP suggesting the osteogenic differentiation of cultivated BMSCs on GG/25%nHA beads.

Qualitative Alizarin Red staining assay also indicated the ability of cultured BMSCs on GG/nHA beads to induce differentiation and bone nodule formation (Figure 5.17B).

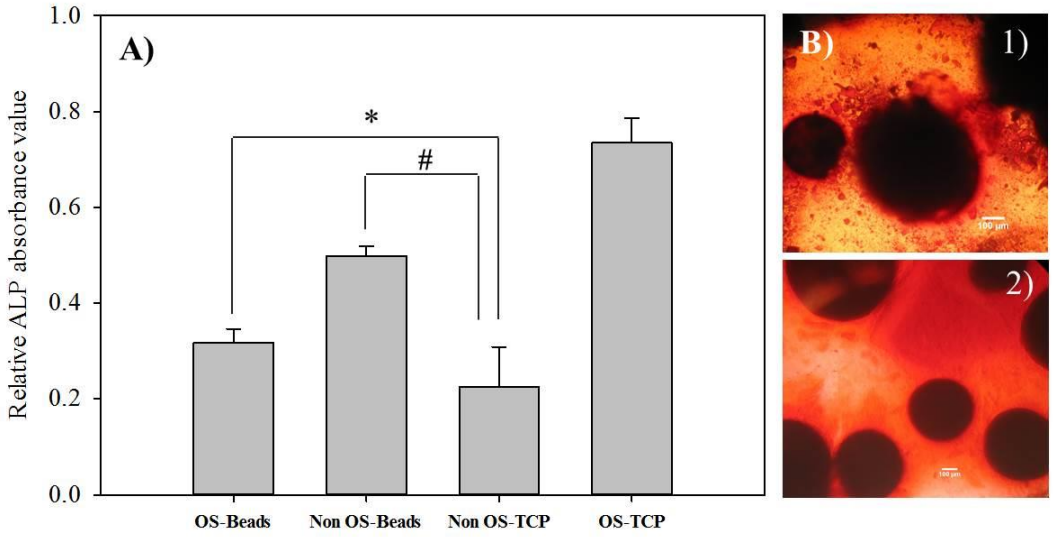


**Figure 5.17: A) Comparison of the ALP activity for the BMSCs cultured on GG/nHA beads in osteogenic media (OS-Beads), non-osteogenic media (Non OS-Beads) and Osteogenic and non-osteogniec tissue culture plastic (OS TCP and NOnOS-TCP). Cells cultured in OS-beads and Non OS-Beads were significantly higher than that of the cells in Non OS- TCP. *p<0.05 when comparing OS-beads and Non OS- TCP. # p<0.001 when comparing Non OST-beads and Non OS-TCP. B) Alizarin red staining of BMSCs in 1) osteogenic media and 2) non-osteogenic media indicating the ability of cells to induce matrix mineralization. Results are displayed as mean of n = 9 specimens ± standard deviation. Scale bar =100µm**

## 5.7. Discussion

In this study, GG/nHA composite culture beads were fabricated and MC3T3 cells were observed to attach, spread, proliferate and form mineralised nodules. It was demonstrated that the incorporation of hydroxyapatite into gellan gum at concentrations of above 5wt% can enhance the ability of gellan hydrogel to support cell attachment and proliferation (Figure .5.10). The cell attachment and proliferation which was examined with an MTT assay was initiated when the nHA content was increased to 5 wt%. The lack of cellular affinity of gellan hydrogel was due to the extremely hydrophilic nature of GG and particularly on the exterior surfaces which prevented the adsorption of ECM proteins and consequently does not allow cell attachment (Wang et al. 2008; Wang et al. 2010). The incorporation of nanocrystalline HA particulates which has been shown to have a strong adsorptive property for ECM proteins overcome this disability and support the binding of cells to its surface (Y.-L. Chang et al. 1999; Zhao et al. 2006). Due to this property of nHA, the cell number on the culture beads increased as the nHA content increased (Figure 5.11).

DAPI staining as well as MTT results qualitatively demonstrated the cell attachment and proliferation of seeded cells on to the GG/5%nHA beads and a significant increase of cell number with increasing of HA content up to 25 wt% by day 5 (Figure 5.12).

As a result, the GG/25%nHA was then selected and considered ideal for further cell culture study. The feasibility of using these beads in spinner flask cultures for cell expansion was evaluated and compared to that of conventional monolayer cultures and static beads cultures. The level of cell attachment and proliferation significantly increased in spinner flask in comparison with static culture conditions (Figure 5.13). The better cell attachment and

proliferation in stirred suspension cultures can be explained by the homogeneous culture environment created in the stirred culture and more availability of the entire free surface of beads in suspension culture, thus cells had a greater chance of coming into contact with microcarriers (Yu et al. 2004). Stirred culture systems have been reported to be suitable candidates for the expansion of cells while maintaining the original phenotypic characteristics (Boo et al. 2011). Dynamic culture systems improve the mass transport of oxygen and nutrients to the culture beads that influence a better cell growth in spinner flask (Sikavitsas et al. 2002) .

Further analysis of cell-beads complexes by SEM (Figure 5.14) following culture spinner flask showed that the cells adhered, proliferated and could form aggregates of cells on to the GG/25%nHA indicating the ability of the fabricated composite beads for cell supporting and aggregate formation which would facilitate their delivery into defect sites (Jos Malda and Frondoza 2006). The cells-beads aggregates can be delivered into the defects through injection and they can be useful to provide larger cell construct which are useful for bigger defects.

The ability of the matrix to stimulate differentiation and cells to produce mineralised matrix and nodules is important with regard to development of materials for bone regeneration. This ability depends on various factors including material composition, the microenvironment, the surface texture of scaffold, and condition of culture system (i.e. dynamic and static culture condition). The functional activity of the MC3T3 pre-osteoblast cells grown on GG/25%nHA beads were quantitatively assessed using ALP activity after culturing for 7 and 14 days, and quantitatively observed using Alizarin Red staining. The ALP activity was enhanced at each time point in cells cultivated on GG/25%nHA beads indicating the ability of fabricated

GG/HA to induce osteogenic differentiation (Figure 5.15) in this cell type. The Alizarin Red staining also demonstrated the mineralized matrix formation by cells onto the composite beads. In this study, the combination of stirred suspension-culture beads system may have the most important effect on differentiation. It has been proposed that the mechanical forces generated by the stirring action result in cellular osteogenesis and mineralization through promotion of growth factor signalling pathways (Edward Andrew Botchwey 2002; Sikavitsas et al. 2002; Yeatts and Fisher 2011; Yu et al. 2004). Differentiation and mineralization phenomena have also been reported to be affected and enhanced on rougher surfaces (Deligianni et al. 2000). However in this study, the fabricated GG/nHA exhibited a smooth surface with a presence of some texture (Figure 5.9), therefore high ALP activity in cells grown on GG/nHA beads and formation of mineralized matrix may be attributed to the matrix composition and dynamic condition of the system.

It is well known that many osteoblast cultures only mineralise in the presence of osteogenic mediator. However here, interestingly, it has been shown that the cells cultivated on beads in unconditioned media when no osteogenic mediators are present, exhibited mineralised matrix and nodules formation as evidenced by increased ALP activity and calcium deposition. This suggests that, the combination of the GG/nHA culture beads composition and its 3D-construct might provide cues that induce osteogenic differentiation. Recently Tseng et al (2012) found that the altering the culture condition from 2D to 3D microcarrier system is sufficient to induce osteogenesis without the need for osteogenic mediator in culture media through alteration of cytoskeletal tension (Tseng et al. 2012). These two mentioned factors alone might be enough to induce osteogenesis and mineralize matrix formation. The elastic modulus of the matrix in which attached cells reside is also an important factor that can have a direct impact on cell differentiation. Tissues are known to be responsive to the stiffness of their

substrate (Discher et al. 2005). As it has been previously shown in this chapter, part A, the incorporation of 25wt% into GG matrix could adjust and increase the elastic modulus by fivefold which might be alone enough to favour the functional activity cultured MC3T3 cells without the need for the presence of osteogenic mediators. The osteogenic potential of these fabricated beads in conditioned and un-conditioned media was also examined with BMSCs cells and the results from ALP activity assay and calcified matrix formation indicated by positive Alizarin Red histochemical staining in both conditions were also confirmed the suitability and ability of these culture beads for cell delivery in bone tissue regeneration. This characteristic of the GG/nHA culture beads can be very crucial in simplifying tissue engineering strategies for therapeutic application in regenerative medicine.

## 5.8. Conclusion

The results presented in this part have shown that the GG/nHA nanocomposites culture beads could be successfully fabricated which are also useful for using in spinner culture. It has been shown that the inclusion of synthetic nHA particles into GG matrix enabled cell attachment to the surface of the composite materials. It has been shown that unmodified GG and the GG/nHA composites with HA concentration up to 2.5% (w/w) did not support cell attachment and proliferation. Cell adhesion and proliferation was significantly improved when the cells cultured on GG/5%nHA and GG/25%nHA beads than when they were cultured on GG beads alone. Furthermore it was found by increasing the content of nHA into GG matrix from 5wt% to 25wt%, the proliferative activity of the MC3T3 cells increased significantly.

Further experiments demonstrated that the dynamic flow environment compared to static conditions enhanced the cell attachment and proliferation of MC-3T3 cells on GG/nHA culture beads**.** The quantitative analysis, ALP activity assessment, on cultured cells

differentiation on to the beads indicated that the ALP activity increased in cells on both conditioned and un-conditioned media compared with TCP in unconditioned media which are only found to be increased when the culture media was supplemented with osteogenic mediator. Positive alizarin red staining also indicated that the MC3T3 osteoblast–like cells cultured on 2.5%GG/25%nHA beads have been shown to form aggregates and synthesize mineralized matrix. Importantly such mineralisation occurred without the need for osteogenic mediator in culture demonstrating the remarkable ability of fabricated GG/nHA culture beads to induce osteogenesis and mineralization. These beads were also found to be capable to stimulate osteogenic differentiation when BMSCs used in the absence of osteogenic media.

# Chapter 6

# CONCLUSION AND FUTURE WORK

## 6.1. Conclusion

In this thesis, novel approaches to develop implantable calcium phosphate containing culture beads for cell therapy in bone and cartilage tissue regeneration were introduced. Two types of culture beads; resorbable calcium phosphate (brushite) culture beads and calcium phosphate (HA)/gellan gum nanocomposite culture beads were fabricated. The capacity of each type of culture bead to facilitate cell adhesion, proliferation and to maintain the phenotype of the seeded cells and deposition of mineralized matrix has been evaluated. In addition in the case of brushite beads, a comparison of methods for fabrication of these beads was also investigated, and in the case of GG/HA culture beads, prior to their fabrication, the effect of size and crystallinity of HA on the mechanical properties of hydrogel was investigated.

### 6.1.1. Novel resorbable brushite-based cell culture beads

Resorbabale brushite-based culture beads were formed using three different methods. Initially the effect of surface chemistry of brushite cement scaffold on cellular behavior was systematically investigated. It has been shown that cell attachment to the surface of the brushite cement (BC) could be inhibited by the presence of an intermediate dicalcium phosphate–citrate complex, formed in the cement as a result of using citric acid, a retardant and viscosity modifier used in many cement formulations. The BC beads formed from the mixture of β-TCP/orthophosphoric acid using citric acid did not allow cell attachment without further treatment. Aging of BC beads in serum-free Dulbecco's Modified Eagle's Medium

(DMEM) solution at 37°C for 1 week greatly enhanced the cell adhesion capacity of the material.

Furthermore, a comparison of cellular responses on three types of brushite beads prepared with different methods has been assessed and the results showed the manufacturing process and subsequent properties of the beads (surface area and topography) influenced the initial cell attachment, proliferative activity of seeded cells and matrix mineralization. Surface topography has been shown to be the most important factor in initial cell attachment and promoting osteogenic induction of osteoblasts- like cells. The proliferation activity of seeded cells was affected by surface area of fabricated brushite granules. It has been shown that the granule with higher surface area exhibited a more favourable cell proliferation. All three types of fabricated brushite granules have exhibited different sphericity and it has been shown that the cellular behaviour of seeded cells did not seem to depend on sphericity of the granules and no correlation was observed between the sphericity and cellular attachment and proliferation. These finding has important applications for cell delivery and also in the development of injectable cements.

### 6.1.2. The development of calcium phosphate/gellan gum nano-composites for cell delivery

Calcium phosphate (HA)/gellan gum nanocomposites with various HA content were developed. The effect of size and crystallinity of HA particles on the mechanical properties of GG matrix has been studied through microstructure and compression testing. It was shown that while the inclusion of nHA significantly increased the compressive strength and bulk modulus of the GG hydrogel, the mHA material acted to weaken it (2.5 wt% HA).

Furthermore, it was found that by increasing the content of the nHA in the composite to 50 wt%, the yield strength and bulk modulus were increased by four- and nine- fold, respectively. The reinforcing effect of nHA was attributed to its higher association with the GG coil structure when compared with the mHA, which disrupted gel structure. By using different levels of nHA reinforcement in the gel matrix, it will therefore be possible to produce materials of defined modulus, which may be investigated in the future to control cell differentiation.

Further to this study, preliminary cellular tests on fabricated GG /nHA culture beads with various HA content demonstrate that the unmodified GG and GG /nHA beads with HA concentration up 2.5% did not support cell attachment and proliferation. The cell attachment and proliferation was initiated when the nHA content was increased to 5wt%. Increasing the HA loading of the composite to 25wt% resulted in significant increase in the cell number on the culture beads as well as gel modulus. The feasibility of using the GG/nHA beads in spinner flask cultures for cell expansion was also evaluated and compared to that of conventional monolayer cultures and static beads cultures. The better cell attachment and proliferation in stirred suspension cultures was observed compared to that of monolayer culture and static GG/nHA beads. It has been also shown that the GG/nHA culture beads have the ability to stimulate osteogenic differentiation of MCT3T osteoblast precursor cells.

In conclusion, from this study, among the formulations tested, all have potential for further use as culture supports, however, the GG/nHA composite beads was the best combination with respect to the feasibility of using these beads in dynamic conditions for cell expansion with higher cell adhesion and proliferation rate as well as capability of these beads to stimulate osteogenic differentiation when BMSCs used interestingly in the absence of

osteogenic media. Moreover the elastic modulus of these beads can be adjusted by manipulation of HA content which has a great interest on controlling new tissue formation. It is clear however that further assessment of the potential of these culture beads for cell therapy would be required in evaluation of these beads with adjusted moulds for formation of tissue of interest and also the feasibility of these beads for scaling up which all are discussed in the following sections.

## 6.2. Future work

In this thesis two different calcium phosphate containing culture beads of resorbable brushite culture beads and GG/nHA culture beads have been formulated and tested for their ability to support cell adhesion, proliferation and controllable differentiation. In each case different studies and methods haven been tried and performed to optimize the potential of these culture beads for cell delivery. By conditioning the brushite beads post manufacture or by using a process of granulation of brushite crystals, it was possible to generate beads that enable attachment and proliferation of the cells. By using of small scale stirred GG/nHA culture beads, it was possible to produce a higher cell yield for osteoblast precursor cells compared to static beads and conventional monolayer culture system. In addition it was proven that the nano-crystalline HA was more effective in the development of GG/HA nano-composite compared to micro crystalline HA for production of materials of defined modulus which is important factor to control cell differentiation.

In each case however, it is clear that further assessment of the potential of these culture beads for cell therapy with the aim of cell expansion and control of cell differentiation are still required. This would concentrate on different aspects for each case:

### 6.2.1. Fabrication of porous brushite culture beads

One of the drawbacks of cements material is their lack of macroporosity which is one of the key requirements for the material design to direct and support tissue ingrowth (M. P. Ginebra et al. 2010). Fabrication of porous culture beads would allow increase in number of adhered cells through their increased surface area (Shi et al. 2009) and also can be beneficial since the expansion of cells internally will protect cells from shear stress during culture process and later for injection. It has been shown that the leaching process in which soluble particulates of sucrose, mannitol, sodium bicarbonate, and sodium hydrogen phosphate can be added during the preparation of the cement paste can produce porous cement materials (Chung and Park 2007).

Various other methods can be investigated to produce porous brushite culture beads. These methods include freeze-drying (Narbat et al. 2006), solid free form fabrication or direct rapid prototyping with a controllable porous formation (Kwon et al. 2013) and selective laser sintering technique (use of 3D computer-aided design to build 3D porous beads) (Shuai et al. 2013).

### 6.2.2. Dynamic culture condition (medium perfusion system) of brushite beads

In this thesis the cell culture study for brushite culture beads was only performed in static conditions. Further work should focus on a dynamic culture condition such as fluidised bed bioreactors can be used for these brushite beads to determine the feasibility of using these beads in dynamic conditions for cell expansion and compare to that of static culture system.

Cement granules, due to their high density and quick sedimentation cannot be used in a spinner flask. A fluidised bed system by medium perfusion can be ideally utilised in which a

flow perfusion enable the diffusion of medium, all required nutrients, onto the surface of each bead and also throughout the internal part of each individual beads in the case of porous brushite beads. The effect of flow rate, shear stress and other processing parameters (e.g. velocity of perfusion, and the effect of fluidised bed column diameter) on cell attachment, proliferation and differentiation can be investigated and how this dynamic condition can be used as a scale up system to produce large quantities of cultured cells.

### 6.2.3. Human MSCs cultivation on fabricated brushite culture beads

This study has proved the potential of the fabricated brushite culture beads for cell attachment, proliferation and bone formation when culturing osteoblast precursor cells. The obtained results from this study may be fully applicable to other cell line such as mesenchymal stem cells (MSCs). The potential of this system should be exploited for human therapy. MSCs can be used as a cell source to determine the suitability of these beads for expansion of stem cells and maintenance of the multipotentiality of these cells.

### 6.2.4. Brushite beads as drug delivery matrices

Cements materials such as brushite have been shown to be an ideal candidate as delivery systems for bioactive molecules and therapeutics in bone tissue engineering as well as a supporting matrix for cell attachment, proliferation and differentiation due to their low-temperature processing of the cements and their injectability characteristics (M. Ginebra et al. 2006). Therefore the methods of incorporating growth factors into the fabricated beads can be investigated. The bioactive molecules can be added into cement paste in the form of liquid or powder. The kinetics of drug release form different brushite beads prepared with different methods should be investigated.

### 6.2.5. Applicability of fabricated GG/nHA with adjusted elastic modulus for controlling new tissue formation

Mammalian cells are known to respond to the elastic modulus of the surface to which they adhere (Discher et al. 2005; Engler et al. 2006). Consequently, there is interest in developing strategies to control the elastic moduli of materials, including hydrogels. In this thesis in the development of GG/nHA nanocomposites, the effect of size and crystallinity of nHA particles on the mechanical properties of GG hydrogel was investigated. It has been shown that the inclusion of nHA particles effectively increased the mechanical properties of GG hydrogel in comparison with micro sized HA particles. By using different levels of nHA reinforcement in the gel matrix, it will therefore be possible to produce materials of defined modulus which has been reported to be vital to control cell differentiation. Further experiments would be interesting to examine whether it is possible to use these composites to control cell differentiation. MSCs can be utilised to investigate the effect of elastic modulus of fabricated GG/nHA nano-composite on behaviour of MSCs cells for various cell differentiation including osteogenic and chondrogenic cells.

### 6.2.6. Scaling- up cultured cells on GG/nHA beads

The applicability of using a small scale stirred GG/nHA culture beads to produce a higher cell yield for osteoblast precursor cells compared to static condition has been proven in this study. Large amount of cells for cell differentiation and subsequent transplantation would be required for human cell therapy (Fernandes et al. 2009). The suitability of these culture beads for stem cell expansion and the preservation of multipotency of seeded stem cells should be investigated and also GG/nHA culture beads in spinner flask for expansion of MSCc can be scaled up as controlled bioreactors in future.

The use of fluidized bed system can also be interesting to investigate for scaling-up of cultured cells on GG/nHA beads. Although spinner flask bioreactors have been reported beneficial to produce a higher cell yield and for scaling-up cultured cells (Fernandes et al. 2009), the mechanical mixing caused by impeller motion can induce unwanted shear gradients in the spinner flask which will influence on cell viability (Temenoff and Mikos 2000). Fluid circulation in fluidized bed instead of impeller motion in spinner flask can be useful to prevent this from occurring.

# 7. References

Alfred, R., Taiani, J. T., Krawetz, R. J., Yamashita, A., Rancourt, D. E., & Kallos, M. S. (2011), 'Large-scale production of murine embryonic stem cell-derived osteoblasts and chondrocytes on microcarriers in serum-free media', Biomaterials, 32 (26), 6006-16.

Amini, Ami R., Laurencin, Cato T., and Nukavarapu, Syam P. (2012), 'Bone Tissue Engineering: Recent Advances and Challenges',Critical Reviews™ in Biomedical Engineering 40 (5), 363-408.

Amit, Bandyopadhyay, Sheldon, B, Weichang, X, Susmita, B. (2006), 'Calcium Phosphate-Based Resorbable Ceramics: Influence of MgO, ZnO, and SiO2 Dopants', Journal of the American Ceramic Society, 89.

Apelt, D., F. Theiss, A. O. El-Warrak, K. Zlinszky, R. Bettschart-Wolfisberger, M. Bohner, S. Matter, J. A. Auer, and B. Von Rechenberg. (2004), 'In vivo behavior of three different injectable hydraulic calcium phosphate cements', Biomaterials, 25 (7–8), 1439-51.

Augello, Andrea, Kurth, Tobias, and De Bari, Cosimo (2010), 'Mesenchymal stem cells: a perspective from in vitro cultures to in vivo migration and niches', European cells & materials, 20, 121-33.

Bačáková, L., Filova, E., Rypáček, F., Švorčík, V., & Starý, V. (2004), 'Cell adhesion on artificial materials for tissue engineering', Physiol Res, 53 (Suppl 1), S35-S45.

Baker, T. and Goodwin, T. (1997), 'Three-dimensional culture of bovine chondrocytes in rotating-wall vessels', In vitro cellular & developmental biology. Animal, 33 (5), 358-65.

Barralet, J. E., Grover, L. M., and Gbureck, U. (2004), 'Ionic modification of calcium phosphate cement viscosity. Part II: hypodermic injection and strength improvement of brushite cement', Biomaterials, 25 (11), 2197-203.

Benya, P. (1982), 'Dedifferentiated chondrocytes reexpress the differentiated collagen phenotype when cultured in agarose gels', Cell, 30, 215-224.

Bhosale, Abhijit and Richardson, James (2008), 'Articular cartilage: structure, injuries and review of management', British medical bulletin, 87, 77-95.

Birdi, G., Bridson, R. H., Smith, A. M., Mohd Bohari, S. P., & Grover, L. M. (2012), 'Modification of alginate degradation properties using orthosilicic acid', Journal of the Mechanical Behavior of Biomedical Materials, 6 (0), 181-87.

Bohner, M. (2000), 'Calcium orthophosphates in medicine: from ceramics to calcium phosphate cements', Injury, 31 Suppl 4, 37-47.

Bohner M, Theiss F, Apelt D, Hirsiger W, Houriet R, Rizzoli G, Gnos E, Frei C, Auer JA, Rechenberg Bv. (2003), 'Compositional changes of a dicalcium phosphate dihydrate cement after implantation in sheep', Biomaterials, 24 (20), 3463-74.

Boo L, Selvaratnam L, Tai CC, Ahmad TS, Kamarul T. (2011), 'Expansion and preservation of multipotentiality of rabbit bone-marrow derived mesenchymal stem cells in dextran-based microcarrier spin culture', Journal of materials science. Materials in medicine, 22 (5), 1343-56.

Botchwey, E. A., Pollack, S. R., Levine, E. M., & Laurencin, C. T. (2001), 'Bone tissue engineering in a rotating bioreactor using a microcarrier matrix system', Journal of Biomedical Materials Research, 55 (2), 242-53.

Botchwey, Edward Andrew (2002), 'Bone tissue engineering in a rotating bioreactor: A quantitative approach'.

Bouffi C, Thomas O, Bony C, Giteau A, Venier-Julienne MC, Jorgensen C. (2010), 'The role of pharmacologically active microcarriers releasing TGF-beta3 in cartilage formation in vivo by mesenchymal stem cells', Biomaterials, 31 (25), 6485-93.

Boyan, B. D., Hummert, T. W., Dean, D. D., & Schwartz, Z (1996), 'Role of material surfaces in regulating bone and cartilage cell response', Biomaterials, 17 (2), 137-46.

Dhandayuthapani, B., Yoshida, Y., Maekawa, T., & Kumar, D. S. (2011), 'Polymeric Scaffolds in Tissue Engineering Application: A Review', International Journal of Polymer Science, 2011.

Brown, W.E. and Chow, L.C. (1990), 'Dental restorative cement pastes', (Google Patents).

Burg, K., Porter, S., and Kellam, J. (2000), 'Biomaterial developments for bone tissue engineering', Biomaterials, 21 (23), 2347-59.

Byrne, D. P., D. Lacroix, J. A. Planell, D. J. Kelly, and P. J. Prendergast (2007), 'Simulation of tissue differentiation in a scaffold as a function of porosity, Young's modulus and dissolution rate: Application of mechanobiological models in tissue engineering', Biomaterials, 28 (36), 5544-54.

Cancedda, R., Dozin, B., Giannoni, P., & Quarto, R. (2003). Tissue engineering and cell therapy of cartilage and bone. Matrix Biology, 22(1), 81-91,

Caplan, A. and Bruder, S. (2001), 'Mesenchymal stem cells: building blocks for molecular medicine in the 21st century', Trends in molecular medicine, 7 (6), 259-64.

Caplan, Arnold I (2005), 'Review: mesenchymal stem cells: cell-based reconstructive therapy in orthopedics', Tissue engineering, 11 (7-8), 1198-211.

Caplan, Arnold I (2007), 'Adult mesenchymal stem cells for tissue engineering versus regenerative medicine', Journal of cellular physiology, 213 (2), 341-47.

Çetinkaya, G., Kahraman, A. S., Gümüşderelioğlu, M., Arat, S., & Onur, M. A. (2011), 'Derivation, characterization and expansion of fetal chondrocytes on different microcarriers', Cytotechnology, 63 (6), 633-43.

Chang, C.H., F.H., Kuo,T.F.,and Liu, H.C.(2005).Cartilage tissue engineering. Biomedical Engineering:Applications, Basis and Communications,17(02),61-71

Chang, Hsin-I and Wang, Yiwei (2011), 'Cell responses to surface and architecture of tissue engineering scaffolds', Regenerative Medicine and Tissue Engineering—Cells and Biomaterials, InTech: Rijeka, Croatia, 569-88.

Chang, Y. L., Stanford, C. M., Wefel, J. S., & Keller, J. C. (1998). Osteoblastic cell attachment to hydroxyapatite-coated implant surfaces in vitro. The International journal of oral & maxillofacial implants, 14(2), 239-247.

Chen, Allen, Reuveny, Shaul, and Oh, Steve (2013), 'Application of human mesenchymal and pluripotent stem cell microcarrier cultures in cellular therapy: Achievements and future direction', Biotechnology advances,**31(7), 1032-1046**

Chen, Tianhong, et al. (2003), 'Enzyme-catalyzed gel formation of gelatin and chitosan: potential for in situ applications', Biomaterials, 24 (17), 2831-41.

Chung, Hyun Jung and Park, Tae Gwan (2007), 'Surface engineered and drug releasing pre-fabricated scaffolds for tissue engineering', Advanced drug delivery reviews, 59 (4), 249-62.

Clarke, Bart (2008), 'Normal bone anatomy and physiology', Clinical journal of the American Society of Nephrology : CJASN, 3 Suppl 3, 9.

Colley, Helen E., et al. (2009), 'Plasma Polymer Coatings to Support Mesenchymal Stem Cell Adhesion, Growth and Differentiation on Variable Stiffness Silicone Elastomers', Plasma Processes and Polymers, 6 (12), 831-39.

Coutinho, Daniela F., et al. (2010), 'Modified Gellan Gum hydrogels with tunable physical and mechanical properties', Biomaterials, 31 (29), 7494-502.

Crane, Nicole J., et al. (2006), 'Raman spectroscopic evidence for octacalcium phosphate and other transient mineral species deposited during intramembranous mineralization', Bone, 39 (3), 434-42.

Dai, Lin, et al. (2008), 'Concentration dependence of critical exponents for gelation in gellan gum aqueous solutions upon cooling', European Polymer Journal, 44 (12), 4012-19.

Davis, Matthew W. and Vacanti, Joseph P. (1996), 'Toward development of an implantable tissue engineered liver', Biomaterials, 17 (3), 365-72.

De Mul, F.F.M., et al. (1986), 'Micro-Raman Line Broadening in Synthetic Carbonated Hydroxyapatite', Journal of Dental Research, 65 (3), 437-40.

Deans, R. and Moseley, A. (2000), 'Mesenchymal stem cells: biology and potential clinical uses', Experimental hematology, 28 (8), 875-84.

Dekker RJ, de Bruijn JD, Stigter M, Barrere F, Layrolle P, van Blitterswijk CA. (2005), 'Bone tissue engineering on amorphous carbonated apatite and crystalline octacalcium phosphate-coated titanium discs', Biomaterials, 26 (25), 5231-39.

Deligianni, Despina D., et al. (2000), 'Effect of surface roughness of hydroxyapatite on human bone marrow cell adhesion, proliferation, differentiation and detachment strength', Biomaterials, 22 (1), 87-96.

Delorme, Bruno, Chateauvieux, Sebastien, and Charbord, Pierre (2006), 'The concept of mesenchymal stem cells', Regenerative medicine, 1 (4), 497-509.

Di Martino, Alberto, Sittinger, Michael, and Risbud, Makarand V. (2005), 'Chitosan: A versatile biopolymer for orthopaedic tissue-engineering', Biomaterials, 26 (30), 5983-90.

Discher, Dennis E., Janmey, Paul, and Wang, Yu-li (2005), 'Tissue Cells Feel and Respond to the Stiffness of Their Substrate', Science, 310 (5751), 1139-43.

Drury, Jeanie and Mooney, David (2003a), 'Hydrogels for tissue engineering: scaffold design variables and applications', Biomaterials, 24 (24), 4337-51.

Drury, Jeanie L. and Mooney, David J. (2003b), 'Hydrogels for tissue engineering: scaffold design variables and applications', Biomaterials, 24 (24), 4337-51.

Ebrahimian-Hosseinabadi, M., et al. (2011), 'Evaluating and Modeling the Mechanical Properties of the Prepared PLGA/nano-BCP Composite Scaffolds for Bone Tissue Engineering', Journal of Materials Science & Technology, 27 (12), 1105-12.

Elliot J.C. (1994). Structure and chemicstry of the apatites and other calcium orthophosphates. (Amsterdam: Elsevier).

Engler, Adam J., et al. (2006), 'Matrix Elasticity Directs Stem Cell Lineage Specification', Cell, 126 (4), 677-89.

Evageliou, Vasiliki, et al. (2010), 'Compression of gellan gels. Part I: effect of salts', International Journal of Food Science & Technology, 45 (5), 1076-80.

Fernandes, A. M., et al. (2009), 'Successful scale-up of human embryonic stem cell production in a stirred microcarrier culture system', Brazilian Journal of Medical and Biological Research, 42 (6).

Fischer, E., et al. (2003), 'Bone formation by mesenchymal progenitor cells cultured on dense and microporous hydroxyapatite particles', Tissue engineering, 9 (6), 1179-88.

Flautre, B., et al. (1999), 'Volume effect on biological properties of a calcium phosphate hydraulic cement: experimental study in sheep', Bone, 25 (2 Suppl).

Francis Suh, J. K. and Matthew, Howard W. T. (2000), 'Application of chitosan-based polysaccharide biomaterials in cartilage tissue engineering: a review', Biomaterials, 21 (24), 2589-98.

Franco, C., Price, J., and West, J. (2011), 'Development and optimization of a dual-photoinitiator, emulsion-based technique for rapid generation of cell-laden hydrogel microspheres', Acta Biomaterialia, 7 (9), 3267-76.

Freed, L., Vunjak-Novakovic, G., and Langer, R. (1993), 'Cultivation of cell-polymer cartilage implants in bioreactors', Journal of cellular biochemistry, 51 (3), 257-64.

Gbureck, Uwe, et al. (2004), 'Ionic modification of calcium phosphate cement viscosity. Part I: hypodermic injection and strength improvement of apatite cement', Biomaterials, 25 (11), 2187-95.

Giannoni, Paolo, et al. (2005), 'Species variability in the differentiation potential of in vitro-expanded articular chondrocytes restricts predictive studies on cartilage repair using animal models', Tissue engineering, 11 (1-2), 237-48.

Ginebra, M. P., et al. (2010), 'New processing approaches in calcium phosphate cements and their applications in regenerative medicine', Acta Biomaterialia, 6 (8), 2863-73.

Ginebra, Maria-Pau, et al. (2012), 'Calcium phosphate cements as drug delivery materials', Advanced Drug Delivery Reviews, 64 (12), 1090-110.

Ginebra, MP, Traykova, T, and Planell, JA (2006), 'Calcium phosphate cements as bone drug delivery systems: a review', Journal of Controlled Release, 113 (2), 102-10.

Glattauer, Veronica, et al. (2010), 'Preparation of resorbable collagen-based beads for direct use in tissue engineering and cell therapy applications', Journal of Biomedical Materials Research Part A, 92A (4), 1301-09.

Griffith, L. G. (2002), 'Tissue Engineering--Current Challenges and Expanding Opportunities', Science, 295.

Grover, L. M., Knowles, J. C., Fleming, G. J. P., & Barralet, J. E (2003), 'In vitro ageing of brushite calcium phosphate cement', Biomaterials, 24 (23), 4133-41.

Grover, L. M., Gbureck, U., Wright, A. J., Tremayne, M., & Barralet, J. E. (2006), 'Biologically mediated resorption of brushite cement in vitro', Biomaterials, 27 (10), 2178-85.

Gunatillake, P. and Adhikari, R. (2003), 'Biodegradable synthetic polymers for tissue engineering', European cells & materials, 5(1), 1-16

Habibovic, Pamela, et al. (2008), 'Osteoconduction and osteoinduction of low-temperature 3D printed bioceramic implants', Biomaterials, 29 (7), 944-53.

Habraken, W., Wolke, J., and Jansen, J. (2007), 'Ceramic composites as matrices and scaffolds for drug delivery in tissue engineering', Advanced Drug Delivery Reviews, 59 (4-5), 234-48.

Hern, D. and Hubbell, J. (1998), 'Incorporation of adhesion peptides into nonadhesive hydrogels useful for tissue resurfacing', Journal of Biomedical Materials Research, 39 (2), 266-76.

Hofmann, Michael P., et al. (2006), 'FTIR-monitoring of a fast setting brushite bone cement: effect of intermediate phases', Journal of Materials Chemistry, 16 (31), 3199-206.

Hollister, Scott J and Murphy, William L (2011), 'Scaffold translation: barriers between concept and clinic', Tissue Engineering Part B: Reviews, 17 (6), 459-74.

Horwitz, E., et al. (1999), 'Transplantability and therapeutic effects of bone marrow-derived mesenchymal cells in children with osteogenesis imperfecta', Nature medicine, 5 (3), 309-13.

Howard, G.A., Turner, R.T., Puzas, J.E., Nichols, F., and Baylink, D.J. (1983), 'Bone cells on microcarrier spheres', JAMA, 249 (2), 258-59.

Hunt, Nicola C and Grover, Liam M (2010), 'Cell encapsulation using biopolymer gels for regenerative medicine', Biotechnology letters, 32 (6), 733-42.

Hwang, Nathaniel, Varghese, Shyni, and Elisseeff, Jennifer (2007), 'Cartilage tissue engineering: Directed differentiation of embryonic stem cells in three-dimensional hydrogel culture', Methods in molecular biology (Clifton, N.J.), 407, 351-73.

Hynes, Richard O (1992), 'Integrins: versatility, modulation, and signaling in cell adhesion', Cell, 69 (1), 11-25.

Ito, Yoshihiro (1999), 'Surface micropatterning to regulate cell functions', Biomaterials, 20 (23), 2333-42.

Jahromi, Shiva H, et al. (2011), 'Degradation of polysaccharide hydrogels seeded with bone marrow stromal cells', Journal of the mechanical behavior of biomedical materials, 4 (7), 1157-66.

Jin, Guang-Zhen, et al. (2012), 'Performance of evacuated calcium phosphate microcarriers loaded with mesenchymal stem cells within a rat calvarium defect', Journal of materials science. Materials in medicine, 23 (7), 1739-48.

Kafienah, Wael, et al. (2007), 'Three-dimensional cartilage tissue engineering using adult stem cells from osteoarthritis patients', Arthritis and rheumatism, 56 (1), 177-87.

Kalita, Samar J., Bhardwaj, Abhilasha, and Bhatt, Himesh A. (2007), 'Nanocrystalline calcium phosphate ceramics in biomedical engineering', Materials Science and Engineering: C, 27 (3), 441-49.

Kasten, Philip, et al. (2008), 'Porosity and pore size of beta-tricalcium phosphate scaffold can influence protein production and osteogenic differentiation of human mesenchymal stem cells: an in vitro and in vivo study', Acta Biomaterialia, 4 (6), 1904-15.

Kieswetter, K, et al. (1996), 'Surface roughness modulates the local production of growth factors and cytokines by osteoblast-like MG-63 cells', Journal of Biomedical Materials Research, 32 (1), 55-63.

Kim, Hae-Won, Knowles, Jonathan C., and Kim, Hyoun-Ee (2004), 'Hydroxyapatite/poly(ε-caprolactone) composite coatings on hydroxyapatite porous bone scaffold for drug delivery', Biomaterials, 25 (7–8), 1279-87.

Klammert, U., et al. (2009), 'Cytocompatibility of brushite and monetite cell culture scaffolds made by three-dimensional powder printing', Acta Biomaterialia, 5 (2), 727-34.

Klammert, Uwe, et al. (2010), 'Phase composition, mechanical performance and in vitro biocompatibility of hydraulic setting calcium magnesium phosphate cement', Acta Biomaterialia, 6 (4), 1529-35.

Kneser, U., et al. (2006), 'Tissue engineering of bone: the reconstructive surgeon's point of view', Journal of cellular and molecular medicine, 10 (1), 7-19.

Kwon, Byeong-Ju, et al. (2013), 'Biological Advantages of Porous Hydroxyapatite Scaffold Made by Solid Freeform Fabrication for Bone Tissue Regeneration', Artificial Organs, 37 (7), 663-70.

Lampin, M, et al. (1997), 'Correlation between substratum roughness and wettability, cell adhesion, and cell migration', Journal of biomedical materials research, 36 (1), 99-108.

Langstaff, S., et al. (1999), 'Resorbable bioceramics based on stabilized calcium phosphates. Part I: rational design, sample preparation and material characterization', Biomaterials, 20 (18), 1727-41.

LaPorta, Thomas, et al. (2012), 'Clinical relevance of scaffolds for cartilage engineering', The Orthopedic clinics of North America, 43 (2), 245.

Lazic´ S, Zec S, Miljevic´ N, Milonjic´ S. (2001), 'The effect of temperature on the properties of hydroxyapatite precipitated from calcium hydroxide and phosphoric acid'. Thermochim Acta, 374: 13–22

Le Nihouannen, Damien, et al. (2008), 'The use of RANKL-coated brushite cement to stimulate bone remodelling', Biomaterials, 29 (22), 3253-59.

Lee, Donghyun and Kumta, Prashant N. (2010), 'Chemical synthesis and stabilization of magnesium substituted brushite', Materials Science and Engineering: C, 30 (7), 934-43.

Lee, Kuen Yong and Mooney, David J (2001), 'Hydrogels for tissue engineering', Chemical reviews, 101 (7), 1869-80.

LeGeros, Racquel (2008), 'Calcium phosphate-based osteoinductive materials', Chemical reviews, 108 (11), 4742-53.

Lin, Hong-Ru and Yeh, Yu-Jen (2004), 'Porous alginate/hydroxyapatite composite scaffolds for bone tissue engineering: Preparation, characterization, and in vitro studies', Journal of Biomedical Materials Research Part B: Applied Biomaterials, 71B (1), 52-65.

Liu, Xiaohua and Ma, Peter (2004), 'Polymeric scaffolds for bone tissue engineering', Annals of biomedical engineering, 32 (3), 477-86.

Liuyun, Jiang, et al. (2008), 'Preparation and properties of a novel bone repair composite: nano-hydroxyapatite/chitosan/carboxymethyl cellulose', Journal of Materials Science: Materials in Medicine, 19 (3), 981-87.

Lotfi, M, Nejib, M, and Naceur, M (2013), 'Cell Adhesion to Biomaterials: Concept of Biocompatibility', Advances in Biomaterials Science and Biomedical Applications.

Lowry, Oliver H, et al. (1951), 'Protein measurement with the Folin phenol reagent', J biol chem, 193 (1), 265-75.

Mackay, A., et al. (1998), 'Chondrogenic differentiation of cultured human mesenchymal stem cells from marrow', Tissue engineering, 4 (4), 415-28.

Madhumathi, K., et al. (2009), 'Preparation and characterization of novel beta-chitin-hydroxyapatite composite membranes for tissue engineering applications', International Journal of Biological Macromolecules, 44 (1), 1-5.

Malafaya, Patrícia B., Silva, Gabriela A., and Reis, Rui L. (2007), 'Natural–origin polymers as carriers and scaffolds for biomolecules and cell delivery in tissue engineering applications', Advanced Drug Delivery Reviews, 59 (4–5), 207-33.

Malda, J., Kreijveld, E., Temenoff, J. S., van Blitterswijk, C. A., & Riesle, J. (2003a), 'Expansion of human nasal chondrocytes on macroporous microcarriers enhances redifferentiation', Biomaterials, 24 (28), 5153-61.

Malda, J., et al. (2003b), 'Expansion of bovine chondrocytes on microcarriers enhances redifferentiation', Tissue engineering, 9 (5), 939-48.

Malda, Jos and Frondoza, Carmelita G. (2006), 'Microcarriers in the engineering of cartilage and bone', Trends in biotechnology, 24 (7), 299-304.

Mandel, Selen and Tas, A. Cuneyt (2010), 'Brushite (CaHPO4·2H2O) to octacalcium phosphate (Ca8(HPO4)2(PO4)4·5H2O) transformation in DMEM solutions at 36.5 °C', Materials Science and Engineering: C, 30 (2), 245-54.

Mariño, F. Tamimi, et al. (2007a), 'Vertical bone augmentation with granulated brushite cement set in glycolic acid', Journal of Biomedical Materials Research Part A, 81A (1), 93-102.

Mariño, Faleh Tamimi, et al. (2007b), 'Advantages of using glycolic acid as a retardant in a brushite forming cement', Journal of Biomedical Materials Research Part B: Applied Biomaterials, 83B (2), 571-79.

Melero-Martin,et al (2006). Expansion of chondroprogenitor cells on macroporous microcarriers as an alternative to conventional monolayer systems. Biomaterials, 27(15), 2970-2979.

Marolt, Darja, et al. (2012), 'Engineering bone tissue from human embryonic stem cells', Proceedings of the National Academy of Sciences of the United States of America, 109 (22), 8705-09.

Miller, Matthew A., et al. (2012), 'Testing of Brushite (CaHPO4·2H2O) in Synthetic Biomineralization Solutions and In Situ Crystallization of Brushite Micro-Granules', Journal of the American Ceramic Society, 95 (7), 2178-88.

Mao, R., et al. (2000), Texture properties of high and low acyl mixed gellan gels. Carbohydrate Polymers, 41, 331–338.

Müller, Petra, et al. (2008), 'Calcium phosphate surfaces promote osteogenic differentiation of mesenchymal stem cells', Journal of cellular and molecular medicine, 12 (1), 281-91.

Nair, Lakshmi and Laurencin, Cato (2006), 'Polymers as biomaterials for tissue engineering and controlled drug delivery', Advances in biochemical engineering/biotechnology, 102, 47-90.

Nam, Jong Hyun, Ermonval, Myriam, and Sharfstein, Susan T. (2007), 'Cell Attachment to Microcarriers Affects Growth, Metabolic Activity, and Culture Productivity in Bioreactor Culture', Biotechnology Progress, 23 (3), 652-60.

Narbat, Mehdi Kazemzadeh, et al. (2006), 'Fabrication of porous hydroxyapatite-gelatin composite scaffolds for bone tissue engineering', Iranian Biomedical Journal, 10 (4), 215-23.

Naveena, N., Venugopal, J., Rajeswari, R., Sundarrajan, S., Sridhar, R., Shayanti, M., ... & Ramakrishna, S. (2012). Biomimetic composites and stem cells interaction for bone and cartilage tissue regeneration. Journal of Materials Chemistry, 22(12), 5239-5253..

Newman, Alan P. (1998), 'Articular Cartilage Repair', The American Journal of Sports Medicine, 26 (2), 309-24.

Oliveira, J. T., et al. (2010a), 'Gellan gum: A new biomaterial for cartilage tissue engineering applications', Journal of Biomedical Materials Research Part A, 93A (3), 852-63.

Oliveira, João, et al. (2010b), 'Gellan gum injectable hydrogels for cartilage tissue engineering applications: in vitro studies and preliminary in vivo evaluation', Tissue engineering. Part A, 16 (1), 343-53.

Oliveira, Mariana and Mano, João (2011), 'Polymer-based microparticles in tissue engineering and regenerative medicine', Biotechnology Progress, 27 (4), 897-912.

Pang, Y. X. and Bao, X. (2003), 'Influence of temperature, ripening time and calcination on the morphology and crystallinity of hydroxyapatite nanoparticles', Journal of the European Ceramic Society, 23 (10), 1697-704.

Park, Jeong-Hui, et al. (2013a), 'Microcarriers designed for cell culture and tissue engineering of bone', Tissue engineering. Part B, Reviews, 19 (2), 172-90.

Park, Jung-Hui, et al. (2013b), 'Preparation of in situ hardening composite microcarriers: Calcium phosphate cement combined with alginate for bone regeneration', Journal of Biomaterials Applications.

Pearle, Andrew, Warren, Russell, and Rodeo, Scott (2005), 'Basic science of articular cartilage and osteoarthritis', Clinics in sports medicine, 24 (1), 1-12.

Penel, G., et al. (1998), 'MicroRaman Spectral Study of the PO<sub>4</sub> and CO<sub>3</sub> Vibrational Modes in Synthetic and Biological Apatites', Calcified Tissue International, 63 (6), 475-81.

Penel, G., et al. (1999), 'Raman microspectrometry studies of brushite cement: in vivo evolution in a sheep model', Bone, 25 (2, Supplement 1), 81S-84S.

Pina, S., et al. (2010), 'In vitro performance assessment of new brushite-forming Zn- and ZnSr-substituted β-TCP bone cements', Journal of Biomedical Materials Research Part B: Applied Biomaterials, 94B (2), 414-20.

Ponsonnet, L., et al. (2002), 'Effect of surface topography and chemistry on adhesion, orientation and growth of fibroblasts on nickel–titanium substrates', Materials Science and Engineering: C, 21 (1–2), 157-65.

Predoi, D, et al. (2008), 'Calcium phosphate ceramics for biomedical applications', Journal of optoelectronics and advanced materials, 10 (8), 2151-55.

Qinghong, Hu, et al. (2007), 'Effect of crystallinity of calcium phosphate nanoparticles on adhesion, proliferation, and differentiation of bone marrow mesenchymal stem cells', Journal of Materials Chemistry, 17.

Qiu, Qing-Qing, Ducheyne, Paul, and Ayyaswamy, Portonovo S. (2000), 'New bioactive, degradable composite microspheres as tissue engineering substrates', Journal of Biomedical Materials Research, 52 (1), 66-76.

Rajkumar, M., Meenakshisundaram, N., and Rajendran, V. (2011), 'Development of nanocomposites based on hydroxyapatite/sodium alginate: Synthesis and characterisation', Materials Characterization, 62 (5), 469-79.

Ratner, B. D. and Bryant, S. J. (2004), 'Biomaterials: where we have been and where we are going', Annu Rev Biomed Eng, 6, 41-75.

Richardson, C. R., et al. (1999), 'Clinical evaluation of Bio-Oss®: a bovine-derived xenograft for the treatment of periodontal osseous defects in humans', Journal of Clinical Periodontology, 26 (7), 421-28.

Rodrigues, Carlos A. V., et al. (2011), 'Stem cell cultivation in bioreactors', Biotechnology advances, 29 (6), 815-29.

Rodrigues, CVM, et al. (2003), 'Characterization of a bovine collagen–hydroxyapatite composite scaffold for bone tissue engineering', Biomaterials, 24 (27), 4987-97.

Rungsiyanont, Sorasun, et al. (2011), 'Evaluation of Biomimetic Scaffold of Gelatin–Hydroxyapatite Crosslink as a Novel Scaffold for Tissue Engineering: Biocompatibility Evaluation with Human PDL Fibroblasts, Human Mesenchymal Stromal Cells, and Primary Bone Cells', Journal of Biomaterials Applications.

Salgado, António, Coutinho, Olga, and Reis, Rui (2004), 'Bone tissue engineering: state of the art and future trends', Macromolecular Bioscience, 4 (8), 743-65.

Salimi, M. Nabil, et al. (2012), 'Effect of processing conditions on the formation of hydroxyapatite nanoparticles', Powder Technology, 218.

Santos, Maria Helena, et al. (2004), 'Synthesis control and characterization of hydroxyapatite prepared by wet precipitation process', Materials Research, 7, 625-30.

Sautier, Jean-Michel, Nefussi, Jean-Raphaël, and Forest, Nadine (1992), 'Mineralization and bone formation on microcarrier beads with isolated rat calvaria cell population', Calcified Tissue International, 50 (6), 527-32.

Selen, Mandel and Tas, A. Cuneyt (2010), 'Brushite (CaHPO4·2H2O) to octacalcium phosphate (Ca8(HPO4)2(PO4)4·5H2O) transformation in DMEM solutions at 36.5°C', Materials Science and Engineering: C, 30, 245-254.

Shen, Hong, et al. (2010), 'An injectable scaffold: rhBMP-2-loaded poly (lactide-co-glycolide)/hydroxyapatite composite microspheres', Acta biomaterialia, 6 (2), 455-65.

Shi, Xudong, et al. (2009), 'Biodegradable Polymeric Microcarriers with Controllable Porous Structure for Tissue Engineering', Macromolecular Bioscience, 9 (12), 1211-18.

Shin, Michael, Yoshimoto, Hiroshi, and Vacanti, Joseph (2004), 'In vivo bone tissue engineering using mesenchymal stem cells on a novel electrospun nanofibrous scaffold', Tissue engineering, 10 (1-2), 33-41.

Shuai, Cijun, et al. (2013), 'In vitro bioactivity and degradability of β-tricalcium phosphate porous scaffold fabricated via selective laser sintering', Biotechnology and Applied Biochemistry, 60 (2), 266-73.

Sikavitsas, Vassilios I., Bancroft, Gregory N., and Mikos, Antonios G. (2002), 'Formation of three-dimensional cell/polymer constructs for bone tissue engineering in a spinner flask and a rotating wall vessel bioreactor', Journal of biomedical materials research, 62 (1), 136-48.

Silva-Correia, J., et al. (2011), 'Gellan gum-based hydrogels for intervertebral disc tissue-engineering applications', Journal of Tissue Engineering and Regenerative Medicine, 5 (6), e97-e107.

Smith, Alan M., et al. (2007), 'An Initial Evaluation of Gellan Gum as a Material for Tissue Engineering Applications', Journal of Biomaterials Applications, 22 (3), 241-54.

Smith, Ian, McCabe, Laura, and Baumann, Melissa (2006), 'MC3T3-E1 osteoblast attachment and proliferation on porous hydroxyapatite scaffolds fabricated with nanophase powder', International journal of nanomedicine, 1 (2), 189-94.

Solaiman, Tarafder, et al. (2013), '3D printed tricalcium phosphate bone tissue engineering scaffolds: effect of SrO and MgO doping on in vivo osteogenesis in a rat distal femoral defect model', Biomaterials Science, 1, 1250-1259.

Sprio, S., et al. (2008), 'Physico-chemical properties and solubility behaviour of multi-substituted hydroxyapatite powders containing silicon', Materials Science and Engineering: C, 28 (1), 179-87.

Su, Kai, et al. (2011), 'A Novel Shell-Structure Cell Microcarrier (SSCM) for Cell Transplantation and Bone Regeneration Medicine', Pharmaceutical Research, 28 (6), 1431-41.

Suh, J. and Matthew, H. (2000), 'Application of chitosan-based polysaccharide biomaterials in cartilage tissue engineering: a review', Biomaterials, 21 (24), 2589-98.

Sun, Jinchen and Tan, Huaping (2013), 'Alginate-Based Biomaterials for Regenerative Medicine Applications', Materials, 6 (4), 1285-309.

Sun, X. T., et al. (2004), 'Angiogenic synergistic effect of basic fibroblast growth factor and vascular endothelial growth factor in an in vitro quantitative microcarrier-based three-dimensional fibrin angiogenesis system', World journal of gastroenterology : WJG, 10 (17), 2524-28.

Suzuki, Osamu, et al. (2006), 'Bone formation enhanced by implanted octacalcium phosphate involving conversion into Ca-deficient hydroxyapatite', Biomaterials, 27 (13), 2671-81.

Swetha, Maddela, et al. (2010), 'Biocomposites containing natural polymers and hydroxyapatite for bone tissue engineering', International Journal of Biological Macromolecules, 47 (1), 1-4.

Tadic, D. and Epple, M. (2004), 'A thorough physicochemical characterisation of 14 calcium phosphate-based bone substitution materials in comparison to natural bone', Biomaterials, 25 (6), 987-94.

Tamimi, F., Sheikh, Z., & Barralet, J. (2012). Dicalcium phosphate cements: Brushite and monetite. Acta biomaterialia, 8(2), 474-487.

Tamimi, Faleh, et al. (2008), 'Brushite–collagen composites for bone regeneration', Acta Biomaterialia, 4 (5), 1315-21.

Tas, A. Cuneyt and Brown, P. (2011), 'Granules of Brushite and Octacalcium Phosphate from Marble', Journal of the American Ceramic Society, 94 (11) 3722–3726

Tebb, T. A., Tsai, S. W., Glattauer, V., White, J. F., Ramshaw, J. A., & Werkmeister, J. A. (2006). Development of porous collagen beads for chondrocyte culture. Cytotechnology, 52(2), 99-106.

Temenoff, Johnna S and Mikos, Antonios G (2000), 'Review: tissue engineering for regeneration of articular cartilage', Biomaterials, 21 (5), 431-40.

Theiss, Felix, et al. (2005), 'Biocompatibility and resorption of a brushite calcium phosphate cement', Biomaterials, 26 (21), 4383-94.

Tseng, Pei-Chi, et al. (2012), 'Spontaneous osteogenesis of MSCs cultured on 3D microcarriers through alteration of cytoskeletal tension', Biomaterials, 33 (2), 556-64.

Tsuda, H. and Arends, J. (1993), 'Raman Spectra of Human Dental Calculus', Journal of Dental Research, 72 (12), 1609-13.

Tuan, Rocky S, Boland, Genevieve, and Tuli, Richard (2003), 'Adult mesenchymal stem cells and cell-based tissue engineering', Arthritis Research and Therapy, 5 (1), 32-45.

Velden-deGroot, C. A. M. (1995), 'Microcarrier technology, present status and perspective', in E. C. Beuvery, J. B. Griffiths, and W. P. Zeijlemaker (eds.), Animal Cell Technology: Developments Towards the 21st Century (Springer Netherlands), 899-905.

Voigt, M., et al. (1999), 'Cultured epidermal keratinocytes on a microspherical transport system are feasible to reconstitute the epidermis in full-thickness wounds', Tissue engineering, 5 (6), 563-72.

Von Recum, AF and Van Kooten, TG (1996), 'The influence of micro-topography on cellular response and the implications for silicone implants', Journal of Biomaterials Science, Polymer Edition, 7 (2), 181-98.

Wakitani, S., et al. (2002), 'Human autologous culture expanded bone marrow mesenchymal cell transplantation for repair of cartilage defects in osteoarthritic knees', Osteoarthritis and cartilage / OARS, Osteoarthritis Research Society, 10 (3), 199-206.

Wall, I., Donos, N., Carlqvist, K., Jones, F., & Brett, P. (2009). Modified titanium surfaces promote accelerated osteogenic differentiation of mesenchymal stromal cells< i> in vitro</i>. Bone, 45(1), 17-26.

Wang, Chunming, Varshney, Rohan R., and Wang, Dong-An (2010), 'Therapeutic cell delivery and fate control in hydrogels and hydrogel hybrids', Advanced Drug Delivery Reviews, 62 (7–8), 699-710.

Wang, Chunming, et al. (2008), 'A novel gellan gel-based microcarrier for anchorage-dependent cell delivery', Acta Biomaterialia, 4 (5), 1226-34.

Weiner, Steve and Wagner, H. Daniel (1998), 'The material bone: structure-mechanical function relations', Annual Review of Materials Science, 28 (1), 271-98.

Xi Lu, Jian, et al. (1999), 'Effects of chitosan on rat knee cartilages', Biomaterials, 20 (20), 1937-44.

Xynos, ID, et al. (2000), 'Bioglass® 45S5 stimulates osteoblast turnover and enhances bone formation in vitro: implications and applications for bone tissue engineering', Calcified Tissue International, 67 (4), 321-29.

Yeatts, Andrew B and Fisher, John P (2011), 'Bone tissue engineering bioreactors: dynamic culture and the influence of shear stress', Bone, 48 (2), 171-81.

Yoshida, Hirohisa and Takahashi, Masato (1993), 'Structural change of gellan hydrogel induced by annealing', Food Hydrocolloids, 7 (5), 387-95.

Yu, Xiaojun, et al. (2004), 'Bioreactor-based bone tissue engineering: the influence of dynamic flow on osteoblast phenotypic expression and matrix mineralization', Proceedings of the National Academy of Sciences of the United States of America, 101 (31), 11203-08.

Yuan, H., & de Groot, K. (2005). Calcium phosphate biomaterials: an overview. In Learning from Nature How to Design New Implantable Biomaterialsis: From Biomineralization Fundamentals to Biomimetic Materials and Processing Routes (pp. 37-57). Springer Netherlands.

Zakharov, N. A., et al. (2004), 'Calcium Hydroxyapatite for Medical Applications', Inorganic Materials, 40 (6), 641-48.

Zhao, Feng, et al. (2006), 'Effects of hydroxyapatite in 3-D chitosan–gelatin polymer network on human mesenchymal stem cell construct development', Biomaterials, 27 (9), 1859-67.

Zhao, Feng, et al. (2002), 'Preparation and histological evaluation of biomimetic three-dimensional hydroxyapatite/chitosan-gelatin network composite scaffolds', Biomaterials, 23 (15), 3227-34.

Zhou, Z., et al. (2009), 'Performance improvement of injectable poly(ethylene glycol) dimethacrylate-based hydrogels with finely dispersed hydroxyapatite', Biomedical materials (Bristol, England), 4 (3), 035007.

# 8. Appendix

## Journal Publications

- **P. Jamshidi,** P. Ma, K. Khosrowyar, A. M. Smith and L. M. Grover, (2012), Tailoring gel modulus using dispersed nanocrystalline hydroxyapatite. Journal of Experimental Nanoscience,7: 652–661.

- **P. Jamshidi**, R.H. Bridson, A.J. Wright, and L.M. Grover, (2013), Brushite cement additives inhibit attachment to cell culture beads. Journal of Biotechnology and Bioengineering, 110: 1487–1494.

- S.C. Cox, **P. Jamshidi**, L.M. Grover, and K.K. Mallick, (2014), Low temperature aqueous precipitation of needle-like nanophase hydroxyapatite. Journal of Materials Science: Materials in Medicine, 25: 37-46.

- S.C. Cox, **P. Jamshidi**, L.M. Grover, and K.K. Mallick, (2014), Preparation and characterisation of nanophase Sr, Mg, and Zn substituted hydroxyapatite by aqueous precipitation. Journal of Materials Science and Engineering: C, 35, 106-114.

- S.C. Cox, **P. Jamshidi**, L.M. Grover, and K.K. Mallick, (2014), Aqueous precipitation of hydroxyapatite – influence of pH conditions on cytocompatibility and proliferation of MC3T3 osteoblast precursor cells. In preparation.

- S.C. Cox, **P. Jamshidi**, L.M. Grover, and K.K. Mallick. (2014), Cellular in vitro evaluation of hydroxyapatite precipitated in mixed solvent systems. In preparation.

- E. Hughes, T. Yanni, **P. Jamshidi**, L. M. Grover, (2014), Inorganic cements for biomedical application: Calcium Phosphate, Calcium Sulphate and Calcium Silicate. Journal of Advances in Applied Ceramics. Under publication.

## Conferences

- **P. Jamshidi**, R.H. Bridson, and L.M. Grover. (2011), Evaluation of the physical and biological properties of a gellan gum-hydroxyapatite composite, Proceedings of $10^{th}$ annual conference of the UK society for biomaterials, london, UK.

- **P. Jamshidi**, R.H. Bridson, A.J. Wright, and L.M. Grover. (2012), A systematic investigation of cell attachment to brushite-based cell culture beads, 9th World Biomaterials Congress, Chengdu, China.

- **P. Jamshidi**, R.H. Bridson, and L.M. Grover. (2012), A comparison of methods for the fabrication of brushite based culture beads, Proceedings of 11th annual conference of the UK society for biomaterials, Nottingham, UK.

## Posters

- **P. Jamshidi**, J.Paxton, and L.M Grover, The development of Calcium phosphate/gellan gum nano-composite culture beads for cell delivery, 25th European Conference on Biomaterials, 2013, Madrid, Spain.

- **P. Jamshidi** and L.M. Grover, Calcium phosphate/gellan gum nano-composite beads for musculoskeletal tissue regeneration**,** Proceedings of 12th annual conference of the UK society for biomaterials, 2013, Birmingham, UK.

- **P. Jamshidi**, R.H. Bridson, and L.M. Grover, A systematic investigation of cell attachment to brushite-based cell culture beads, Research Poster Conference, 2012, Birmingham, UK.

- **P. Jamshidi**, R.H. Bridson, and L.M. Grover, Tailoring gel modulus using dispersed nanocrystalline hydroxyapatite, Doctoral Training Centre Joint Conference - Tissue Engineering and Regenerative Medicine, 2012, Keele, UK.
- **P. Jamshidi**, R.H. Bridson, and L.M. Grover, Tailoring gel modulus using dispersed nanocrystalline hydroxyapatite, Biochemical Engineering Special Interest Group Young researchers meeting, 2012, Manchester, UK.

ARTICLE

BIOTECHNOLOGY and BIOENGINEERING

# Brushite Cement Additives Inhibit Attachment to Cell Culture Beads

Parastoo Jamshidi,[1] Rachel H. Bridson,[1] Adrian J. Wright,[2] Liam M. Grover[1]

[1]School of Chemical Engineering, University of Birmingham, Edgbaston B15 2TT, UK; telephone: +44-121-414-3887; fax: +44-121-414-5324; e-mail: l.m.grover@bham.ac.uk

[2]School of Chemistry, University of Birmingham, Edgbaston, UK

**ABSTRACT:** Brushite-forming calcium phosphate cements are of great interest as bone replacement materials because they are resorbable in physiological conditions. Cell-attached culture beads formed from this material could be of great use for cell therapy. Despite a significant amount of work on optimizing the physicochemical properties of these materials, there are very few studies that have evaluated the capacity of the materials to facilitate cell adhesion. In this study, we have formed resorbable calcium phosphate (brushite) culture beads and for the first time we showed that cell attachment to the surface of the brushite cement (BC) could be inhibited by the presence of an intermediate dicalcium phosphate–citrate complex, formed in the cement as a result of using citric acid, a retardant and viscosity modifier used in many cement formulations. The BC beads formed from the mixture of β-TCP/orthophosphoric acid using citric acid did not allow cell attachment without further treatment. Ageing of BC beads in serum-free Dulbecco's Modified Eagle's Medium (DMEM) solution at 37°C for 1 week greatly enhanced the cell adhesion capacity of the material. Scanning electron microscopy, X-ray diffraction (XRD), and confocal Raman microspectrometry indicated the increased capacity for cell adhesion was due to the changes in phase composition of BC. XRD patterns collected before and after ageing in aqueous solution and a high initial mass loss, suggest the formation of a dicalcium phosphate–citrate complex within the matrix. Since compacts formed from brushite powder supported cell attachment, it was hypothesized that the dicalcium phosphate–citrate complex prevented attachment to the cement surface.

Biotechnol. Bioeng. 2013;xxx: xxx–xxx.



**KEYWORDS:** brushite; ageing; cell attachment; Raman; phase composition; X-ray diffraction

Correspondence to: L. M. Grover

Received 10 September 2012; Revision received 30 November 2012;
Accepted 3 December 2012
Accepted manuscript online xx Month 2012;
Article first published online in Wiley Online Library (wileyonlinelibrary.wiley.com).
DOI 10.1002/bit.24806

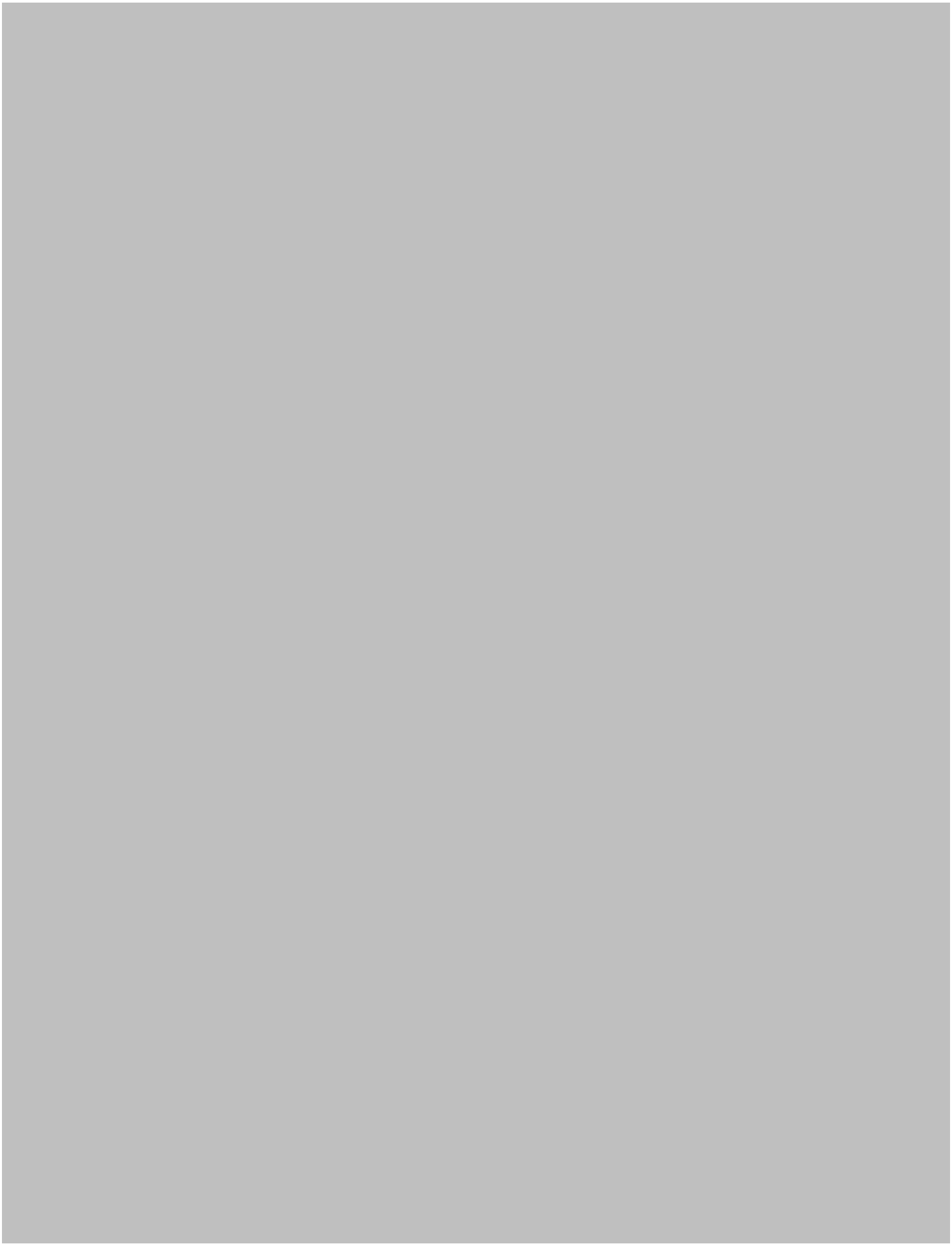

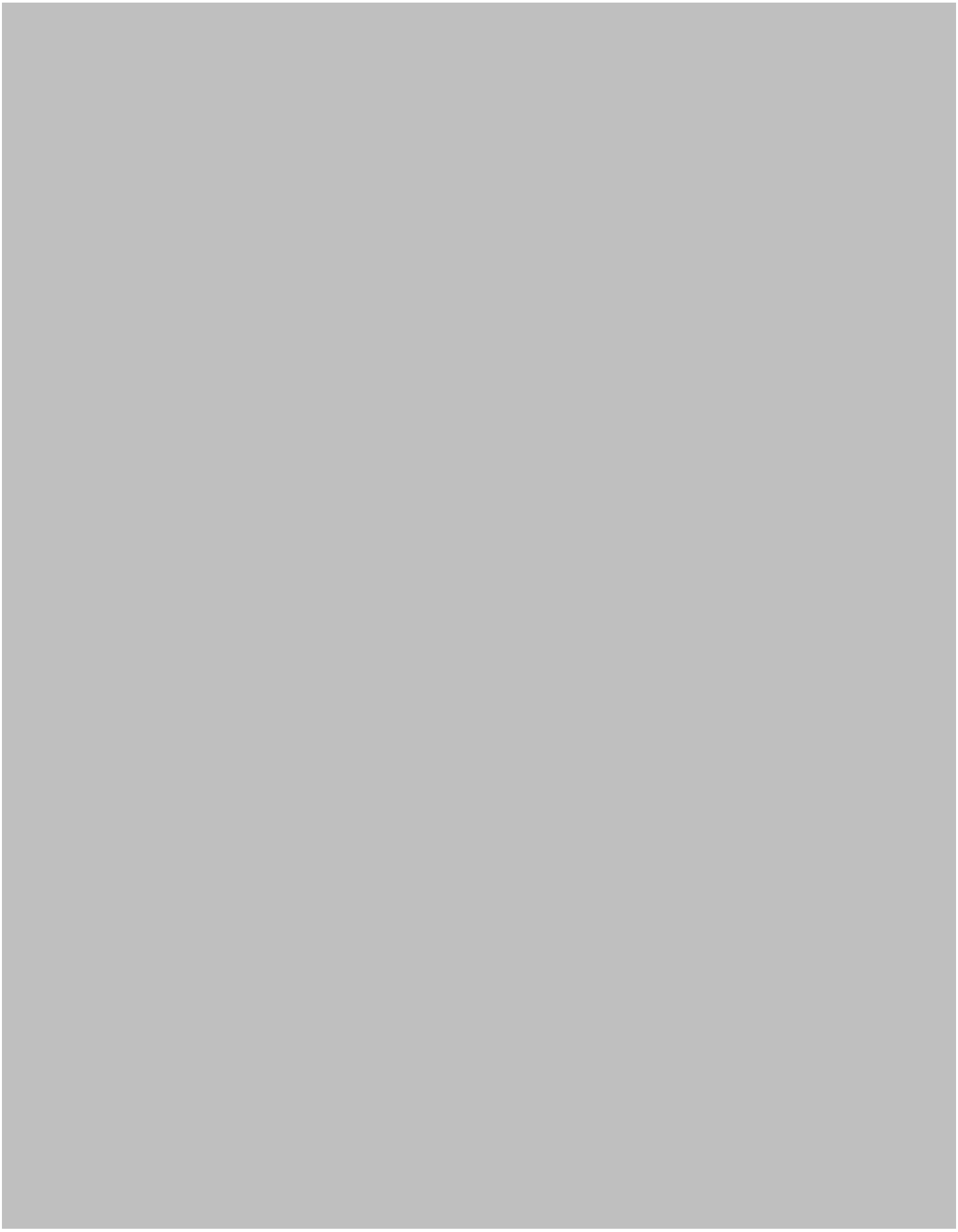

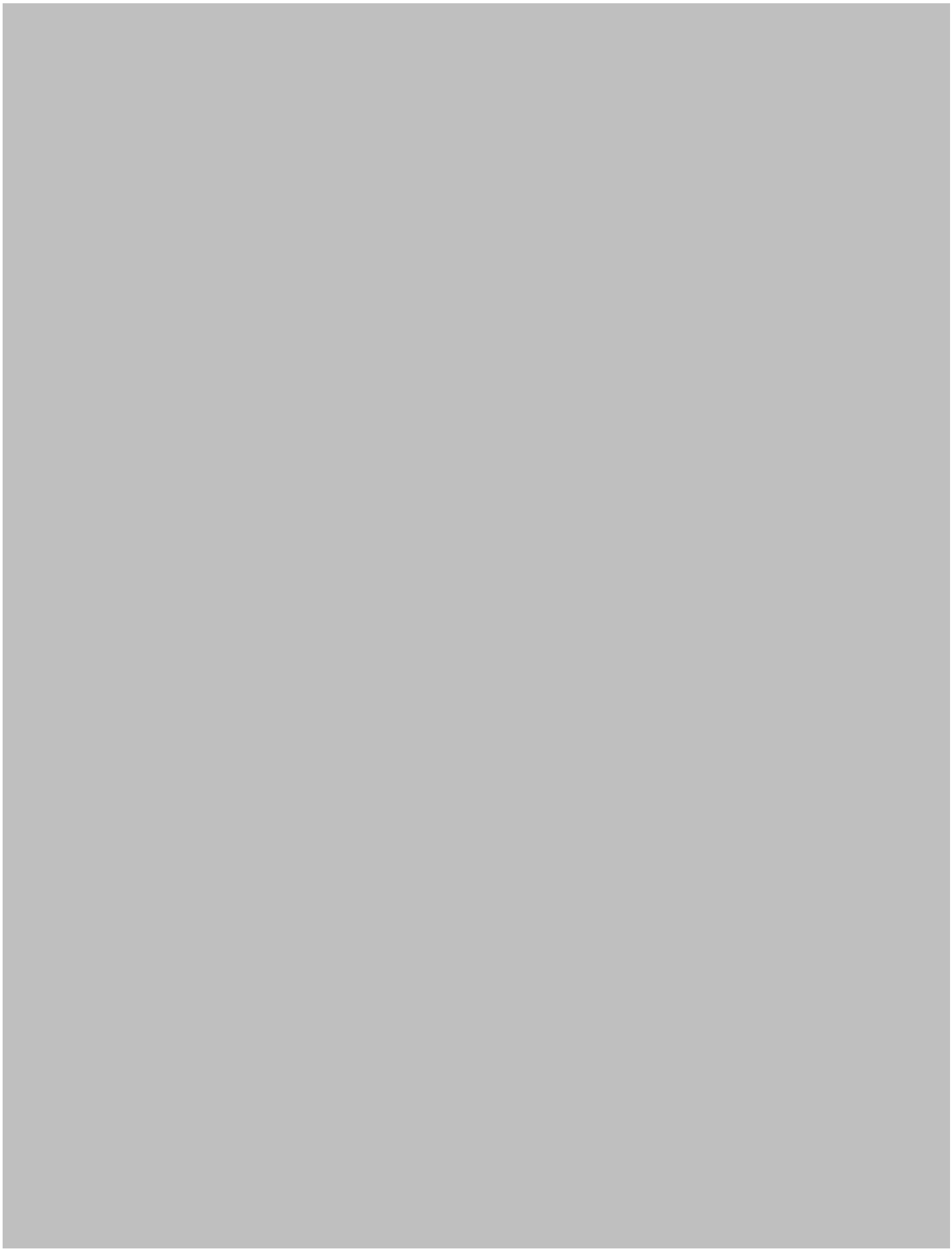

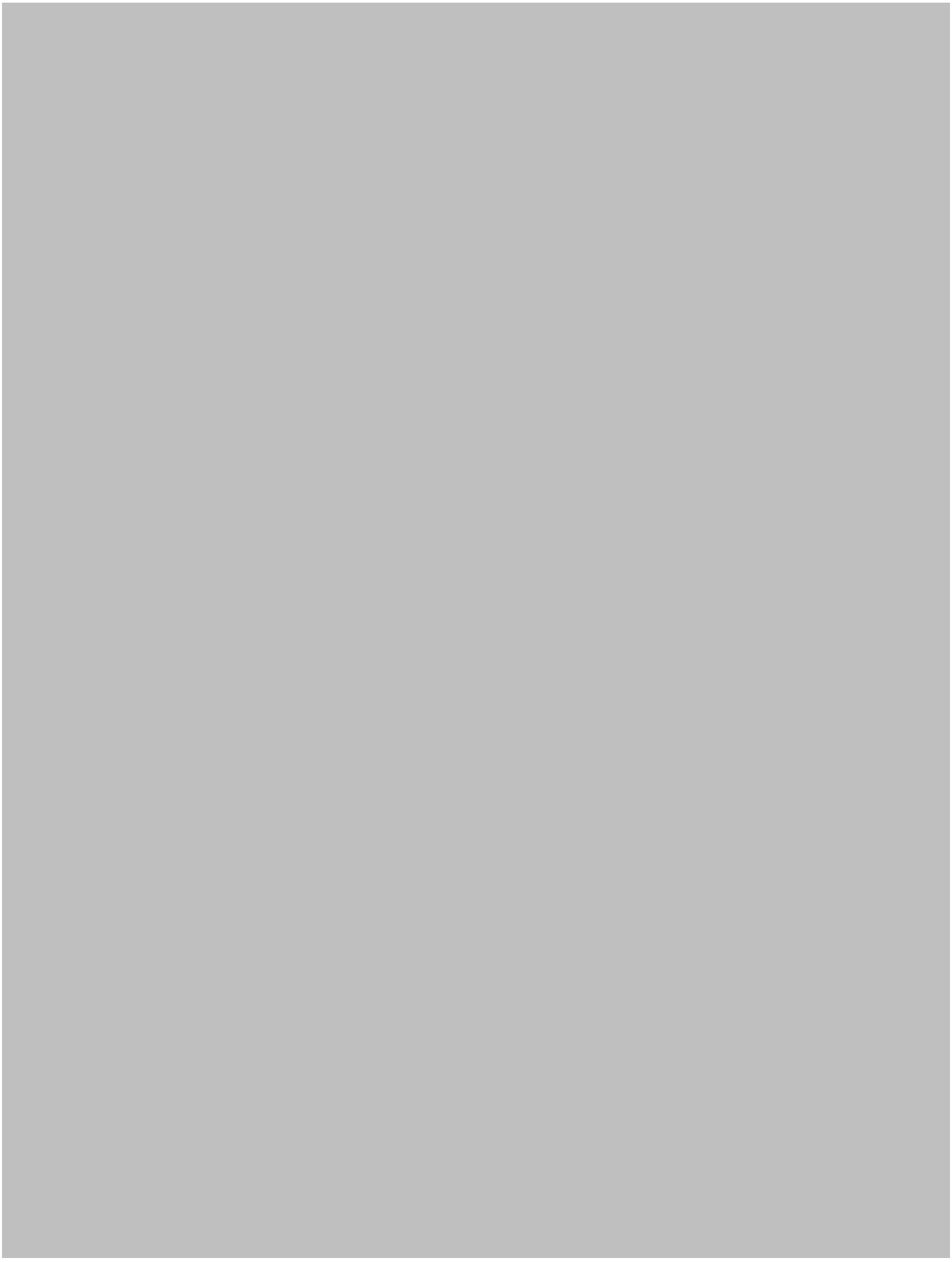

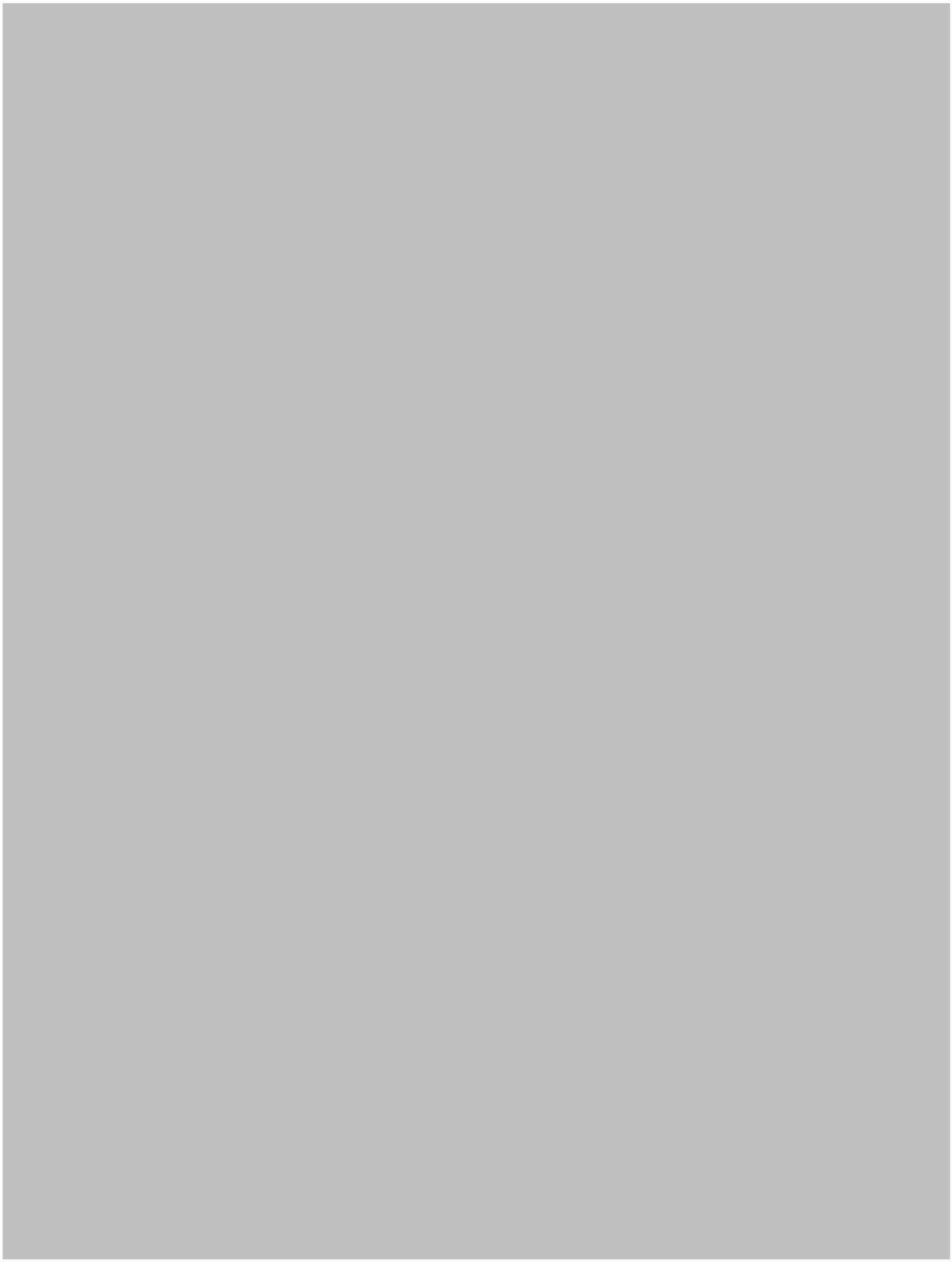

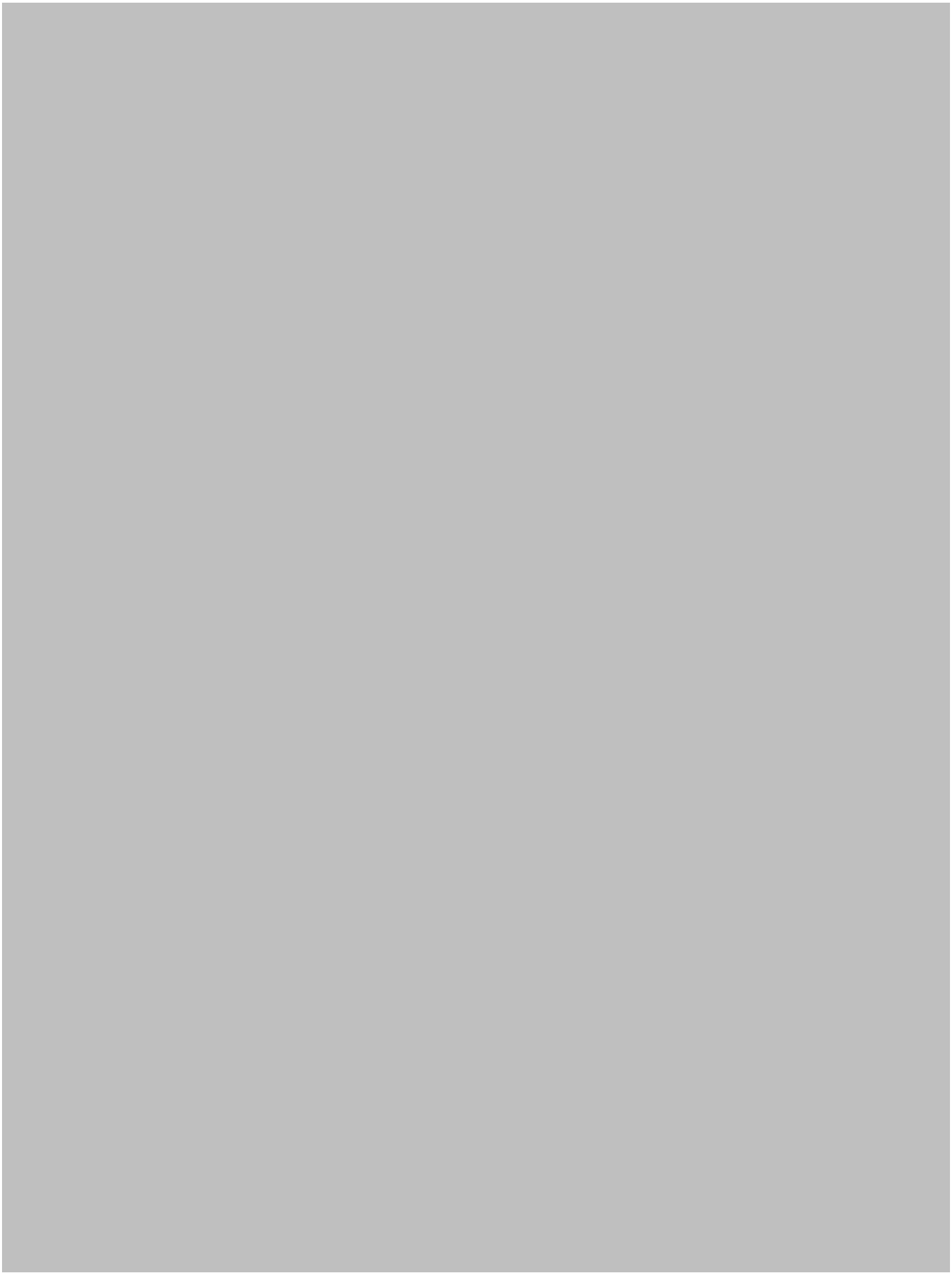

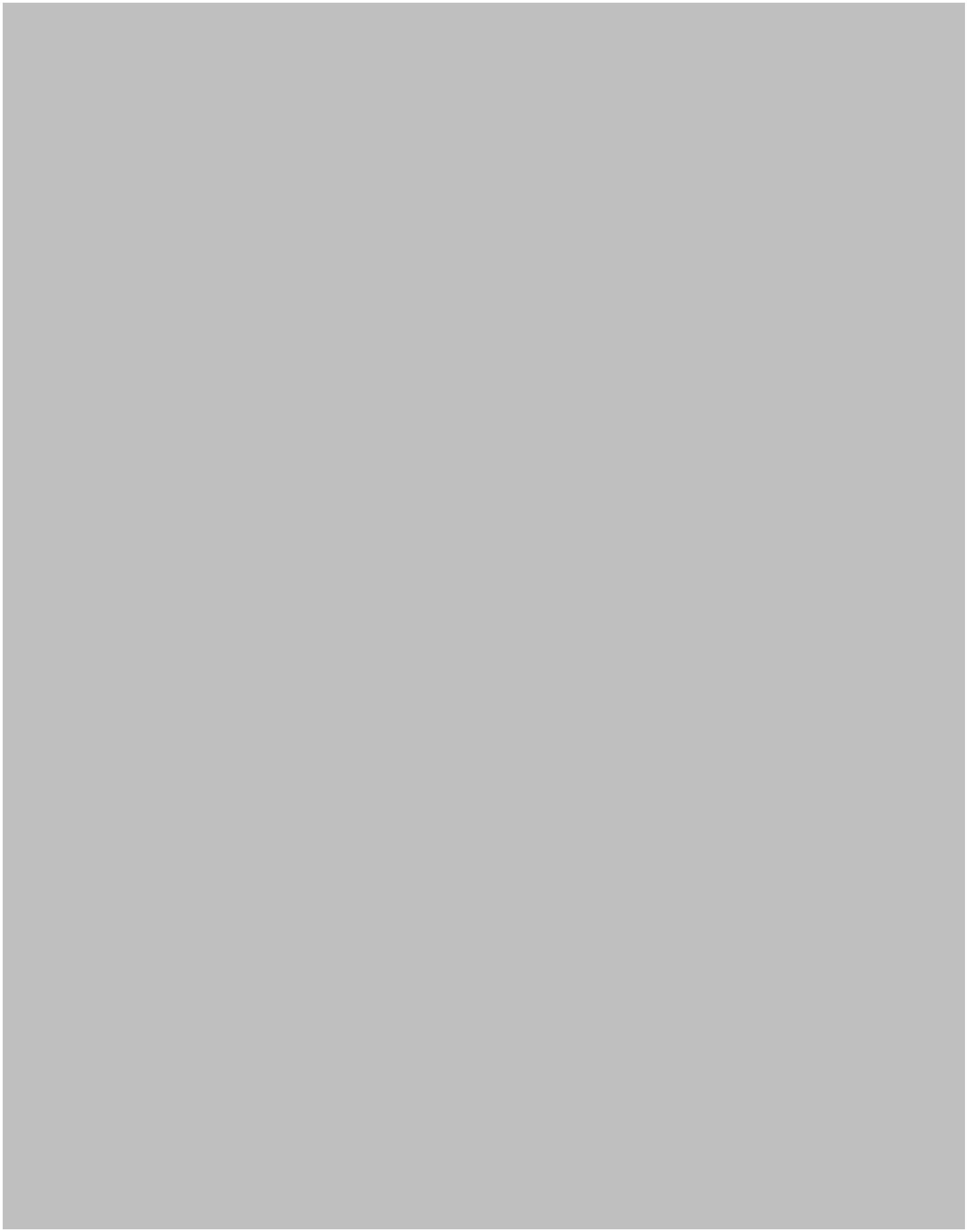

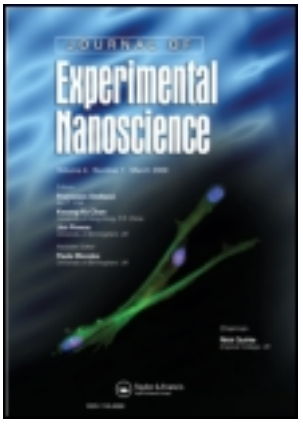

Journal of Experimental Nanoscience
Publication details, including instructions for authors and subscription information:
http://www.tandfonline.com/loi/tjen20

# Tailoring gel modulus using dispersed nanocrystalline hydroxyapatite

Parastoo Jamshidi [a], Paul Ma [a], Katahyunne Khosrowyar [a], Alan M. Smith [b] & Liam M. Grover [a]

[a] School of Chemical Engineering, University of Birmingham, Birmingham, B15 2TT, UK

[b] School of Applied Sciences, University of Huddersfield, Huddersfield, HD1 3DH, UK

Version of record first published: 21 Nov 2012.

To cite this article: Parastoo Jamshidi , Paul Ma , Katahyunne Khosrowyar , Alan M. Smith & Liam M. Grover (2012): Tailoring gel modulus using dispersed nanocrystalline hydroxyapatite, Journal of Experimental Nanoscience, 7:6, 652-661

To link to this article: http://dx.doi.org/10.1080/17458080.2012.724182

*Journal of Experimental Nanoscience*
Vol. 7, No. 6, October–November 2012, 652–661

Taylor & Francis
Taylor & Francis Group

# Tailoring gel modulus using dispersed nanocrystalline hydroxyapatite

Parastoo Jamshidi[a], Paul Ma[a], Katahyunne Khosrowyar[a], Alan M. Smith[b] and Liam M. Grover[a]*

[a]*School of Chemical Engineering, University of Birmingham, Birmingham, B15 2TT, UK;*
[b]*School of Applied Sciences, University of Huddersfield, Huddersfield, HD1 3DH, UK*

(*Received 24 May 2012; final version received 20 August 2012*)

Mammalian cells are known to respond to the elastic modulus of the surface to which they adhere. Consequently, there is interest in developing strategies to control the elastic moduli of materials, including hydrogels. One way of controlling modulus in hydrogels is to introduce reinforcing agents such as inorganic materials, for example hydroxyapatite (HA). Although several authors have reported the reinforcement of hydrogels with ceramic particles, there have not been any studies to investigate the effect of size and crystallinity of HA particles on the mechanical properties of hydrogel. In this study, synthetic Calcium phosphate of two different crystallite sizes: one on the nano-scale (~50 nm) and the other on the micro-scale (~150 nm) have been used to manufacture HA/gellan gum (GG) composites. It was shown that while nano-scale HA (nHA) reinforced the hydrogel structure, the micro-scale HA (mHA) material acted to weaken it (2.5 wt% HA). Furthermore, it was found that by increasing the content of the nHA in the composite to 50 wt%, the yield strength and bulk modulus was increased by four- and nine-fold, respectively. The reinforcing effect of nHA was attributed to its higher association with the GG coil structure when compared with the mHA, which disrupted gel structure.

**Keywords:** hydrogel; gellan; mechanical properties; hydroxyapatite; crystallite size



*Corresponding author. Email: l.m.grover@bham.ac.uk

ISSN 1745–8080 print/ISSN 1745–8099 online

http://dx.doi.org/10.1080/17458080.2012.724182
http://www.tandfonline.com